Charles University in Prague
First Faculty of Medicine

Studijní program: Biomedicína
Studijní obor: Biologie a patologie buňky

Titul. Jméno Příjmení (Autor/Author): **M.Sc. Jana Šmigová**

Název závěrečné práce*:* **Vztah vyšších chromatinových struktur a genového umlčování**

Podnázev závěrečné práce: ***Polycomb (PcG) tělíska***

Title: **The relationship between higher order chromatin structure and gene silencing**

Subtitle: ***Polycomb (PcG) bodies***

Typ závěrečné práce

Disertační / **Ph.D. thesis**

Ústav buněčné biologie a patologie/
Institute of Cellular Biology and Pathology **Prague, 2012**

I would especially like to thank **Dr. Pavel Jůda** for his great personal and scientific support during my Ph.D. studies and stunning tolerance. Pavel is the most important person on my way to get the Ph.D. degree.

I would like to thank the **professor Dr. Ivan Raška**, the chairman of the Institute of Cellular Biology and Pathology, First Faculty of Medicine, Charles University in Prague, for necessary (financial, scientific and personal) support, guidance and his help with writing my first scientific texts.

I would like to thank the **associate professor Dr. Dušan Cmarko** for giving me the opportunity to work at the Institute of Cellular Biology and Pathology and his support and friendship during my Ph.D. studies and all the former and present staff members.

I would like to thank **Dr. Paul Verkade** for hosting me in his laboratory and helpful consultations and all staff of Wolfson Bioimaging Facility at University of Bristol for the friendly atmosphere in the laboratory.

I thank **Dr. Guy M. Hagen** for careful reading of my English texts and for his friendship.

I am deeply grateful to **my parents** and two **brothers** for their unconditional support throughout my life.

I would like to thank to **my friends** for their encouragement and friendship.

Financially, my work was supported by the **grants** from the Ministry of Education, Youth and Sports of the Czech Republic, the Academy of Sciences of the Czech Republic, the Grant Agency of the Czech Republic and the Grant Agency of Charles University in Prague.

Prohlašuji, že jsem tuto disertační práci vypracovala samostatně a výhradně s použitím citovaných pramenů, literatury a dalších odborných zdrojů. Současně prohlašuji, že práce nebyla využita k získání jiného nebo stejného titulu.

Souhlasím s trvalým uložením elektronické verze mé práce v databázi systému meziuniverzitního projektu Theses.cz za účelem soustavné kontroly podobnosti kvalifikačních prací.

V Praze, 20.6.2012 Podpis JANA ŠMIGOVÁ

ŠMIGOVÁ, Jana. *Vztah vyšších chromatinových struktur a genového umlčování. Polycomb (PcG) tělíska. [The relationship between higher order chromain structure and gene silencing. Polycomb (PcG) bodies]*. Praha, 2012. 111 s., 0 příl. Disertační práce (Ph.D.). Univerzita Karlova v Praze, 1. lékařská fakulta, Ústav buněčné biologie a patologie. Vedoucí záverečné práce/Školitel Cmarko, Dušan.

Abstrakt

Eukaryotické interfázní buněčné jádro sestává z různých strukturně a funkčně odlišných subkompartmentů, neboli domén, které na rozdíl od cytoplazmatických organel nejsou ohraničeny biologickou membránou. Kompartmentalizace jádra je generována stochastickou interakcí jeho komponenentů a je podmíněna molekulárním crowding-em. Obecně mohou být jaderné subkompartmenty rozděleny na chromatinové a interchromatinové domény. Na rozdíl od chromatinových domén, interchromatinové subkompartmenty obsahují jen málo nebo žádnou DNA a sestávají zejména z proteinů nebo ribonukleoproteinů. Interchromatinové subkompartmenty mohou být rozděleny na jaderné továrny, tělíska a skvrny. V naší práci jsme se zabývali takzvanými Polycomb (PcG) tělísky, která byla dosud považována za typická jadérná tělíska tvořená akumulací proteinů skupiny Polycomb (PcG proteiny). PcG proteiny jsou důležité epigenetické regulátory genové exprese. Jejich regulační funkce spočívá ve změně funkčního stavu chromatinu změnou chemických modifikací histonů, jeho následné kompaktaci a umlčení příslušných genů. Cílem naší práce bylo zjistit ultrastrukturu PcG tělíska a studovat jeho chování v podmínkách experimentálního crowding-u. Avšak, pomocí korelační světelné a elektronové mikroskopie jsme zistili, že PcG tělíska nepředstavují typická jaderná tělíska, ale spíše jadernou doménu tvořenou lokálním nakupením značených heterochromatinových snopců. Denzita imunoznačení vztažená na plochu heterochromatinu v oblasti odpovídající florescenčním PcG tělískům se nelišila od denzity imunoznačení heterochromatinu mimo tělíska. Dále jsme pozorovali, že v podmínkách experimentálního crowding-u se chování PcG tělísek výrazně liší od chování typických jaderných tělísek. Zatímco je známo, že typická jaderná tělíska se v podmínkách experimentálního crowding-u formují, u PcG tělísek jako akumulací BMI1 proteinu jsme během inkubace buněk v hyperosmotickém prostředí pozorovali jejich reverzibilní zmizení, avšak PcG tělíska jako chromatinové domény v hypertonickém prostředí přetrvávala. Použití experimentálního modelu molekulárního crowding-u nám umožnilo nejen potvrdit chromatinovou podstatu PcG tělísek, ale také poukázat na možnou nezávislost udržování kompaktace chromatinu v Polycomb tělíscích na Polycomb proteinech.

Klíčová slova: Polycomb proteiny, Polycomb tělísko, BMI1 protein, jaderná architektura, interchromatin, heterochromatin, hyperkondenzovaný chromatin, post-translační chemické modifikace, korelační světelná a elektronová mikroskopie

Abstract

The interphase eukaryotic nucleus is a highly organized organelle consisting of various structurally and functionally different subcompartments or domains that are not separated by biological membranes. Thus, the nuclear higher order structure is established by the stochastic (although initially regulated) interaction of its components that mostly arise from macromolecular crowding. Generally, the nuclear subcompartments can be divided into chromatin or interchromatin domains. In contrast to chromatin domains, interchromatin subcompartments contain little or no DNA and are of a proteinaceous or ribonucleoproteinaceous nature; and can be divided into nuclear factories, speckles and bodies. In our work, we were interested in Polycomb (PcG) bodies that were thought to be formed by accumulations of Polycomb group (PcG) proteins. PcG proteins are important epigenetic factors that regulate gene expression by chromatin modification followed by chromatin compaction. The aim of our work was to established the fine structure of the PcG body and to follow its behaviour within the frame of the experimental model of molecular crowding. We found out that the essence of the fluorescent PcG foci is associated with the local accumulation of heterochromatin fascicles with the same labeling density against polycomb BMI1 protein per area of dense chromatin throughout the nucleus. We defined a "PcG body" as a chromatin domain rather than a nuclear body. Further, we observed that the behaviour of the fluorescent PcG foci in cells grown in hyperosmotic medium vastly differs from the behaviour of nuclear bodies. Whereas a typical nuclear bodies are formed/reassembled under condition of experimental crowding, we found that PcG foci reversibly disappeared. Importantly, "PcG bodies" as condensed chromatin accumulations persist. Thus, we revealed that the nature of so-called "PcG body" is in condensed chromatin that shows no dependance on polycomb BMI1 and RING1a proteins to stay condensed under (not only) molecular crowding conditions. Importantly, by using the correlative microscopy, our research was performed at the single cell level.

Key words: Polycomb group proteins, Polycomb body, BMI1 protein, nuclear architecture, interchromatin, heterochromatin, hypercondensed chromatin, post-translational chromatin modifications, correlative light-electron microscopy

2-/3-D, two-/three-dimensional

BMI1, B lymphoma Mo-MLV insertion region 1 homolog

BSA, bovine serum albumin

CBX family of proteins, chromodomain-containing proteins that are thought to mediate chromatin association by PRC1 complexes

CLEM, correlative light-electron microscopy

CSK buffer, hyperosmotic cytoskleton buffer

DAPI, 4',6-diamidino-2-phenylindole

DA/DAPI, distamycin A/DAPI

EM, electron microscopy

FISH, fluorescence *in situ* hybridization

3meK27H3/ H3K27me3, trimethylation at lysine 27 of histone H3

H3K4me3, trimethylation at lysine 4 of histone H3

Hep G2, human hepatocellular carcinoma cell line

HPC1-3 proteins, human polycomb 1-3 proteins

HPF, high-pressure freezing

HPH 1-3 protein, human polyhomeotic 1-3 protein

IC, interchromatin compartment

NGS, normal goat serum

OPT domain, Oct1/PTF/transcription domain

PC, Polycomb protein (a member of the PRC1 complex)

PcG proteins, Polycomb group proteins

PH, Polyhomeotic protein (a member of the PRC1 complex)

PML bodies /PML NBs, promyelocytic leukaemia nuclear bodies

PNC, perinucleolar compartment

PRC1(2), Polycomb repressive complex 1(2)

PRE, Polycomb response element

PSC, Posterior sex comb (a member of the PRC1 complex)

RING1/ 2 proteins, ring finger 1/ 2 proteins (members of the PRC1 complex)

Sam68 protein, Src-associated in mitosis 68 kDa protein

SCML, sex comb on midleg–like protein (a member of the PRC1 complex)

SUMO, small ubiquitin-like modifier

U-2 OS cell line, human osteosarcoma cell line

U-2 OS BMI1-GFP cells, U-2 OS cells expressing the recombinant BMI1-GFP protein

List of figures

1. Theoretical background

1.1. Nucleus and its functional organization: a major challenge for cell biology

The interphase eukaryotic nucleus is a cellular compartment consisting of various structurally and functionally different subcompartments or domains that are not separated by membranes (Taddei et al., 2004). It appears likely that the overall structural stability of the nucleus is generated by the stochastic interaction of its components (Hubner and Spector, 2010). The compartmentalization into domains is non-random and exhibits features of self-organization in space and time (Rajapakse and Groudine, 2011). Each domain has a specific function and macromolecular composition (Spector, 2001). The nuclear subcompartments play a role by offering rich microenvironments and thus support the efficient and precise coordination of diverse processes (Caudron-Herger and Rippe, 2012; Rajapakse and Groudine, 2011), including transcription, splicing, silencing, DNA repair, and replication. *Vice versa*, the morphology of nuclear subcompartments is largely determined by the activities of the nucleus (Misteli, 2000).

So far, the basic mechanisms involved in genes function have been characterized at the molecular level (Misteli, 2000). However, a consensus on basic principles of the global nuclear architecture has not been achieved (Albiez et al., 2006). A major challenge is now to uncover how replication, transcription, gene silencing, RNA processing and RNA export are organized within the space of the cell nucleus, how these processes are coordinated with each other and how nuclear architecture influences gene expression and regulation (Misteli, 2000; Misteli, 2001). A significant contribution to this field has come from cell biological approaches (Misteli, 2000), which validate many findings about the genomic organization at the single-cell level (Rouquette et al., 2010).

1.2. Organization of the genome within the cell nucleus

The structural complexity of the eukaryotic cell nucleus is important for its function to carry and read genetic information and execute the first steps of gene expression. An extremely efficient way of storing the DNA within the nucleus is its packing into chromatin (Schneider and Grosschedl, 2007). DNA is highly packed through its association with histone proteins forming 10 nm (11 nm) chromatin fibers and

further compacted into higher order structures to fit within the restricted volume of the nucleus (Eltsov et al., 2008; Amouroux et al., 2010; Fussner et al., 2011). Concernig reading and translating of genetic information, DNA has to become accessible for DNA dependent processes such as transcription, replication, DNA repair and others. Importantly, this accessibility is regulated, as not all regions of the genome are active at a given time during the cell cycle (Schneider and Grosschedl, 2007). Together, the polymorphic nature of the chromatin structure is required to allow the DNA to be used and managed while minimizing the risk of damage (Miyoshi and Sugimoto, 2008).

1.2.1. From genes to chromatin domains: three regulatory levels

To explore the problem of how the genome is organized and how it functions it is useful to discriminate three regulatory levels: the sequence level, the chromatin level and the nuclear level (van Driel et al., 2003) (see Fig. 1.1).

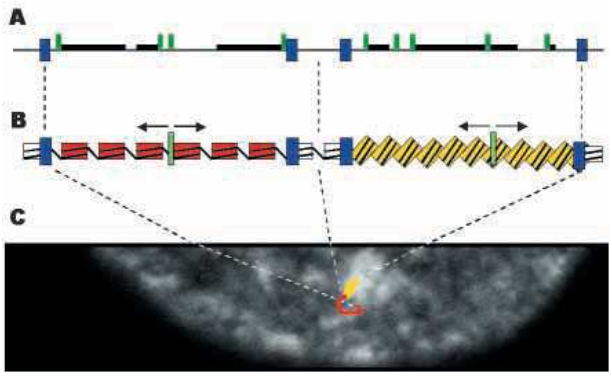

Figure 1.1. Schematic representation of the three levels in genome organization. (A) The sequence level. The black line is the DNA (fat black lines represent coding regions, thin line intergenic DNA), green bars are promoters and enhancers and blue boxes are boundary elements. (B) The chromatin level. Red, yellow and white boxes depict nucleosomes, blue boxes are boundary elements, green bars are recruitment sites for proteins that change the histone code, or otherwise induce a change in the structural and functional state of chromatin. From here the change in chromatin state may spread along the chromatin fiber, as indicated by the arrows. The red and the yellow chromatin domains are in a different state. While the chromatin with yellow nucleosomes is closed and transcriptionally inactive, the chromatin with red nucleosomes is open and transcriptionally active. (C) The nuclear level. The image shows part of a HeLa cell nucleus in which chromatin was labelled by integration of GFP-histone H2B (Verschure et al., 1999). Light areas (local high GFP-concentration) represent condensed chromatin, whereas black areas correspond to the interchromatin compartment. The red and the yellow chromatin domains depicted in B have been drawn in the image. The silenced domain (yellow) is part of condensed chromatin. The active domain (red) loops out into the interchromatin space. Adapted from van Driel et al. (2003).

1.2.1.1. The sequence level

At the lowest level of hierarchy of chromatin organization, DNA wraps around nucleosomes like a beads-on-a-string structure (Miyoshi and Sugimoto, 2008). This level is called the sequence level and is represented by the 1D organization of functional sequence elements in the genome. The level includes all coding regions, the wide variety of regulatory sequences (e.g. promoters, enhancers, silencers) that bind sequence-specific protein factors (e.g. DNA-binding transcription factors, RNA polymerases, cofactors), and sequence elements that may have a role in determining the 3D folding of the chromatin fibre (e.g. chromatin-remodeling complex) (Maniatis and Reed, 2002; van Driel et al., 2003).

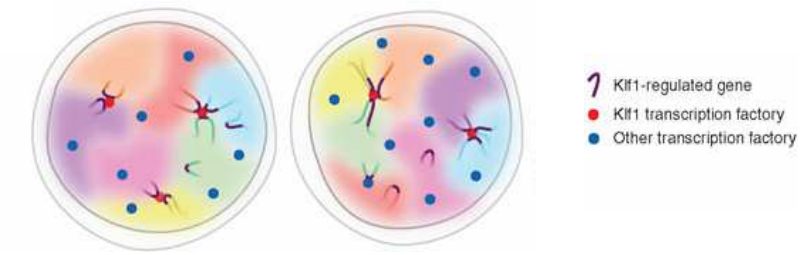

Figure 1.2. Preferential associations between co-regulated genes. Schematic representation of two cells that could represent the same cell at different times, or two cells with differing genome conformations within a population. The gene clustering is shown on the example of transcription factories. Transcription factories are depicted as blue dots; Klf1-containing transcription factories (Klf1 is a transcription factor associated with RNA polymerase II) are shown as red dots. Chromatin loops containing Klf1-regulated genes (purple segments) from the same or different chromosomes territories (colored areas) preferentially co-transcribe in the limited number of specialized Klf1-containing transcription factories. Temporarily non-transcribed alleles are positioned away from transcription factories. Interactions between transcription network members are dynamic and may change over time. Adapted from Schoenfelder et al. (2009).

The regulation at the level of the individual gene is the best-studied level. However, a fundamental question is whether the activity of genes is controlled individually or whether genes form intra-/inter-chromosomal interactions and major regulatory decisions are made at the cluster level. At least 20% of genes are present in co-regulated clusters (Spellman and Rubin, 2002; van Driel et al., 2003). There is growing evidence that many genes are clustered and co-regulated, although they are not otherwise functionally related. Clusters of functionally related genes are relatively rare (e.g. clusters of the α-globin genes, ß-globin genes, histone genes and *Hox* genes) (van Driel et al., 2003).

1.2.1.2. The chromatin level

As mentioned, the regulation of gene expression cannot be accounted for only by the information encoded in the regulatory elements contained in the linear DNA sequence. Genome-sequence data tell us how genes and regulatory sequences are organized linearly on chromosomes, but they reveal little about the spatial organization of these sequences in the cell nucleus or how spatial genome organization contributes to gene regulation (Parada and Misteli, 2002). DNA in the eukaryotic nucleus is packed into chromatin that occurs in different functional states. Fluctuation between open and closed chromatin, respectively the presence of various epigenetic marks, represents the next level, the chromatin level of gene regulation.

Traditionally, chromatin can be divided into heterochromatin and euchromatin. Heterochromatin was originally defined well before the discovery of DNA as regions of nuclei that stained intensively with basic dyes (Heitz, 1928). Heterochromatin is correlated with the transcriptionally inactive chromatin, whereas euchromatin is considered to be transcriptionally active (Schneider and Grosschedl, 2007). Actively transcribed genes, localized into euchromatin, are more loosely packaged and are easily accessible for regulatory complexes such as transcription factors, recombination and DNA repair enzymes and polymerases (Rapkin et al., 2012), while silenced genes of heterochromatin are more tightly packaged and are found associated with chromatin architectural proteins (Luger and Hansen, 2005). Today the term heterochromatin is more loosely applied and is extended to include newly observed functional differences. An important distinction is made between constitutive and facultative heterochromatin (Woodcock and Ghosh, 2010). Constitutive heterochromatin is stably compact and usually contains repetitive, gene-poor and late replicating DNA sequences, whereas facultative heterochromatin can reversibly undergo transitions from a compact, transcriptionally inactive state to become more open and transcriptionally competent (Woodcock and Ghosh, 2010). It means that facultative (facultas means opportunity) heterochromatin has the opportunity to adopt open or compact conformation depending on circumstances (Berger, 2007).

The terms constitutive or facultative heterochromatin and euchromatin refer to states of compaction and transcriptional potential rather than categories of chromatin higher-order structure *per se* (as thought initially) (Woodcock and Ghosh, 2010).

Although initially, based on data from *in vitro* studies (Bednar et al., 1998), it was expected that the silenced/closed chromatin occurs in the form of the 30 nm chromatin fiber, which is organized as a zig-zag helix and excludes activating regulatory factors (Bednar et al., 1998; Woodcock, 2006), whereas euchromatin occurs in the form of the 10 nm chromatin fibers (Derenzini, 1979; Derenzini et al., 1984; Fussner et al., 2011).

New experimental approaches, however, including chromatin conformation capture and cryo-electron microscopy, call into question the *in situ* evidence for the 30 nm chromatin fiber. New data (van Holde and Zlatanova, 1995; Eltsov et al., 2008; Ahmed et al., 2009; Fussner et al., 2011) suggest that the organization of the genome based on 10 nm chromatin fibers is sufficient to describe the complexities of nuclear organization and gene regulation. The above mentioned authors argue that the mammalian genome can be organized based on the 10 nm fiber and does not require the 30 nm fiber. The idea is that the genome is separated into distinct active and silenced compartments which arise through variations in the packing densities of 10 nm chromatin fibers, in a manner that would reflect both differentiation and cell type (Fussner et al., 2011; Rapkin et al., 2012). Thus, chromatin exists as a series of globules, which cluster together forming yet larger globules, until the final stage of clumping represents a complete chromosome territory. These studies support a model of uniform chromatin structure based on a single chromatin fiber type, which can give rise to both open and closed chromatin compartments. Whether in closed or open contexts, no change in the underlying chromatin configuration is detected (Fussner et al., 2011). This model is consistent with the observations from both cryo-EM of mitotic chromosomes (Eltsov et al., 2008) and ESI (electron spectroscopic imaging) of compact chromatin domains consisting of densely packed 10 nm fibers (Ahmed et al., 2009). Because of the fact that the thin chromatin fibers, of 10 and 30 nm diameters, are poorly contrasted *in situ* by conventional microscopy, the highest impact data come from ESI analysis, a high-contrast technique that is not reliant on heavy metal contrast agents (Ahmed et al., 2009; Ahmed et al., 2010). This technique allows to visualize nucleosomes and even linker DNA of 10 nm chromatin *in situ* (Ahmed et al., 2009). However, the big disadvantage of the presented studies is that the ESI analysis was done on chemically fixed samples.

However, the studies of chromatin exhibit further difficulties. The ability of genes to be activated is not necessarily lost when chromatin is packed into compact domains (Schneider and Grosschedl, 2007). Bickmore´s group (Gilbert et al., 2004) found a link between chromatin structure and gene density, independent of the status of gene activity. They found out that whereas open chromatin correlates with highest gene density, but not gene expression levels, compact chromatin generally has a low gene density, but can also contain active genes. Also, several other studies (Nye et al., 2002; Tumbar et al., 1999; Volpi et al., 2000) show that chromatin decondensation alone is not sufficient for transcriptional activation. This is consistent with the notion that regulation at the chromatin domain level prepares DNA for regulation at the level of individual genes, but does not necessarily transcriptionally activate them (van Driel et al., 2003).

The rapidly evolving field of epigenetics has provided possibilities to characterize functionally different types of chromatin at the molecular level (Berger, 2007; Rouquette et al., 2010). The major source of chromatin variation is the large number of post-translational modifications of histone tails and DNA (Kouzarides, 2007). Whereas DNA methylation is usually associated with more or less permanent silencing of, for example, transposons and imprinted genes, histone modifications are involved in the differential expression patterns governing cell fate decisions (Jaenisch and Bird, 2003).

Genome-wide mapping studies of histone modifications have revealed that actively transcribed chromatin regions are enriched in H3K4 mono-, di-, or tri-methylation, H3K36 trimethylation, and monomethylation of H3K9, H3K27, and H4K20 (Grandjean et al., 2001; Barski et al., 2007; Schneider and Grosschedl, 2007). In contrast to this, the methylation of H3K9 has been thought to be a mark for constitutive heterochromatin. Methylated H3K9 can be “read out” by the Heterochromatin Protein 1 (HP1), a structural component of condensed chromatin (Bannister et al., 2001; Lachner et al., 2001; Schneider and Grosschedl, 2007). Common signature of facultative heterochromatin is trimethylation of H3K27, dimethylation of H3K9, monoubiquitinylation of H2AK119 and presence of histone variant macroH2A (Trojer and Reinberg, 2007).

Furthermore, in so-called “bivalent chromatin domains” repressive marks (H3K27me3) and activating marks (H3K4me3) can coexist (Fig. 1.3) (Azuara et al.,

2006; Bernstein et al., 2006; Lee et al., 2006). Genes with bivalent domains are primed for differential expression upon differentiation (Fig. 1.4). Bivalent modifications seem to be a part of a flexible silencing system that allows the postponement of lineage choices and contribute to pluripotency until the appropriate signals are received (Pietersen et al., 2008; Pietersen and Lohuizen, 2008). The large-scale chromatin structure in embryonic stem cells and how it changes during development was examined by Ahmed et al. (2010). They used ESI analysis to follow the chromatin structural changes during the founding and loss of pluripotency that occurs in preimplantation mouse development. They found out that in one-cell embryos chromatin was extensively dispersed with no noticeable accumulation at the nuclear envelope. Major changes were observed from one-cell to two-cell stage embryos, where chromatin became confined to discrete blocks of compaction and with an increased concentration at the nuclear envelope. In eight-cell embryos and pluripotent epiblast cells, chromatin was primarily distributed as an extended meshwork of uncompacted fibres and was indistinguishable from chromatin organization in embryonic stem cells. In contrast, lineage-committed trophectoderm and primitive endoderm cells, and the stem cell lines derived from these tissues, displayed higher levels of chromatin compaction (Ahmed et al., 2010).

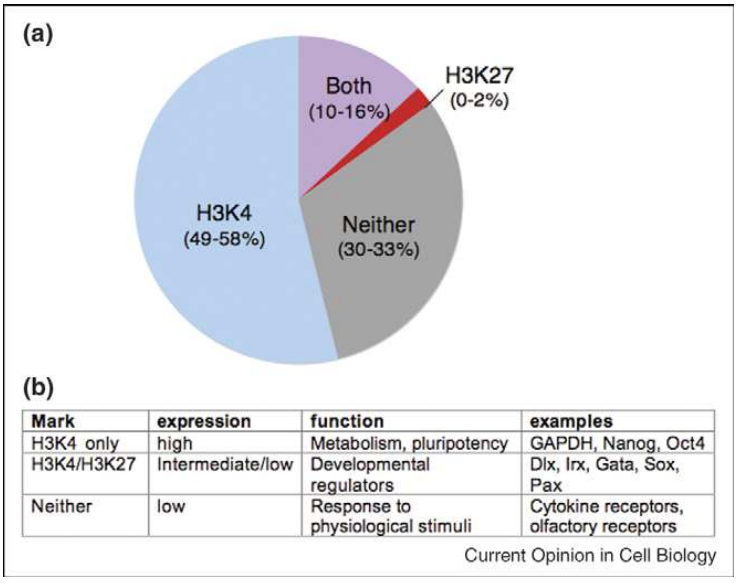

(b)

Mark	expression	function	examples
H3K4 only	high	Metabolism, pluripotency	GAPDH, Nanog, Oct4
H3K4/H3K27	Intermediate/low	Developmental regulators	Dlx, Irx, Gata, Sox, Pax
Neither	low	Response to physiological stimuli	Cytokine receptors, olfactory receptors

Current Opinion in Cell Biology

Figure 1.3. Bivalent domains in human ES cells. (a) Distribution of H3K4me3 and H3K27me3. The percentage of genes that was marked by trimethylation of H3K4 (blue), H3K27 (red), both (purple) or neither (grey), based on two studies (Pan et al., 2007; Zhao et al., 2007) in human ES cells. (b) Functionally distinct groups based on histone modifications. Genes classified by the presence or absence of H3K4me3 and H3K27me3 are associated with different expression levels and gene

function in both human and mouse ES cells (Mikkelsen et al., 2007; Pan et al., 2007; Zhao et al., 2007). Adapted form Pietersen and Lohuizen (2008). Abbrev.: pluripotent embryonic stem (ES) cells, mouse embryonic fibroblasts (MEFs), mouse neural precursor cells (NPCs).

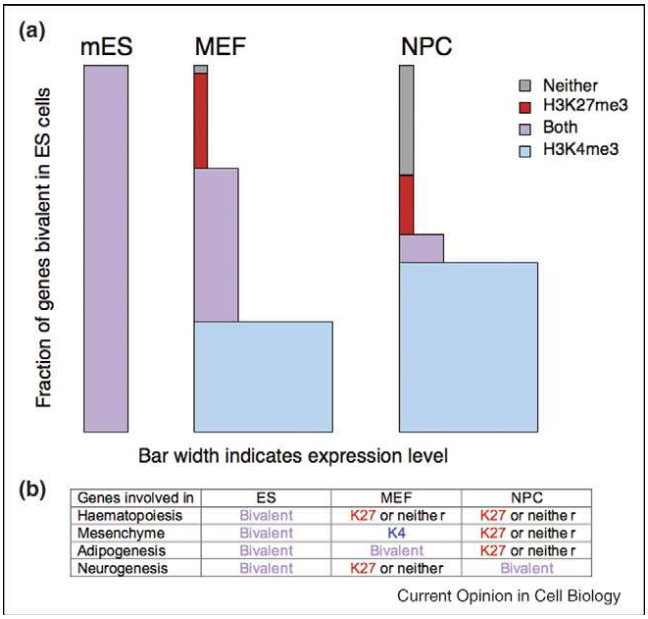

Figure 1.4. The fate of bivalent domains during differentiation. (a) Resolution of bivalent domains in MEFs and NPC. About 22% of CpG-rich promoters are bivalently marked in mouse ES cells. These bivalent domains (purple) have an intermediate expression. In MEFs, 43% of regions remain bivalent, which may be related to their less differentiated state. In more committed NPCs, approximately half of the bivalent domains in ES cells become marked by H3K4me, the other half remains to be bivalent and the rest resolves into domains containing only H3K27me3 or losing both marks. Based on Mikkelsen et al. (2007). Adapted from Pietersen and Lohuizen (2008).

Studing chromatin modifications, Bas van Steensel (van Steensel et al., 2001; Filion and van Steensel, 2010; van Steensel, 2011; preview in Schubeler, 2010) found out that the division of chromatin into open euchromatin and compacted heterochromatin is an oversimplified and outdated, and could be even incorrect. Based on data from DamID technique applied on *Drosophila* genome, they came up with the new division of the chromatin into five types. They maped a set of 53 proteins, representing a cross-section of the known functional classes of chromatin components as well as several histone marks (van Steensel et al., 2001; Filion and van Steensel, 2010). Integrative analysis of these maps revealed that much of the binding profiles is explained by five distinct chromatin types, which are each made up of unique combinations of proteins. While some proteins mark only one of these chromatin types, many proteins are shared by two to four types. Because the Greek

word chroma means "colour", they named the five chromatin states by the colours YELLOW, RED, BLUE, BLACK and GREEN. Most transcriptionally active genes the authors assigned to YELLOW or RED chromatin. YELLOW chromatin contains active genes with components of transcription machinery and enzymes that control histone acetylation. RED chromatin also harbours active genes, however, in contrast to YELLOW chromatin, which has a strong preference for ubiquitously expressed housekeeping genes, RED chromatin marks primarily genes that are tissue specific. Moreover, RED chromatin does not exhibit the histone mark H3K36me3. The absence of H3K36me3 is surprising, because it is thought to be a general mark of transcription elongation. Another specific feature of RED chromatin is its great diversity of proteins. Little is known about BLUE chromatin that is characterized by the presence of Polycomb proteins and the histone mark H3K27me3 (Filion and van Steensel, 2010). About 50% of the genome is BLACK chromatin. BLACK chromatin is enriched in inactive tissue-specific genes and specific marks such as the linker histone H1 and Lamin, the main component of the nuclear lamina. Interestingly, no histone modification has been identified in BLACK chromatin. GREEN chromatin is specifically marked by heterochromatin protein HP1 and the histone modifications H3K9me2 and H3K9me3 (van Steensel, 2011). It is traditionally called as "heterochromatin," the transcriptionally inactive chromatin. Steensel´s group assumed that the GREEN chromatin rather represents a neutral alternative.

Although, the authors criticize the traditionally used terms "euchromatin" and "heterochromatin", they do not want to generalize the results obtained from *Drosophila*, and *vice versa*, they highlight the necessity to compare the presence of the five chromatin types across species. They are aware of the fact that during evolution, some proteins and histone marks have adopted new functions and localization within the nucleus. For example, in *Drosophila*, lamin B is primarily associated with nuclear lamina, or BLACK chromatin, whereas H3K9me2 is located in GREEN chromatin. In contrast, in mouse and human cells, both, H3K9me2 and lamin B1 binding patterns are localized to BLACK chromatin (Peric-Hupkes et al., 2010). These data also point to a direct role of the nuclear lamina in gene repression.

Together, the regulation of gene expression at the histone code level creates a regulatory system that switches chromatin between different functional states.

Combinations of chromatin modifications might constitute an epigenetic code that defines the condensation state of chromatin and the transcriptional state of genes (Turner, 2007); Thus, one genome can be translated into the many epigenomes (Jenuwein and Allis, 2001).

1.2.1.3. / 1.3. The nuclear level: nuclear domains

In order to understand the control mechanisms of gene expression *in vivo*, it will be essential to uncover how genomes are spatially and temporally organized. This is the reason why the study of gene expression is rapidly evolving. Rather than analysing in detail the molecular mechanisms involved in regulation of genes, nowadays, the focus in the genome era is on the global understanding of the genome within the context of the entire nucleus (Parada and Misteli, 2002). Thus, the third studied regulation level is the nuclear level - the organization of the eukaryotic genome into topologically independent domains (Mishra and Karch, 1999).

1.2.1.3.1. / 1.3.1. Chromatin compartment

During interphase, individual chromosomes reside in distinct regions known as chromosome territories (Boveri, 1909; Stack et al., 1977; Mao et al., 2011). Extensive studies on chromosome territories, including gene densities, radial arrangement of chromosome territories, their changes during differentiation or distance between homologous chromosomes, were done by Cremer´s group (Kreth et al., 2004; Stadler et al., 2004; Heride et al., 2010). Although, chromosome territories are relatively compact regions, they do not have rigid boundaries and their organization is plastic (Fraser and Bickmore, 2007). There is some intermingling of chromatin from different chromosomes (Visser et al., 2000) and chromosomal stretches that are strongly decondensed can loop out and intrude into other chromosome territories (Volpi et al., 2000; Mahy et al., 2002). Interchromosomal interactions among looped genes are also termed “chromosome-kissing” (Schneider and Grosschedl, 2007). Chromatin loops carrying specific clusters of genes can expand up to several micrometers away from the surface of their home chromosome territory (Volpi et al., 2000; Mahy et al., 2002; Rouquette et al., 2010). The looping the chromosomal stretches out from the chromosomal territory allows colocalization of the widely separated genes in the nuclear space (Rouquette et al., 2010). Although, it is yet unclear whether gene looping is the primary mechanism for colocalization of

distant loci or whether a higher order rearrangement of chromatin mediates the interaction (Strickfaden et al., 2010).

Some studies probed deeper into the substructure of chromosome territories to analyse subchromosomal domains (Fraser and Bickmore, 2007). Subchromosomal domains are functionally specialized areas associated with active or silent gene regions. The activity of domains can be defined in molecular terms by the presence of specific post-translational histone modifications (Shneider and Grosschedl, 2007). Electron microscopy results indicate that the irregularly shaped well-visualized condensed chromatin domains measure from 100 to 800 nm or sometimes even more. Assuming that an average condensed chromatin domain is a sphere with a diameter of 300 nm and the nucleosome concentration of 200 μM (Langowski and Heermann, 2007), such domain could contain several Mb of DNA (Fakan and van Driel, 2007). However, human transcriptome map shows that chromosomes contain many domains that are highly enriched in genes, whereas other domains are gene-poor (Caron et al., 2001). Generally, it is believed that the eukaryotic genome is organized in 5-200 kb domains, however, highly expressed genes tend to reside in smaller domains of 4-13 kb (Gasser and Laemmli, 1987; Mishra and Karch, 1999).

1.3.2. Interchromatin compartment

Although much of the nuclear space is taken up by chromatin of varying degrees of condensation, a significant part of the nuclei (41.7% for endothelial cells, including nuclear space occupied by nucleoli) is left to the interchromatin space (interchromatin compartment, IC) (Verschure et al., 1999; Visser et al., 2000; Verschure et al., 2002; Albiez et al., 2006; Rouquette et al., 2009). Although, in some cell types even inverse volume occupation was found; e.g. in hepatic cells the IC fills 66.2% of the nuclear volume, including nuclear space with nucleoli (Rouquette et al., 2010).

The IC constitutes a highly convoluted set of channels and lacunae, which allow diffusion of macromolecular components through the nucleus (Politz et al., 1999). It occurs around the periphery and inside chromosome territories (Visser et al., 2000). Clearly, the current view is that the chromatin territories have a spongelike architecture with the IC meandering into them (Schneider and Grosscheld, 2007). This meshwork configuration of chromatin was revealed by electron microscopy studies using BrdU to observe individual chromatin territories (Visser et al., 2000)

and by ESI analysis (Dehghani et al., 2005). A mesh of chromatin fibers would permit the free diffusion of enzymatic (e.g. transcription) machineries into the interior of chromatin territories (Albiez et al., 2006). However, it is considered that genes to be active would need to become exposed to interchromatin channels (Cremer et al., 1993; Cremer and Cremer, 2006). In support of this concept, actively transcribed genes lie at the surface of chromatin bulks (Kurz et al., 1996; Rouquette et al., 2010). Although, it has not been conclusively determined whether the transcriptional activity of a gene is the cause or the consequence of, or is independent of, its location within a chromosome territory or within the three-dimensional nuclear space (Hubner and Spector, 2010).

Thus, the IC consists of the regions that are free of DNA and the regions that contain loops of decondensed chromatin. To make difference between these regions, some scientists apply also the term "perichromatin region." This concept was originally established, based on results from electron microscopy observations, by Monneron and Bernhard (1969). Later, the perichromatin region was defined as a narrow border zone of decondensed chromatin at the surface of higher-order chromatin domains. Its width has been estimated to be about 100-200 nm, according to the length of chromatin fibers looping out from the chromosome territory (Fakan and van Driel, 2007). The perichromatin region represents a functionally important nuclear compartment, where DNA and RNA synthesis, as well as co-transcriptional splicing take place (Fakan, 2004). Moreover, Cmarko et al. (2003) have presented evidence that Polycomb-silenced loci are located in the same perichromatin area. The perichromatin region is directly exposed to the IC and therefore is likely to be well accesible to factors and machineries. However, recent reports analyzing the accesibility of large molecular complexes to interphase condensed chromatin (Verschure et al., 2003) or even to mitotic chromatin (Chen et al., 2005) demonstrate that this phenomenon may not play an essential role in determining the functional domains in the nucleus (Fakan and van Driel, 2007). Structurally, the perichromatin region is rich in fibrogranular material, where dispersed chromatin cannot be morphologically distinguished from ribonucleoprotein perichromatin fibrils (Bouchet-Marquis et al., 2006; Fakan and van Driel, 2007). Perichromatin fibrils are considered to be the primary products of transcription (Monneron and Bernhard, 1969) and perichromatin granules are RNA and hnRNP core protein containing component (Smetana et al., 1979; Fakan and van Driel, 2007).

1.3.2.1. Interchromatin subcompartments

Interchromatin space occupies almost half of the available nuclear volume and harbors important nuclear subcompartments and soluble components involved in DNA metabolism. Interchromatin subcompartments consist of nuclear proteins and ribonucleoprotein particles and have characteristic size, shape and composition (Richter et al., 2007). The structure of some of these subcompartments, notably nucleoli, replication foci and transcription factories, relates to their dedicated activity. Thus, the typical organization of nucleoli into fibrillar centers, fibrillar components and granular components expresses distinct processes in the formation of ribosomal subunits (Hernandez-Verdun, 2006). The structural integrity of other entities, such as speckles, Cajal bodies and PML bodies, appears less determined by productive activity (Albiez et al., 2006). Generally, interchromatin subcompartments could be devided into nuclear factories, speckles and bodies.

1.3.2.1.1. Transcription factory

Actively transcribed genes localized at focal concentrations of RNA polymerases and transcription factors are called "transcription factories." Because the number of expressed genes seems to be higher than the number of discrete factories, it is suggested that multiple genes share the same factory (Fraser and Bickmore, 2007). Genes are dynamically recruited to transcription factories (not *vice versa*), and they can move in and out of these sites, resulting in activation or decreasing of their transcription (Osborne et al., 2004). According to the "transcription factory" model, RNA polymerase complexes, and transcription factors cluster and form a “cloud” of up to 20 DNA loops around the transcription factory (Cook, 1999; Faro-Trindade and Cook 2006). The polymerase would be an immobile component of the factory, and DNA loops would appear and disappear as polymerases initiate, elongate, and terminate transcription (Bartlett et al., 2006). When released after termination, a gene would still be near a factory and still carry the active histone modifications that could keep it in an open state, leading to efficient re-initiation (Bartlett et al., 2006). In agreement with this concept, domains of decondensed and recently transcribed chromatin carry histone marks that are associated with active transcription (Muller et al., 2007; Schneider and Grosschedl, 2007). The transcription factory measures 80 nm in diameter (Jackson et al., 1998) and can colocalize even widely separated active genes (Osborne et al., 2004). Studies aiming at visualizing the sites of RNA

synthesis by electron microscopy identified the perichromatin fibrils to be associated with different transcription components (Fakan et al., 1984; Cmarko et al., 1999).

1.3.2.1.2. Splicing factor compartment

A large volume of interchromatin space is occupied by a compartment termed splicing factor compartments (SFCs or speckles) (Spector, 1993; Misteli and Spector, 1998). Speckles occupy approximately 20% of total nuclear volume and were originally defined on the basis of the presence of high concentrations of pre-mRNA splicing factors (Beck, 1961; Spector, 1990; Spector et al., 1991; Misteli, 2000). In addition to pre-mRNA splicing factors and snRNAs, speckles also contain transcription factors (Larsson et al., 1995; Mortillaro et al., 1996; Zeng et al., 1997), 3′-processing factors (Krause et al., 1994; Schul et al., 1998b) and ribosomal proteins (Mintz et al., 1999). By electron microscopy, SFCs correspond to two morphologically distinct structures: the central regions consist of clusters of 20 nm granules, the so-called interchromatin granule clusters; and the peripheral regions are perichromatin fibrils, which are believed to represent nascent transcripts (Fakan, 1994).

1.3.2.1.3. Nuclear bodies

A nuclear body is a prominent interchromatin structure that is morphologically distinct from its surroundings when observed by transmission electron microscopy (Matera, 1999). It constitutes a well-distinguished nuclear domain with specialized functional significance (Spector, 2006). This excludes structures that are only detected upon over-expression of tagged nuclear proteins and that most likely result from non-physiological aggregation of excess protein (Matera, 1999; Spector, 2006). Moreover, nuclear bodies have a non-random positioning relative to specific nuclear regions (Schneider and Grosscheld, 2007). Concerning composition, a nuclear body is primarily of a proteinaceous or ribonucleoproteinaceous nature (Carmo-Fonseca et al., 2010), but some nuclear bodies are also associated with chromatin (genes). Physical contacts of 10 nm chromatin fibres with the protein-based core of the nuclear body (PML NBs) was observed by electron spectroscopic imaging (Dellaire et al., 2006).

Functionally, by concentrating proteins and RNAs required for specific biological processes, nuclear bodies can serve as reaction sites to efficiently facilitate these

processes (Fig. 1.5A) or hubs to regulate the expression of recruited gene loci (Fig. 1.5B). They can also function as modification sites to recycle and modify RNAs and proteins (Fig. 1.5C). Notably, one nuclear body is very likely to combine different themes to execute diverse functions and accommodate different processes at the same time (reviewed in Mao et al., 2011).

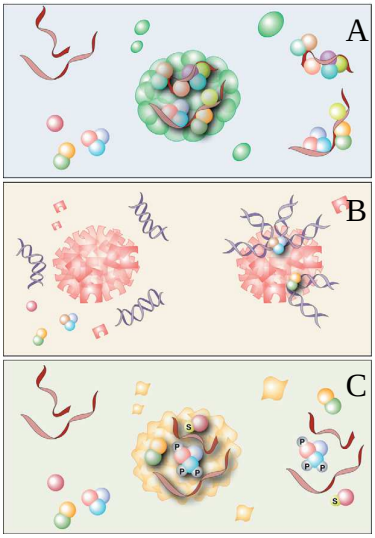

Figure 1.5. Different mechanisms of nuclear bodies function. Although, many nuclear bodies combine multiple mechanisms to perform their diverse cellular functions. (A) Reaction site. Nuclear bodies can concentrate the substrates and enzymes in a confined volume, thereby enhancing the specificity and efficiency of biological reactions. (B) Hub. Nuclear bodies can act as hot spots to activate or repress gene expression by recruiting gene loci. (C) Modification site. Nuclear bodies can recycle proteins and RNAs. Adapted from Mao et al. (2011).

On the basis of their structure observed at the electron microscopic level, nuclear bodies have been classified as either simple or complex (Bouteille et al., 1974). The simple nuclear bodies are small (0.2–0.5 µm), round, compact and finely fibrillar, whereas the complex nuclear bodies are larger (0.2–1.2 µm), heterogeneous in shape and texture, and enveloped by a peripheral capsule, which gives them a doughnut-shaped appearance (reviewed in Carmo-Fonseca et al., 2010).

The most prominent nuclear body is a nucleolus. A nucleolus emerges from the congregation of multiple tandem repeats of ribosomal DNA from several different chromosomes (Raska et al., 2006). It is the site of ribosomal RNA (rRNA) transcription by RNA polymerase I, posttranscriptional processing of the rRNA, and assembly of ribosomal subunits (Raska et al., 1995; Raska et al., 2004; Raska et al., 2006; Boisvert et al., 2007; Kalmarova et al., 2007). Moreover, several lines of

evidence now show that the nucleolus has also numerous non-ribosomal functions (reviewed in Pederson, 1998; Raska et al., 2006; Cmarko et al., 2008). The characteristic composition of the nucleolus has been already mentioned in other place (see Interchromatin subcompartments).

In addition to the nucleolus, a growing family of small nuclear bodies, often referred to as foci because of their appearance by fluorescence microscopy, is present in nuclei (Matera, 1999). The two best-characterized nuclear bodies, the PML body (promyelocytic leukemia body; Gorisch et al., 2004; Bernardi and Pandolfi, 2007) and the Cajal body (Raska et al., 1990; Schul et al., 1996), are both thought to form in response to transcriptional activity of genes (Misteli, 2000). The nuclear bodies that have been less well studied compared with other well-characterized structures in the nucleus are termed "orphan nuclear bodies" (Carmo-Fonseca et al., 2010).

1.3.2.1.3.1. Orphan nuclear bodies

This group of bodies includes the clastosome, the cleavage body, the OPT domain, the SUMO body, the Sam68 body, and also the Polycomb (PcG) body (Carmo-Fonseca et al., 2010; see Tab 1.1).

Table 1.1. Orphan nuclear bodies. Adapted from Carmo-Fonseca et al. (2010)

Nuclear body	*Description*	*Number per cell*	*Diameter*	*Reference*
Clastosome	Concentrates the proteosomal 20 S and 19 S complexes, and ubiquitin conjugates. Detected predominantly when the activity of proteasome is stimulated (for degradation of short-lived regulatory proteins, misfolded or aggregated proteins), disassembles upon proteosomal inhibition.	0-3	0.2-1.2 µm	Lafarga et al. 2002
SUMO body	Enriched in SUMO-1 and SUMO-conjugating enzyme Ubc9. Concentrates transcription factors pCREB, CBP, c-Jun.	1-3	1.0-3.0 µm	Navascue´s et al. 2007
PcG body	Enriched in Polycomb proteins: RING1, BMI1, HPC. It is suggested to be a site of gene silencing.	12-16	0.3-1.0 µm	Buchenau et al. 1998; Saurin et al. 1998
OPT domain	Enriched in transcription factors Oct1 and PTF. Partial colocalization with transcription sites. Disassembles upon transcription inhibition.	1-3	1.0-1.5 µm	Pombo et al. 1998
Cleavage body	Enriched in cleveage factors. Detected predominantly during S phase, is not affected by transcription inhibition.	1-4	0.2-1.0 µm	Li et al. 2006

In our work, we were interested in PcG bodies that are thought to be formed by accumulation of Polycomb group (PcG) proteins.

1.4. Polycomb group proteins

PcG proteins are important epigenetic factors that regulate gene expression by chromatin modification (Martin-Perez et al., 2010). They act as histone-code ″readers″ and ″writers″ and are essential for establishing cell identity. PcG proteins were first identifed in *Drosophila* (Lewis, 1978), where they are responsible for maintaining homeotic gene activity in the appropriate segments during fly development (Martin-Perez et al., 2010). Polycomb proteins are so named because of mutations that affect the patterning of the male sex combs (to poly-combs) in *Drosophila* (Maertens et al., 2009). Although, PcG proteins are the best known for regulation of HOX gene expression during embryogenesis (Liang and Biggin, 1998), they also repress the genes whose products are implicated in cellular processes like cell cycle control, senescence, X-chromosome inactivation, cell fate decision, and stem cell differentiation (Plath et al., 2004; Sparmann and van Lohuizen, 2006; Villa et al., 2007; Boukarabila et al., 2009).

Polycomb proteins repress the transcription of their target genes through the assembly on key regulatory DNA elements (Tuckfield et al., 2002; Sawarkar and Paro, 2010; Hodgson and Brock, 2011). In *Drosophila*, most of the genes regulated by PcG proteins contain consensus sequences called Polycomb response elements (PREs) (Zink and Paro, 1989; Horard et al., 2000; Martin-Perez et al., 2010; see Fig. 1.8). However, although some specific regions in the human genome have been shown to have a similar function than PREs, a general DNA sequence specific for Polycomb binding in mammals has not been identified (Martin-Perez et al., 2010).

PcG proteins execute their repressive function in at least two distinct multiprotein complexes: the Polycomb repressive complex 1 (PRC1) and the Polycomb repressive complex 2 (PRC2; in mammals also known as the Eed-Ezh2 complex) (Martinez and Cavalli, 2006; Enderle et al., 2011). PRC2 is thought to be involved in the initiation of gene silencing by methylation of histone H3 at lysine 27 (H3K27) (Cao et al., 2002; Czermin et al, 2002; Trojer and Reinberg, 2007), whereas PRC1 is implicated in stable maintenance of the repressed state of the genes (Lund and van Lohuizen, 2004; Ringrose and Paro, 2004; see Fig. 1.6). Recently, some scientists have postulated even the existence of PRC3 and PRC4 (Kuzmichev et al., 2004;

Kuzmichev et al., 2005). PRC3 and PRC4 complexes possess histone lysine methyltransferase activity and are considered to be the variants of the PRC2 complex (Kuzmichev et al., 2005). The maintenance complex, PRC1, binds to the H3K27 trimethylation and catalyses the monoubiquitination at K119 of histone H2A that triggers a compaction of the chromatin into a heterochromatin state (Wang et al., 2004; Cao et al., 2005; in Martin-Perez et al., 2010). Thus, PRC1 and PRC2 make changes at chromatin level (Francis et al., 2004) that result to gene silencing (Simon and Kingston, 2009; see Fig. 1.6).

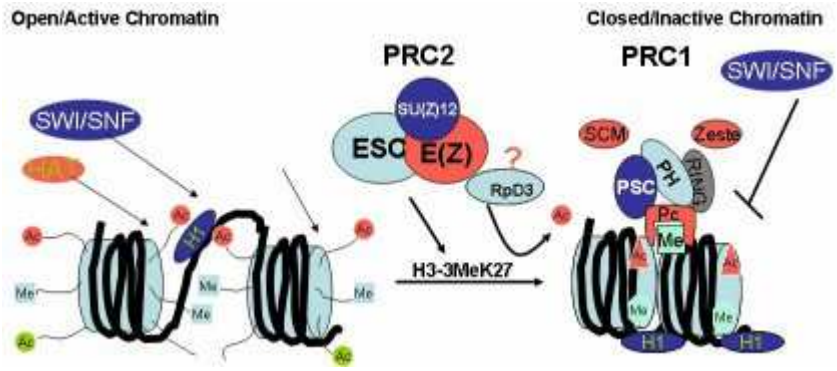

Figure 1.6. PcG-mediated gene silencing. PRC1 and PRC2 complexes suppress an active chromatin environment into silent chromatin structure. Adapted from Aggarwal (AbCam pages). PRC2 complexes trimethylate the Lys27 residue of H3 (a blue rectangle with Me inside) and induce a silenced state of the chromatin at the target locus. This mark is recognized by the PRC1 complex that triggers the compaction of chromatin. Chromatin suppression & structural integrity; by Bhagwan D. Aggarwal; http://www.abcam.com/index.html?pageconfig=resource&rid=10189&pid=5

These epigenetic modifications of histone proteins and chromatin conformational changes seem to be the main way by which PcG proteins mediate gene silencing (Otte and Kwaks, 2003). Although, the only evidence of PcG-mediated chromatin compaction comes from *in vitro* studies where condensation has been addressed by measuring the compaction of nucleosomal fibers in electron microscope (Francis et al., 2004; Cheutin and Cavalli, 2012). Simultaneously, PcG proteins can block the binding of ATP-dependent chromatin remodeling complex (e.g. SWI/SNF) (Otte and Kwaks, 2003; see Fig. 1.6) and transcriptional machinery association (Stock et al., 2007).

Concerning composition, the PRC2 complex has three core components, including histone methyltransferase EZH2 (Cao et al., 2002; Czermin et al, 2002). PRC1 consists of proteins such as HPC, HPH, RING1-2, SCML and BMI1 (Levine et al., 2004). See Fig. 1.7 that is adapted from (Otte and Kwaks, 2003).

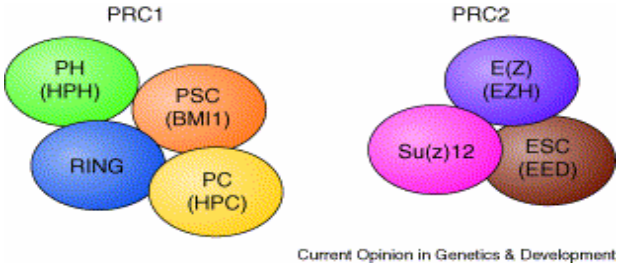

Figure 1.7. Core components of PRC1 and PRC2. The *Drosophila* components are indicated, with their human homologs in parenthesis. PRC1 comprises the PcG proteins PC (Polycomb), PH (Polyhomeotic), PSC (Posterior sex comb) and RING (Ring finger). The respective human homologs are HPC, HPH, BMI1 and RING. PRC2 comprises E(Z), Su(z)12 and ESC, their respective human homologs being EZH, Su(z)12 and EED. Adapted from Otte and Kwaks (2003).

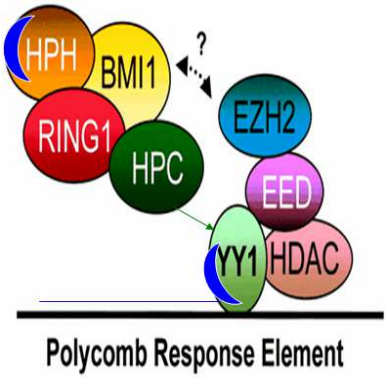

Figure 1.8. Importance of RNA for the binding of PcG complexes to DNA (e.g. Rinn et al., 2007; Yap et al., 2010). (RNA is depicted in blue line; RNA binding domains on proteins are drawn as blue moon-like objects). Adapted from Ekstrom lab (www.bch.msu.edu/faculty/ekstrom.htm) and modified.

However, the composition of PRC complexes, especially in mammals, is variable and dynamic (Gunster et al., 2001). The patterns of expression of the complexes depend mainly on the differentiated status of the cell (Kuzmichev et al., 2005; Martin-Perez et al., 2010; see Fig. 1.9). PRC1 is even more heterogeneous than PRC2 (Maertens et al., 2009).

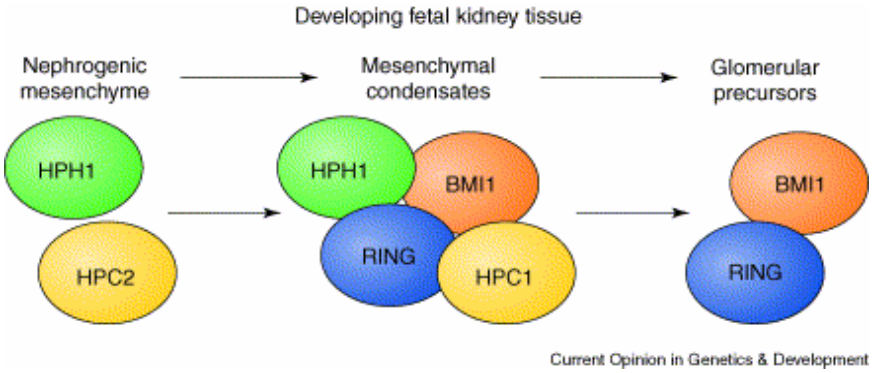

Figure 1.9. Expression pattern of PRC1 core components during the development of the fetal kidney. Nephrogenic mesenchyme cells develop through mesenchymal condensates to become glomerular precursor cells. In nephrogeneic mesenchymal cells BMI expression is repressed but is activated later on in the mesenchymal condensate and glomerular precursor cells along with RING1 (reviewed in Otte and Kwaks, 2003). Adapted from Otte and Kwaks (2003).

Moreover, in mammalian cells, the situation is complicated by the presence of multiple orthologs of the archetypal PRC1 proteins (Maertens et al., 2009). With five PC proteins (CBX2, CBX4, CBX6, CBX7 and CBX8), six PSC proteins (BMI1, MEL18, MBLR, NSPC1, RNF159 and RNF3), three PH proteins (HPH1, HPH2 and HPH3) and two SCE proteins (RING1 and RING2) there is enormous scope for combinatorial diversity (Gil and Peters, 2006; Whitcomb et al., 2007). The reasons for such diversification and the interplay between the different family members remain unclear (reviewed in Maertens et al., 2009).

Concerning nuclear level, PcG proteins are usually distributed diffusely in the nucleus. However, core components of PRC1 are also found in intensely fluorescent foci, whether imaged using GFP fusion proteins or conventional immunofluorescence, with a high accumulation of PcG proteins termed Polycomb (PcG) bodies (Gunster et al., 1997; Satijn et al., 1997; Schoorlemmer et al., 1997; Buchenau et al., 1998; Saurin et al., 1998).
Besides mammalian cells, PcG bodies have been described in cells of a number of other species including *Drosophila* and *C. elegans* (Buchenau et al., 1998; Zhang et al., 2006).

1.5. Polycomb (PcG) bodies

Polycomb bodies are considered to arise from accumulations of PcG proteins. The expression levels of PcG proteins vastly differ in human cell lines (for a review see Otte and Kwaks, 2003). Reflecting the expression level, PcG bodies are conspicuous in human osteosarcoma U-2 OS cells where their relative sizes differ from 0.2 to 1.5 μm and their number varies between six and fourteen per nucleus (Satijn et al., 1997; Saurin et al., 1998). According to immuno-FISH data and karyotype analysis, these variations in expression also apparently result from karyotypic differences between cell lines (Voncken et al., 1999). In addition, nuclear positioning of PcG bodies is not completely random as the bodies appear to be preferentially associated with some loci on particular mitotic chromosomes (Saurin et al., 1998; Voncken et al., 1999). In interphase nucleus, PcG bodies are found in DAPI poor euchromatic regions (Cheutin and Cavalli, 2012). There are no observable colocalizations between PcG bodies and Cajal bodies, gemini of Cajal bodies and possibly also PML bodies (Saurin et al., 1998). PcG bodies thus appear to be unrelated to any other known nuclear body and are thought to represent a genuine structure within the nucleus.

Functionally, PcG bodies are considered to be the hubs for gene repression. However, the number of PcG bodies is too small to encounter for the high number of genetic loci targeted by PcG proteins (Carmo-Fonseca et al., 2010). This implies that multiple gene targets are associated with each Polycomb body or that gene silencing by PcG proteins can occur outside Polycomb bodies (Carmo-Fonseca et al., 2010). Nowadays, clear evidence exists that PcG bodies can recruit multiple target gene loci to stabilize their interactions and subsequently co-regulate their expression (Bantignies et al., 2011; Mao et al., 2011). Because of genes pairing and their co-regulation, PcG bodies are in various PcG body models also compared to transcription factories (Bantignies et al., 2011) and they were termed as gene silencing factories (Bantignies et al., 2011; Hodgson and Brock, 2011). It is assumed that whereas transcription factories cluster actively transcribing genes, in the same way PcG bodies cluster genes to be silenced (Bantignies et al., 2011; Hodgson and Brock, 2011). However, in contrast to transcription factories, which clearly mediate gene expression, it is not known whether PcG bodies contribute to gene silencing directly through their components of PcG repressive complexes or indirectly by

positioning their target genes into heterochromatin domains (Hodgson and Brock, 2011).

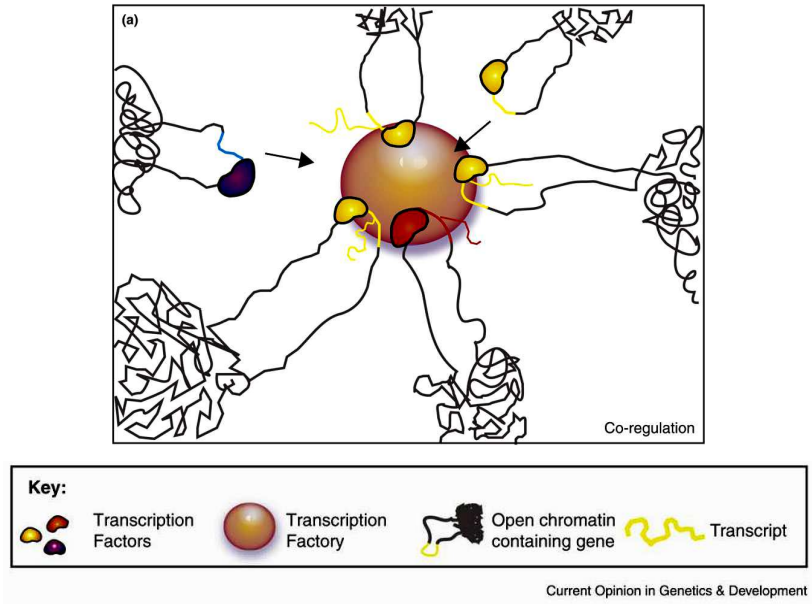

Figure 1.10. Co-regulated genes cluster in a specialized factory. Here, co-regulation is shown on the example of transcription factory. Adapted from Schoenfelder et al. (2010). Genes are dynamically recruited to transcription factories, and they can move in and out of these sites, resulting in activation or decreasing of their transcription (Osborne et al. 2004). However, the nature of factory is in focal concentrations of RNA polymerases and transcription factors (a purple-brown ball).

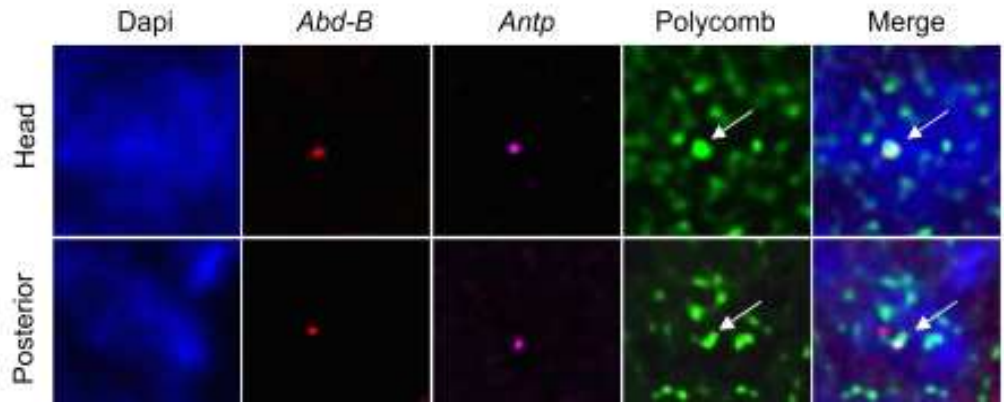

Figure 1.11. A representative example of co-localization of repressed genes in PcG bodies. The Abd-B and the Antp gene (two clusters of Hox genes in *Drosophila*) rarely colocalized in the thoracic parasegments and in the posterior parasegments, with colocalization rates of 4% and 7.6%, respectively. In contrast, the association between the loci was stronger (18%) in cells in anterior regions of the embryo or larval head tissues where both genes are silenced and localized into PcG body. Adapted from Bantignies et al. (2011).

The genes appear to cluster at PcG bodies by a mechanism that requires non-coding RNAs (Simon and Kingston, 2009). It was shown that the RNA interference machinery associated with the PcG body cleaves dsRNA to produce siRNA, which is proposed to participate in stabilizing the genes pairing and maintenance of gene silencing (Grimaud et al., 2006; Mao et al., 2011).

Taken together, PcG body is considered to be mostly a ribonucleoproteinous structure, an accumulation of PcG proteins and non-coding RNAs, localized into interchromatin compartment where genes are looped into such a nuclear body to be co-silenced. Because of its size and unrelation to any other nuclear structure, it is considered to be a novel nuclear body.

2. The aims of the work

The polycomb group (PcG) proteins play a primordial role in gene silencing accompanied by chromatin condensation. The aim of this thesis was to expand the knowledge on the structural basis of the Polycomb-mediated gene silencing. Specifically, we focused our endeavour on the so-called PcG bodies.

The PcG bodies were described by fluorescence microscopy 15 years ago as a novel kind of nuclear bodies situated in the nuclear interchromatin compartment. Interestingly enough, nuclear bodies are defined via their distinct ultrastructure, but no electron microscopy description of these bodies has been provided to date. Because of the missing information on the PcG body architecture, a number of different hypothetical models, how a PcG body looks like and how gene silencing could occur, were generated.

The aim of the first study was **to established the fine structure of the PcG body**. To be able to achieve the aim, we were forced to use the correlative light-electron microscopy applied on the U-2 OS cell line expressing recombinant BMI1-GFP protein. U-2 OS cells, that contain a number of well distinct PcG bodies at the fluorescence level, represents a mammalian model cell line to study PcG proteins and silencing.

The aim of the second study was **to follow the fate of PcG bodies** within the frame of the experimental model of **molecular crowding** that leads to chromatin condensation. We focused on the compaction of chromatin encompassed in PcG bodies and the behavior of PcG proteins under conditions of molecular crowding.

3. Material and Methods

3.1. Cell cultures

U-2 OS (human osteosarcoma) cell line, U-2 OS cell line stably expressing BMI1-GFP and Hep G2 (human hepatocellular carcinoma) cell line were cultured in Dulbeco´s modified Eagle´s medium (DMEM; GIBCO) supplemented with 10% fetal bovine serum (GIBCO) and 1% *penicillin*/*streptomycin* sulfate (PAA Laboratories) under normal conditions.

3.2. Correlation of live cell imaging and immunofluorescence

U-2 OS BMI1-GFP cells (kindly provided by Dr. Maarten van Lohuizen, Amsterdam) grown on the gridded Petri dish were imaged for PcG bodies using a confocal microscope Leica TCS SP5 with 40×/1.25 NA oil immersion objective. After acquiring a Z-series of cells with a distinct, point-like GFP signal, the cells were fixed with 4% formaldehyde in 0.2 mM PIPES (pH 7.2) for 10 minutes, permeabilized with 0.3% TritonX-100 for 5 minutes and washed several times in PBS. Nonspecific sites were blocked with 5% normal goat serum (NGS; Sigma) in PBS. The cells were incubated with mouse anti-BMI1 (1:300, Clone F6, Upstate) and rabbit anti-GFP (1:300, Abcam) antibodies in 1% (w/v) BSA in PBS containing 0.5% Tween20 for 1 hour, then washed and incubated with secondary goat anti-mouse and goat anti-rabbit antibodies conjugated with TRITC or FITC (Jackson ImmunoResearch Laboratories) in PBS for 45 minutes. DNA was counterstained with DAPI (4',6-diamidino-2-phenylindole, Sigma). Gridded Petri dishes were then mounted using a Polyvinyl alcohol mounting medium with DABCO (BioChemika, Fluka). Immunofluorescence images were taken with the Leica TCS SP5 confocal microscope. Non-transfected U-2 OS cells were processed for immunofluorescence in the same way as transfected cells.

3.3. Correlation of "PcG bodies" fluorescence with DA/DAPI staining and DNA immunocytochemistry

For staining of the U-2 OS BMI1-GFP cells with DAPI (Sigma) in combination with distamycin A-HCl (Chemos), the cells were fixed with 4% formaldehyde in 0.2 mM PIPES (pH 7.2) for 10 minutes, permeabilized with 0.3% TritonX-100 for 5 minutes and washed several times in PBS. Then the cells were counterstained with DA/DAPI

according to protocol of Schweizer and Ambros (1994). Briefly, the cells were incubated in 0.2 mg/ml distamycin A-HCl for 15 minutes, rinsed in McIlvaine`s buffer (pH 7.0), counterstained with 0.2 µg/ml DAPI for 15 minutes and rinsed again.

Concerning the DNA detection, live cell images of U-2 OS BMI1-GFP cells were taken and correlated with the immunocytochemical images of GFP (anti-GFP antibody, Abcam) and DNA (anti-DNA antibody, Progen) taken after 2% formaldehyde in PBS (pH 7.2) fixation for 10 minutes and permeabilization with an increasing concentrations of TritonX-100 (from 0.3% up to 2% TritonX-100) for 5 minutes and several washes in PBS. In the immunocytochemical approach, the cells were incubated with diluted mouse monoclonal anti-DNA (1:30) and rabbit polyclonal anti-GFP (1:300) in 1% (w/v) BSA in PBS containing 0.5% Tween20 for 2 hours, washed and incubated with secondary goat anti-mouse and goat anti-rabbit antibodies conjugated with cy5 or TRITC (Jackson ImmunoResearch Laboratories) in PBS for 90 minutes. The results with the 2% concentration of TritonX-100 provided an evidence that there is an increased density of DNA in the nuclear regions/domains that contain PcG bodies.

In both approaches, the coverslips were then mounted using a Polyvinyl alcohol mounting medium with DABCO. The cells were imaged using a confocal microscope Leica TCS SP5 with 63×/1.4 NA oil immersion objective.

3.4. High-pressure freezing (HPF) and freeze substitution

U-2 OS cells were grown on 1.4 mm sapphire discs (Leica Microsystems) in Petri dishes. Only a single sapphire disc was placed in a given Petri dish. Samples were then dipped into cryofiller, 20% BSA (Sigma) in CO_2 independent medium supplemented with L-glutamin (GIBCO, Invitrogen) and the addition of 10% FCS (GIBCO), transferred into the rapid loader under a stereomicroscope and frozen. For the high-pressure freezing (HPF) the Leica EM PACT2 with the rapid transfer system (Leica EM RTS) was used.

Frozen samples were then processed using a freeze substitution apparatus (Leica EM AFS2) equipped with an automatic processor (Leica EM FSP). As a freeze substitution medium, 0.1% uranyl acetate (10% stock solution in methanol) in aceton (EM grade, Polysciences) was used. Cells were freeze substituted at -90°C for 48

hours. Thereafter, the temperature was raised to -50°C (5°C per hour). The samples were then kept in the freeze substitution medium for 24 hours. After freeze substitution, the cells were washed with acetone and gradually infiltrated with increasing concentrations of Lowicryl HM20 monostep (Electron Microscopy Sciences) in acetone (2h with 25% HM20, 3h with 50% HM20, 3h with 75% HM20, 4h with 100% HM20, 8 h with 100% HM20). During all steps of substitution, washing and infiltration the automatic processor agitated the samples using a syringe. Lowicryl used for low temperature embedding was bubbled with a stream of dry nitrogen to remove oxygen, which can interfere with the polymerization process. Polymerization was performed at -50°C for 26 hours and followed by gradual warming to 20°C over a 14 hour period (with a slope 5°C/h). Final hardening process of resin blocks was performed at 20°C for 24 hours. The polymerization ran under a UV lamp (a component of the Leica EM FSP).

3.4.1. Correlative light-electron microscopy (CLEM) on high-pressure frozen cells

U-2 OS cells expressing BMI1-GFP were grown on sapphire discs in Petri dishes. A sapphire disc was placed into a gold-coated live cell carrier (1.5 mm in diameter, 140 µm deep; Leica Microsystems) with the cells facing up. On top of this system, a molybdenum finder grid (1.48 mm; Leica Microsystems) was clamped. Such a sandwich was flipped over and transferred into a Fluorodish (World Precision Instruments, Inc.) with CO_2-independent medium containing 10% FCS. After acquiring a Z series using the inverted Leica TCS SP5 confocal microscope using a long working distance, 63×/1.3 NA glycerol immersion objective, the sandwich was frozen. Frozen samples were processed in the freeze substitution apparatus with the mounted automatic processor according to the protocol described above.

Step	T_{Start}	T_{End}	Slope	Time	Reagent	%	Transfer	Agit.	UV	P
01	-90	-90	0	26:00	FS med	100%	stay	on		
02	-90	-50	5	08:00	FS med	100%	stay	on		
03	-50	-50	0	25:00	FS med	100%	exch/fill	on		
04	-50	-50	0	00:02	Acetone	100%	exch/fill	on		
05	-50	-50	0	00:02	Acetone	100%	exch/fill	on		
06	-50	-50	0	03:00	HM20	25%	mix	on		
07	-50	-50	0	04:00	HM20	50%	mix	on		
08	-50	-50	0	06:00	HM20	75%	mix	on		
09	-50	-50	0	04:00	HM20	100%	exch/fill	on		
10	-50	-50	0	09:00	HM20	100%	exch/fill	on		
11	-50	-50	0	26:00	HM20	100%	stay	off	X	
12	-50	20	5	14:00	HM20	100%	stay	off	X	
13	20	20	0	24:00	HM20	100%	stay	off	X	X

Tab.3.1. Freeze substitution protocol for the apparatus Leica EM AFS2 with the mounted automatic processor Leica EM FSP. The same protocol can be used for any freeze substitution apparatus. Freeze substitution running in an apparatus without the automatic processor should be agitated manually (with the syringe or the transfer pipette), the process should be paused at the end of impregnation and the cover must be changed for the UV lamp. Our protocol for the automatic processor was first published in Brown et al. (2009) where we are acknowledged. Abbrev: T (temperature in °C), FS med (freeze substitution medium): 0,1% uranyl acetate (from 10% methanol stock) in acetone, HM20 (embedding medium Lowicryl HM20), exch/fill (exchange/fill), Agit. (agitation), P (pause).

3.4.1.1. Retracting and sectioning

Polymerized blocks were then removed from the plastic flow through rings (accessories for the AFS2, Leica). To release the carrier from the block, the residual resin was trimmed, and the blocks were dipped into liquid nitrogen and attached to a 40°C razor blade. Blocks prepared for CLEM experiments had the cells on the surface and the finder grid deeper. A pyramid was made to only leave the quadrant in which the cell of the interest was located as described by Verkade (2008). Serial ultrathin sections (70 nm) cut with Leica Ultracut S ultramicrotome were collected on nickel slot grids coated with formvar-carbon film. Ultrathin resin sections not further stained with heavy metal salts were then viewed with a FEI Tecnai G2 Sphera electron microscope.

3.4.1.2. Immunolabeling on resin sections

With respect to on-section immunolabeling, the BMI1 monoclonal antibody was purchased from Upstate (Millipore), TRITC-conjugated and 15 nm gold-conjugated secondary antibodies from Aurion and 18 nm gold-conjugated antibody from

Jackson ImmunoResearch. NGS pretreated sections were incubated for 1h at room temperature with a primary antibody (diluted at 1:35) in PBS with 2% BSA and 0.5% Tween 20 (Sigma). After a second treatment with 5% NGS, 15 nm gold-conjugated secondary antibodies (goat anti-mouse) diluted in 1.2% BSA in PBS (1:3, Aurion or 1:10, Jackson ImmunoResearch) were reacted with sections for 45 minutes at room temperature. For immunofluorescence on resin sections with the TRITC-conjugated goat anti-mouse secondary antibody (diluted 1:100), the same protocol was used.

The quantitative evaluation of the density of the post-embedding immunogold labeling in heterochromatin was estimated by comparing the outside, with respect to the inside, of the "PcG bodies" in thin sectioned cells by counting the number of gold particles per unit area of heterochromatin. In the case of the "PcG body" domain, attention was paid that the evaluated heterochromatin area in thin section is a part of the "PcG body", as judged from its immunofluorescence image. For the chosen heterochromatin domains outside of the "PcG body", attention was paid to only include the heterochromatin area distant from any "PcG body" identified by fluorescence microscopy. The ratio of these two estimates gave us information about how much of the immunogold labeling was found per heterochromatin area outside the "PcG body" compared to heterochromatin inside the "PcG body." Statistical measurements were obtained by averaging these ratios over six sectioned "PcG bodies."

In all control immunocytochemical experiments, the primary antibodies were omitted resulting in negligible background signals.

3.5. Correlative light-electron microscopy on chemically fixed cells

For all CLEM approaches using chemical fixation, the U-2 OS cells stably expressing BMI1-GFP were grown either on CELLocate coverslips (Eppendorf) or on gridded Petri dishes (MatTek Corporation). Before electron microscopy procedure (prior fixation if not mentioned otherwise), Z series from the inverted confocal microscope (Leica TCS SP5) were obtained.

After the EM embedding procedure, a pyramid was made to only leave the small area with the cells of the interest. 70 nm sections were then cut and collected on formvar carbon coated nickel slot grids. The sections were counterstained using 3.7% uranyl acetate for 15 minutes and lead citrate (Reynolds, 1963) for 2 minutes. The

ultrastructural images were recorded with a FEI Tecnai G2 Sphera or Zeiss EM 900 electron microscopes.

3.5.1. CLEM with pre-embedding labeling procedure

For pre-embedding labeling, the cells were first fixed with the 2% formaldehyde in 0.2M PIPES (pH 7.2) for 15 minutes and permeabilized with 0.1% TritonX-100 in PBS for 10 minutes. Prior to antibody incubation, the cells were blocked with 5% NGS in PBS for 30 minutes. The BMI1 monoclonal antibody (diluted 1:50 in BSA/PBS/Tween 20) was followed by the goat anti-mouse ultrasmall gold conjugate (diluted 1:50 in 1%BSA/PBS). After the immunogold labeling the cells were washed and postfixed with 2.5% glutaraldehyde in PBS. Finally, several important washing steps with distilled water were performed and the cells were incubated with Aurion R-Gent Silver Enhancement Kit (equal parts of the developer, enhancer and gum arabic mixed just before applying) for 23 minutes. The cells were again washed extensively with distilled water, dehydrated in increasing concentrations of ethanol (30%, 50%, 70%, 90% and 100%) and flat embeded into Araldite, Embed 812 (Epon-812) (Electron Microscopy Sciences).

3.5.2. CLEM with pre-embedding labeling of cells extracted prior fixation

U-2 OS BMI1-GFP cells were permeabilized in CSK buffer (100mM NaCl, 300mM sucrose, 3mM $MgCl_2$ and 10Mm PIPES; pH 6.8) with 0.1% TritonX-100 for 10 minutes (Martini et al., 1998). Then the cells were fixed with 2% formaldehyde in CSK for 30 minutes at RT and the CELLocate coverslip was transferred (face down) into a fluorodish with PBS. After acquiring serial confocal sections, the cells were processed for EM, sectioned and viewed as in the previous pre-embedding approach.

3.6. Induction of chromatin hypercondensation

Macromolecular crowding was induced by supplying the live cells with a dilution of 1.6 M sucrose, sorbitol or NaCl in growth medium to yield the 320 mOsm or 640 mOsm concentration of used hyper-osmotic agents. To study the reversibility of this phenomenon the cells were incubated in their physiological medium (290mOsm). The influence of the hyperosmotic media on the ultrastructure of cells was studied by Richter et al. (2007).

3.7. Correlation of live cell imaging before and after hyperosmotic treatment with immunofluorescence

U-2 OS BMI1-GFP cells grown on the glass bottom gridded Petri dish (MatTek Corporation´s) were imaged for PcG bodies under a confocal microscope Leica TCS SP5 accessorized with large size temperature incubator with CO_2 controller and using 63× plan-apochromat 1.4 NA oil immersion objective. After acquiring Z-series, the cells were incubated in hyperosmotic medium (for from 10 minutes to 2 hours) and imaged for fluorescence again. Then the cells were fixed with 4% formaldehyde in 0.2 mM PIPES (pH 7.2) for 10 minutes, permeabilized with 0.3% TritonX-100 for 5 minutes and washed several times in PBS. Nonspecific sites were blocked with 5% normal goat serum (NGS; Sigma) in PBS. The cells were incubated with mouse anti-BMI1 (1:300, Clone F6, Upstate), rabbit anti-GFP (1:300, Abcam), rabbit anti-3meK27H3 (1:350, Millipore) and mouse anti-DNA (IgM; 1:30, Progen) antibodies in 1% (w/v) BSA in PBS containing 0.5% Tween20 for 1-2 hours, then washed and incubated with secondary goat anti-mouse goat anti-rabbit antibodies conjugated with TRITC or FITC (Jackson ImmunoResearch Laboratories) in PBS for 45 minutes. Gridded Petri dishes were then mounted using a Polyvinyl alcohol mounting medium with DABCO (BioChemika, Fluka). Individual fluorescence signals were detected by sequential excitation to avoid possible cross-talks.

3.8. Applying of a live cell DNA marker DRAQ5

DRAQ5 (Biostatus Limited) was added to the live cells grown on the glass bottom gridded Petri dish in DMEM at a 5 µM final concentration according to the supplier´s protocol. Cells were incubated in DRAQ5 medium for 30 minutes, then immunolabeled and imaged under the confocal microscope as described before.

3.9. Western blot analysis

Cells, which were grown to confluence, were scraped into 1x Laemmli sample lysis buffer (60 mM Tris-HCl, 2% SDS, 10% glycerol) containing the Protease Inhibitor Cocktail Set III, EDTA-free (Calbiochem). Lysed cells were sheared by passing the solution through a 27 G needle.Then lysates were boiled and cleared by centrifugation. Protein concentrations in supernatants were determined using the bicinchoninic assay kit (Sigma). Lysates were supplemented with 5% ß-mercaptoethanol and 0.01% bromophenol blue, and equal amounts of total proteins

(20-80 µg) was loaded into 8-12% polyacrylamide gels. Proteins were separated by SDS–PAGE (at 180 volts constant) and electrotransferred onto nitrocellulose membranes (at 100 volts) (Protran).

After blocking in 5% non-fat milk (Biorad), the membranes were incubated at room temperature for 2-3 hours with affinity-purified primary antibodies (mouse BMI1 (1:300, clone F6, Upstate); rabbit RING1a (1:1000, AbCam); rabbit Akt and rabbit P-Akt (1:1000, Cell Signaling). Antigen-antibody complexes were labeled using secondary antibodies coupled with horseradish peroxidase (Biorad) that were diluted according to the manufacturer´s instructions. Horseradish peroxidase activity was visualized by chemiluminiscence (ECL detection kit, Pierce Chemical Co.) and captured onto X-ray films (Foma).

3.9.1. *In vitro* phosphatase treatment

Lyzates for phosphatase treatment were prepared according a protocol published by Noguchi et al. (2002): Cells were scraped into 1x NEB3 buffer (BioLabs) supplemented with 0.6% SDS and Protease Inhibitor Cocktail Set III, EDTA-free (Calbiochem). The cells were lysed for 15 minutes on ice and then boiled for 5 minutes. Lysates were passed throught a 27 G needle ten times and finally diluted with four volumes of NEB3 buffer. Protein concentrations were measured.

Seventy units of Calf Intestinal Alkaline Phosphatase (CIAP; Promega) were added to 350 µl of lyzate and incubated for dephosphorylation at 37°C for 1 hour. In a half-time of the incubation fresh CIAP was added. CIAP reaction was terminated by adding 25 µl of 4x Laemmli sample lysis buffer (Noguchi et al., 2002) and by heat.

Sample loading, ELFO and immunoblotting was performed in the same way as written before (see Western blot analysis).

4. Results

4.1. Paper I

Fine structure of the "PcG body" in human U-2 OS cells established by correlative light-electron microscopy.

Šmigová J, Juda P, Cmarko D, Raška I.

Nucleus. 2011 May-Jun;2(3):219-28. doi: 10.4161/nucl.2.3.15737.

Abstract

Polycomb group (PcG) proteins of the Polycomb repressive complex 1 (PRC1) are found to be diffusely distributed in nuclei of cells from various species. However they can also be localized in intensely fluorescent foci, whether imaged using GFP fusions to proteins of PRC1 complex, or by conventional immunofluorescence microscopy. Such foci are termed PcG bodies, and are believed to be situated in the nuclear intechromatin compartment. However, an ultrastructural description of the PcG body has not been reported to date. To establish the ultrastructure of PcG bodies in human U-2 OS cells stably expressing recombinant polycomb BMI1-GFP protein, we used correlative light-electron microscopy (CLEM) implemented with high-pressure freezing, cryosubstitution and on-section labeling of BMI1 protein with immunogold. This approach allowed us to clearly identify fluorescent PcG bodies, not as distinct nuclear bodies, but as nuclear domains enriched in separated heterochromatin fascicles. Importantly, high-pressure freezing and cryosubstitution allowed for a high and clear-cut immunogold BMI1 labeling of heterochromatin structures throughout the nucleus. The density of immunogold labeled BMI1 in the heterochromatin fascicles corresponding to fluorescent "PcG bodies" did not differ from the density of labeling of heterochromatin fascicles outside of the "PcG bodies". Accordingly, an appearance of the fluorescent "PcG bodies" seems to reflect a local accumulation of the labeled heterochromatin structures in the investigated cells. The results of this study should allow expansion of the knowledge about the biological relevance of the "PcG bodies" in human cells.

Results I

All presented experiments were performed with the U-2 OS cell line since these cells contain a number of distinct PcG bodies, already studied in several reports (Saurin et al., 1998; Voncken et al., 1999; Hernandez-Munoz et al., 2005). U-2 OS cells stably expressing BMI1-GFP fusion protein (Hernandez-Munoz et al., 2005) furthermore allowed us to link the live cell imaging of the localization of BMI1-GFP with imaging, at the ultrastructural level, of immunolabeled ultrathin sections. It should be, however, mentioned that prior applying the CLEM technique, we tried to identify PcG bodies in non-transfected U-2 OS cells via post-embedding immunogold labeling procedures. Even though we were able to achieve a clean immunogold signal in heterochromatin (Fig. 4.S1), we failed to identify distinct PcG bodies.

4.1.1. Correlation of live cell imaging and immunofluorescence

With the transfected U-2 OS cells, we correlated BMI1-GFP fluorescent signals (Fig. 4.1A) with signals from the same cells which were immediately fixed and immunolabeled (Fig. 4.1B). Within the resolution limit of light microscopy, we did not observe any major difference between fluorescence patterns generated by the two approaches (Fig. 4.1). At the same time, we compared patterns of BMI1 immunolabeling in both normal (non-transfected) U-2 OS cells and stably transfected U-2 OS BMI1-GFP cells. The two patterns were comparable and in agreement with their previous description (e.g. ref. Hernandez-Munoz et al., 2005). Except for an absence of an intranucleolar signal in most cells, the nuclear fluorescence consisted of the overall weaker nucleoplasmic signal together with several bright PcG foci/bodies of various size. The PcG bodies were often situated in a close proximity to nucleoli. Individual cells exhibited differences both concerning the number and size of PcG foci. These results from light microscopy were in agreement with the results of previous studies (Saurin et al., 1998; Hernandez-Munoz et al., 2005).

4.1.2. PcG foci represent DNA-rich structures

We wanted to know whether there is an increased density of DNA in the nuclear regions/domains that contain PcG bodies. Concerning DNA detection, there is a known cytogenetic problem due to the probe (e.g. DAPI, antibodies) penetration/epitope accessibility within compacted chromatin structures.

To overcome this problem, we first imaged GFP in fixed and permeabilized cells and then used the established counterstaining with DAPI in combination with distamycin A (DA/DAPI staining) (Schweizer and Ambros, 1994; Voncken et al., 1999). A co-localization of the PcG bodies with an increased DAPI signal in the regions of the PcG bodies was observed (Fig. 4.1C). Our results on the co-localization of PcG bodies with the DA/DAPI stained areas are in agreement with those of Voncken et al (1999).

Alternatively, we first visualized PcG bodies in live U2-OS BMI-GFP cells, and, after fixation, we permeabilized the cells with increasing concentrations of TritonX-100 up to 2% followed by immunocytochemistry using antibodies to GFP and DNA. The 2% detergent concentration allowed for a convenient co-localization of the PcG bodies with an increased DNA density in the regions of the PcG bodies (Fig. 4.1D).

Taken together, we were able to show that there is an increased density of DNA in the nuclear domains that contain PcG bodies.

Figure 4.1 (See next page). Correlation of live cell imaging and fluorescence immunocytochemistry, and correlation of "PcG bodies" fluorescence with DA/DAPI staining and DNA immunofluorescence. (**A_1**) U-2 OS BMI1-GFP cells were imaged *in vivo* in gridded Petri dishes. Live cell images are shown consecutively: localization of the cells in phase contrast, with the chosen cell of the interest being delineated in the rectangle (overview phase), differential interference contrast microscopy of the cell of interest (DIC), and Z-projection of fluorescence of GFP-tagged BMI1protein in the same cell (*in vivo* GFP). (**A_2**) Subsequently, the cells were aldehyde fixed, permeabilized and immunolabeled with antibodies. Maximum intensity projections of BMI1 (BMI1) and GFP (GFP) signals are shown. DNA was counterstained with DAPI (DAPI, middle confocal section). The *in vivo* fluorescence signal of the PcG bodies matches well both the BMI1 and GFP immunofluorescence signals. (**B**) Counterstaining of the fixed and permeabilized U-2 OS BMI1-GFP cells with DAPI in combination with distamycin A (DA/DAPI) to show the co-localization of increased DNA density with the PcG bodies identified with a anti-GFP antibody (GFP). The highest intensities of DA/DAPI fluorescence on maximum intensity projection co-localized with the fluorescence of the PcG bodies (white arrows). (**C**) Live cell imaging of the PcG bodies (*in vivo* GFP) was, after weak fixation accompanied by the use of 2% Triton X-100 treatment, correlated with the GFP (GFP) and DNA (DNA) immunocytochemistry images. The anti-DNA labeling revealed a high accumulation of DNA in the PcG bodies (white arrows).

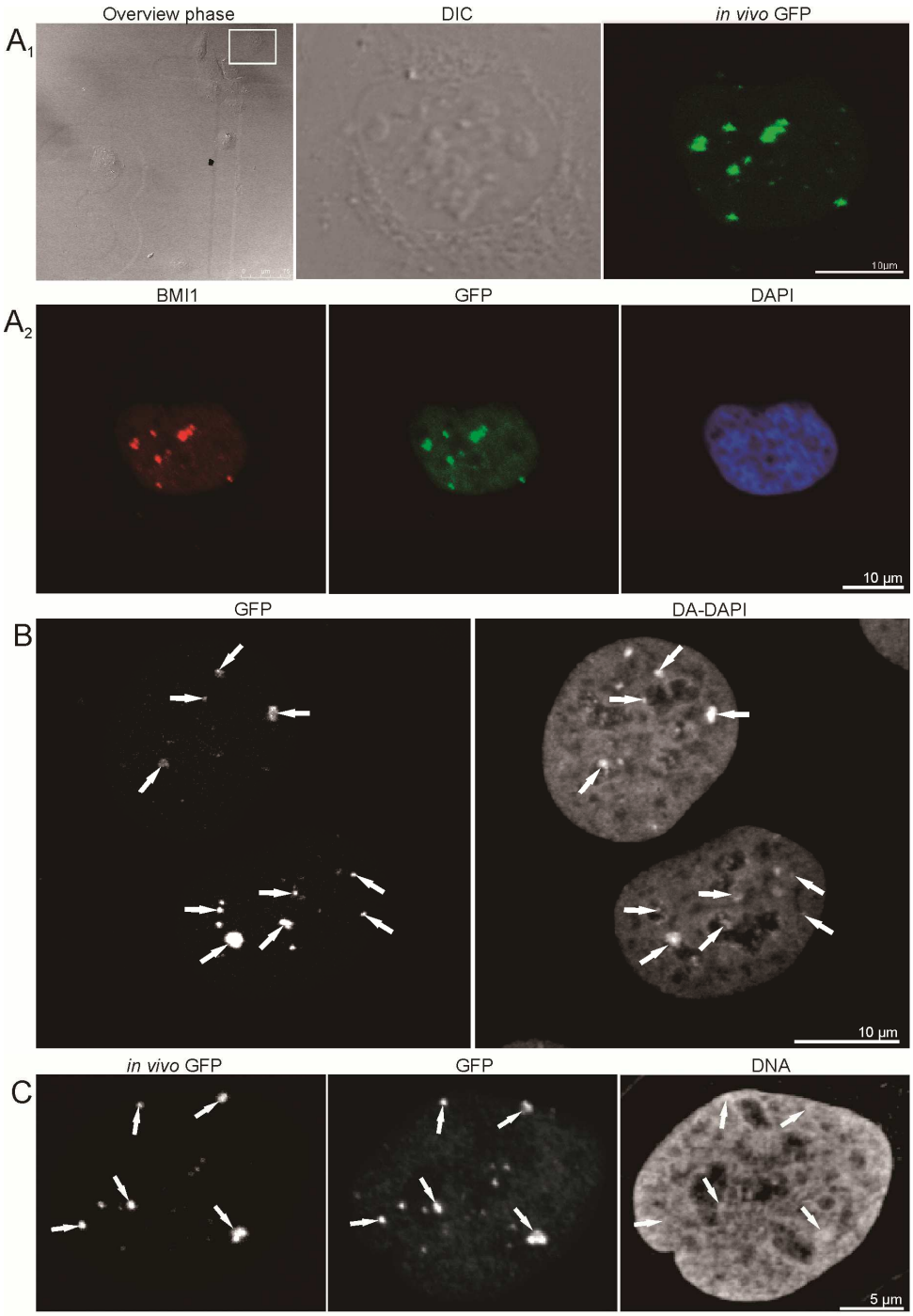

4.1.3. PcG foci correspond to chromatin domains rather than to nuclear bodies

To achieve structural preservation of the PcG bodies and high efficiency of the post-embedding immunocytochemistry we performed, together with CLEM, high-pressure freezing and cryosubstitution of transfected U-2 OS cells (Figs. 4.2, 4.3).

Using this approach, the ultrastructure of the cells was well preserved (Figs. 4.2D, 4.3A, 4.S2). Thin sectioned cells exhibited well delineated electron-dense heterochromatin structures in the form of heterochromatin fascicles termed also

large-scale chromatin fibres (Hu et al., 2009). In addition, they frequently exhibited nuclear envelope invaginations seen in their longitudinal or transverse sections (Figs. 4.2, 4.3, black arrows and black arrowheads), this phenomena is typical for cultured, transformed cells (Fricker et al., 1997). The immunogold BMI1 label was specifically enriched within heterochromatin fascicles throughout the nucleus (Figs. 4.2D, 4.3A; see also Fig. 4.S2) and appeared sometimes to line the heterochromatin borders (insert in Fig. 4.3A). In contrast, the label in the IC and nucleoli (see insert in Fig. 4.2D) was much lower, and was basically missing in the cytoplasm. With respect to the IC label, the gold particles were preferentially found in the vicinity of heterochromatin structures. The nucleolar label was usually found in intranucleolar heterochromatin clumps (insert in Fig. 4.2D); the nucleoli are known to exhibit such heterochromatin structures (e.g. refs. Raska et al., 1983a, b).

Such a clear-cut immunogold signal thus does not necessitate any quantitative evaluation, and is of primary importance within the frame of this study. But it has to be mentioned that we were not able to achieve, in contrast to immunofluorescence light microscopy of fixed, non-embedded cells (Fig 4.1B), a convenient post-embedding on-section labeling with several antibodies to GFP. This illustrates a well known fact that the antibodies convenient for the fluorescence microscopy of fixed cells are frequently not useful for the detection of their respective targets in on-section labeling of resin embedded cells.

Figure 4.2 (See next page). CLEM of high pressure frozen and cryosubstituted cells (the images of the same cell are also shown in Fig. 4.3; however, Fig. 4.3 encompasses different thin sections and documents images of a different "PcG body" in this same cell). U-2 OS BMI1-GFP cells grown on the sapphire discs were clamped in the live cell carrier with the finder grid and imaged face down. After live cell imaging the cells were high-pressure frozen, cryosubstituted and immunolabeled with anti-BMI1 antibody. In fluorescence and EM images in Figs. 4.2 and 4.3, the white and yellow arrows point to a nuclear region/domain corresponding to the two GFP "PcG bodies." Invaginations of the nuclear envelope are designated by black arrows and arrowheads. (**A**) An overview image (merge of fluorescence and phase contrast) to determine the quadrant of interest on the finder grid, (**B**) higher magnification of the quadrant with the cells of interest delineated in the rectangle. ($\mathbf{B_1}$) Phase contrast and ($\mathbf{B_2}$) maximum intensity projection of fluorescence of the cells from the rectangle. (**C**) The same two thin sectioned cells seen in the electron microscope. Some of the serial thin sections we also processed for on-section fluorescence immunocytochemistry (see inserts in Figs. 4.3B, 4.3C as well as Figs. 4.S3-4.S5 in the Supplementary Material). (**D**) Anti-BMI1 immunogold labeling on ultrathin sections (15 nm gold particles). The electron-dense heterochromatin structures (he) are specifically

enriched in the BMI1 immunogold label while the cytoplasm (cy) rich in ribosomes is devoid of the label. The nucleolus (nu) in the insert of **D** shows two BMI1 labeled intranucleolar heterochromatin clumps (white arrowheads). The white arrow points to a nuclear region/domain that correlates with (a section of) the "PcG body" fluorescence seen in **B_2**, with the local accumulation of heterochromatin structures in this domain.

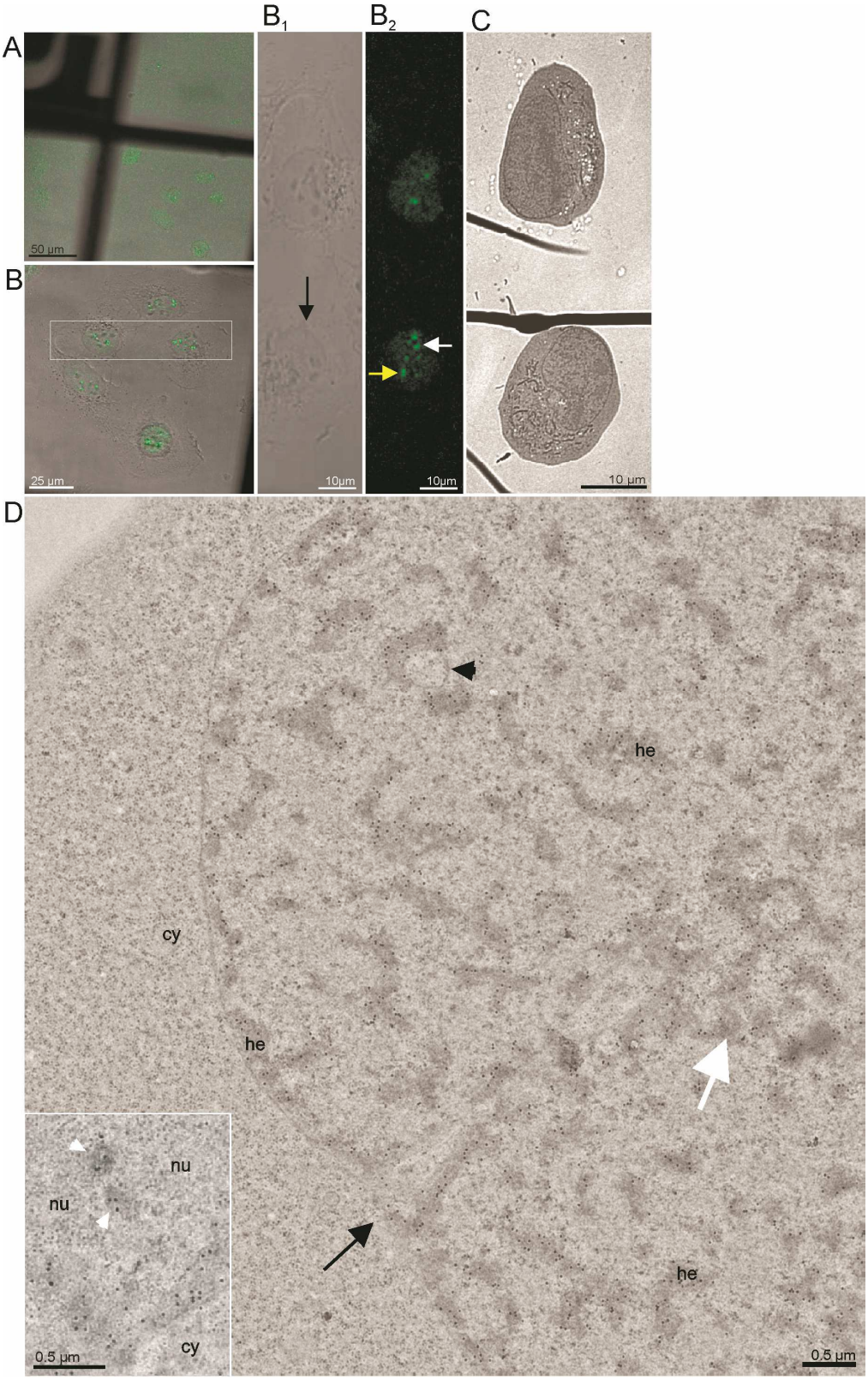

To identify the PcG bodies *per se* we correlated the snapshots (Z series) from live cell imaging with electron microscopy images. Because of the very small thickness of thin sections, we had to analyze serial sections in order to identify the EM area that fit well with the PcG body fluorescence signal (Fig. 4.2; for on-section immunofluorescence of the BMI1 signal see inserts in Figs. 4.3B, 4.3C). We never observed a nuclear region/domain with a locally increased immunogold label present outside of the heterochromatin structures. However, importantly, we found that there was a higher local accumulation of heterochromatin fascicles in the nuclear region/domain corresponding to the PcG body fluorescence signal (white and yellow arrows in Figs. 4.2, 4.3; for a more detailed description of the analysis concerning the "PcG body" identification see Figs. 4.S3-4.S5) as compared to other nuclear domains seen in the thin sections. Accordingly, we cannot use the term "nuclear body" for the description of such a nuclear domain. Also, we cannot exactly draw a line delimiting a "PcG body" in thin sectioned nuclei as it is impossible to establish which part of a given heterochromatin fascicle still does, or does not, belong to the "PcG body" that is defined through its fluorescence signal. "PcG bodies" were frequenly associated with the nuclear envelope, together with its invaginations (black arrows and arrowheads in Figs. 4.2, 4.3), and with nucleoli. In this respect, the vicinity of the nuclear envelope and the nucleoli are well known to be enriched in heterochromatin that is termed perinuclear and perinucleolar heterochromatin, respectively.

Figure 4.3 (See next page). CLEM of a high pressure frozen, cryosubstituted and serially sectioned cell. (**A**) Anti-BMI1 immunogold labeling of heterochromatin structures (15nm gold particles) of the same cell as in the Fig. 4.2D, but a different thin section is shown here. The yellow arrow points to the nuclear region/domain that correlates with (the section of) the "PcG body" fluorescence seen in Figs. 4.2B_2 with the local density of heterochromatin structures being enriched in this domain. The heterochromatin structures are specifically enriched in the BMI1 immunogold label. Gold particles are sometimes situated towards the periphery of the heterochromatin structures (insert). (**B**-**E**) Four consecutive serial sections from the same area as shown in **A**. In **B** and **C**, the thin sections were first used for on-section immunofluorescence mapping of the BMI1 protein (inserts; note that the intensity of the "PcG body" in **B** is higher than that in **C**) to identify the position of the "PcG bodies", and subsequently observed in the electron microscope (for a detailed analysis of the ultrastructural identification of the "PcG body", see Figs. 4.S3-4.S5 in the Supplementary Material). The two remaining serial thin sections (**D, E**) were on-section immunogold labeled for the BMI1 protein. Nucleolus (nu), cytoplasm (cy) and invaginagions of the nuclear envelope (black arrowheads) are designated in **A**-**E**.

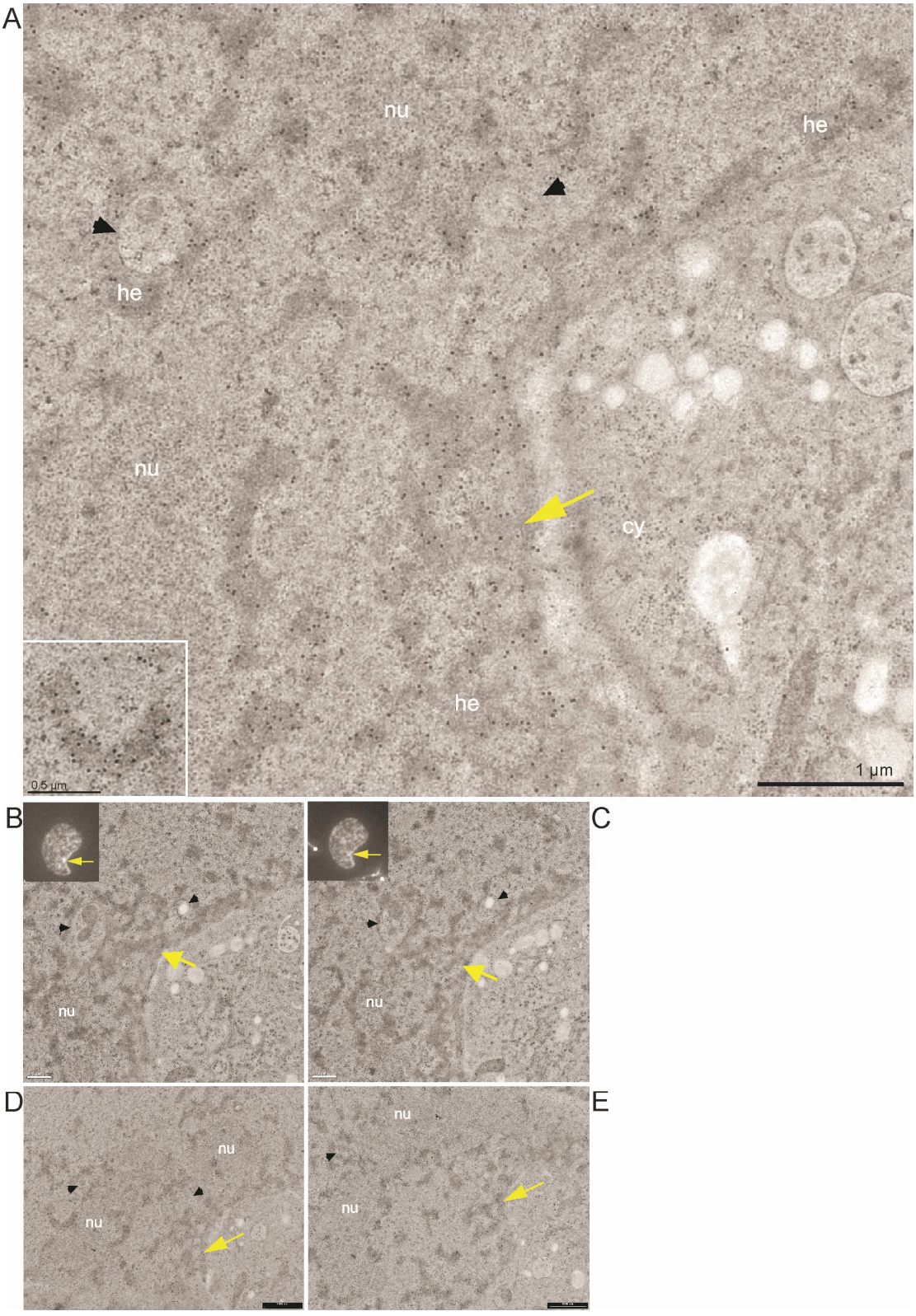
A
nu
he
he
nu
cy
he
0.5 µm
1 µm
B
nu
C
nu
D
nu
nu
E
nu
nu

Importantly, the morphometric analysis did show that the number of gold particles per unit area of heterochromatin outside and inside the "PcG body" was about the same. The relative density of the immunolabeling of heterochromatin outside the "PcG body" compared to that inside of the "PcG body" was 1.05 ± 0.24.

Taken together, using this CLEM approach, we identified, and established the structure of "PcG bodies" at the ultrastructural level. Immunogold labeling provided high and clean labeling of nuclear heterochromatin structures, and the densities of gold particles confined to heterochromatin structures outside and inside the "PcG body" were comparable. However, the fine structure of "PcG bodies" did not correspond to the nuclear bodies as such, but to locally accumulated and BMI1 immunogold labeled heterochromatin structures. Generally speaking, nuclear regions/domains with higher 3-D (Fig. 4.2B$_2$) or 2-D (inserts in Figs. 4.2B, 4.2C) BMI1 or GFP fluorescence intensity (including that of the "PcG bodies") seen in the fluorescence microscope find thus their counterpart in the nuclear regions/domains with higher local accumulations of the thin sectioned (and BMI1 2-D immunogold labeled) heterochromatin fascicles seen in the EM (see also Figs. 4.S3-4.S5).

We ultrastructurally identified "PcG bodies" by additional CLEM approaches in which the chemical fixation of cells was performed. Since we consider only the above mentioned results as representing the convenient description of the "PcG body" (e.g. refs. Dubochet and Sartori-Blanc, 2001; Hancock 2004a, b), we also document the two additional approaches (Figs. 4.S6, 4.S7). In summary, chromatin structures exhibit extraordinary sensitivity to enviromental factors, including the processing of cells for microscopy. While the resolution power of the fluorescence approaches we used does not allow for the detection of significant structural chromatin changes accompanying the processing of cells, such changes are put in evidence by electron microscopy.

4.1.4. Discussion I

PcG bodies have been so far identified only by fluorescence microscopy as distinct accumulations of PcG proteins of the PRC1 (e.g. Gunster et al., 1997; Satijn et al., 1997). With a help of CLEM, we were here able to ultrastructurally identify the "PcG bodies" in thin sectioned U-2 OS cells expressing BMI1-GFP proteins. Further, we were also able to describe the well preserved structure of the "PcG body" together with its reference nuclear space. Importantly, the transfected cells and commercial antibody used in this study were explored and characterized in several previous studies (e.g. Alkema et al, 1997; Voncken et al., 1999; Hernandez-Munoz et al, 2005).

To establish the fine structure of the "PcG body" we used the HPF followed by the cryosubstitution, nowadays the method of choice for the best preservation of cellular ultrastructure, and the basis for an achieving of convenient on section labeling (e.g. McDonald et al., 2007; Muller-Reichert et al., 2007; Verkade; 2008). This approach revealed that PcG fluorescence signals do not correspond to a nuclear body, but to a heterochromatin area (domain) represented by an accumulation of the heterochromatin fascicles.

Importantly, this approach also allowed for a high and clear-cut imunogold BMI1 label of heterochromatin fascicles throughout the nucleus. Importantly, the densities of gold particles per unit area of the thin sectioned and 2D labeled heterochromatin structures were comparable, whatever was the chosen heterochromatin area within the nucleus, either inside or outside of the "PcG body". Accordingly, the appearance of the fluorescent "PcG bodies" should reflect a local accumulation of the BMI1 labeled heterochromatin in the investigated cells.

This being said we have to discuss two relevant matters. First, we provided in Figs. 4.2, 4.3 and 4.S1 only static snapshots of the cell at the moment of rapid freezing. But chromatin is highly dynamic, and specifically, BMI1 protein exhibits high mobility (Hernandez-Munoz et al., 2005). Most chromatin proteins have a high turnover on chromatin with a residence time on the order of seconds (Misteli, 2001; Phair et al, 2004). This transient binding is a common property of chromatin-associated proteins, but the major fraction of each protein is bound to chromatin at steady state (Misteli, 2001; Phair et al, 2004). The immunocytochemical result presented here, with most gold particles localized in heterochromatin structures

(Figs. 4.2D, 4.3A, 4.S1), describes exactly such a steady state. In other words, low BMI1 immunogold label found outside of heterochromatin structures seems to be in agreement with such a steady state concept.

Second, the ultrastructural immunogold results presented here in Figs. 4.2D and 4.3A (see also Fig. 4.S1) differ from those of the previous study (Cmarko et al., 2003). In cultured transformed cells of human origin and in somatic rat liver cells, the authors mapped BMI1 protein, as well other PRC1 proteins, mainly outside of heterochromatin. They established that with respect to the BMI1 labeling density of heterochromatin, this density was 100 times and 10 times higher over the perichromatin region (region in the vicinity of heterochromatin) and over the IC, respectively (Cmarko et al., 2003). The likely explanation could be that different cells and different antibodies were used in the two studies. In a reconciliation tone, even though the present immunogold label was mostly found in heterochromatin, it was sometimes lining the periphery of heterochromatin structures, and the low label in the IC was preferentially found in the vicinity of heterochromatin. But at the same time, the strength of the present study is based on the high and clear-cut immunogold labeling of heterochromatin structures throughout the whole nucleus.

Through the previous comment we touched the third matter. We were dealing here with heterochromatin structures since such electron-dense structures are morphologically well definable (Figs. 4.2, 4.3). How about euchromatin structures? The perichromatin region is considered to encompass transcriptionally active genes (Cmarko et al., 2003), i.e. euchromatin structures. The aim of the present study was to establish the fine structure of the "PcG body", and based just on the BMI1 immunogold labeling results, it is anyway impossible to speculate in whatever terms on euchromatin structures.

The current models of the "PcG body" arise mainly from the biochemical and fluorescence microscopy studies (e.g. refs. Cavalli, 2007; Sexton et al., 2007). PcG bodies have been compared to transcription factories in these models (Cavalli, 2007). This presumption raises from the fact that Polycomb mediated gene silencing involves chromosome-kissing events, and that such events occur at PcG bodies. Similar kissing phenomena are thought to be induced also by the active or activation-prone genes and occur at the structures like transcription factories, splicing speckles or CTCF sites (Cavalli, 2007). Coming up from the expectation that the "PcG bodies" are typical nuclear bodies and the fact that the light microscopy does not

allow to study the reference space in details, the "PcG bodies" have been, in such models, situated in the IC (e.g. refs. Cavalli, 2007; Zhao et al., 2009). In the present study, the essence of "PcG bodies" was, at the EM level, associated with the accumulated and highly immunogold labeled heterochromatin structures, and not with a nuclear body situated in the IC. It should be also mentioned here that the progress in the field of Polycomb proteins has been initiated and is, with a great success, being carried out in the *Drosophila* model (e.g. refs. Platero et al., 1995; Cavalli and Paro, 1998; Dellino et al., 2004) that can be to greater or lesser extent transposed to human cells.

The present results are related just to the transfected U-2 OS cell line. If such results are confirmed in other human cell lines, they will, in a straightforward way, help to expand the knowledge with respect to the biological relevance of the "PcG body" observed in human cells.

4.1.5. Supplementary I

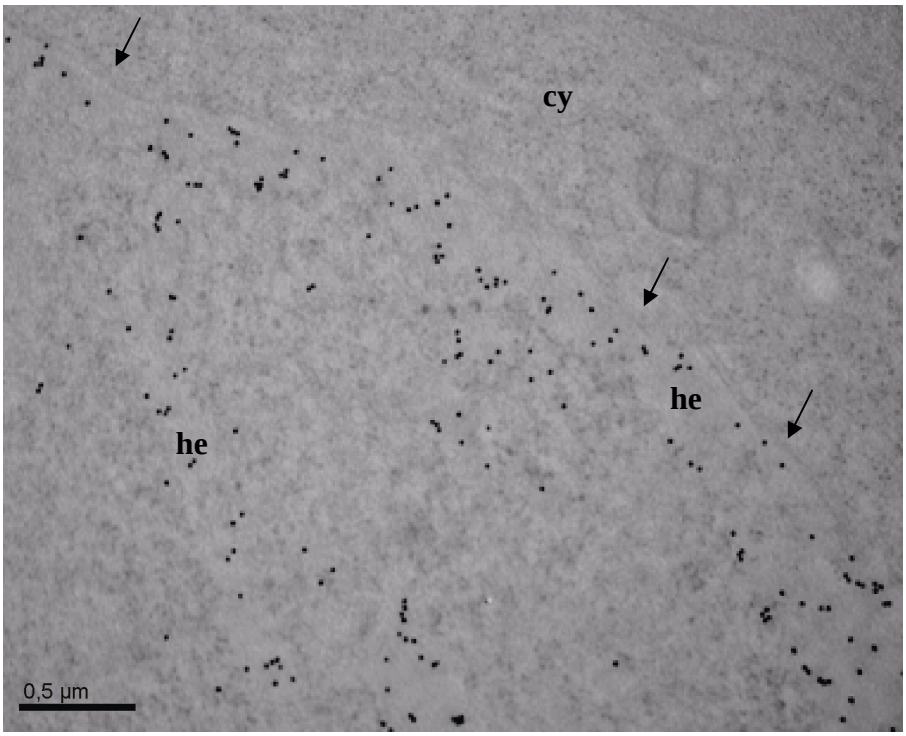

Figure 4.S1. BMI1 protein immunogold labeling of non-transfected U-2 OS cells. High-pressure frozen and cryosubstituted cells were on-section labeled with the primary monoclonal mouse anti-BMI1 antibody and the secondary goat anti-mouse antibody-gold complex (18 nm gold particles) as described in the main results. The heterochromatin, which is specifically enriched in the immunogold label, appears to be bleached. Due to the bleached heterochromatin phenomenon, sometimes observed after HPF and cryosubstitution (Paul Verkade, personal communication), the gold particles are clearly visible. Note that gold particles are often observed towards the periphery of the heterochromatin structures (he). Cytoplasm (cy), nuclear envelope (black arrows).

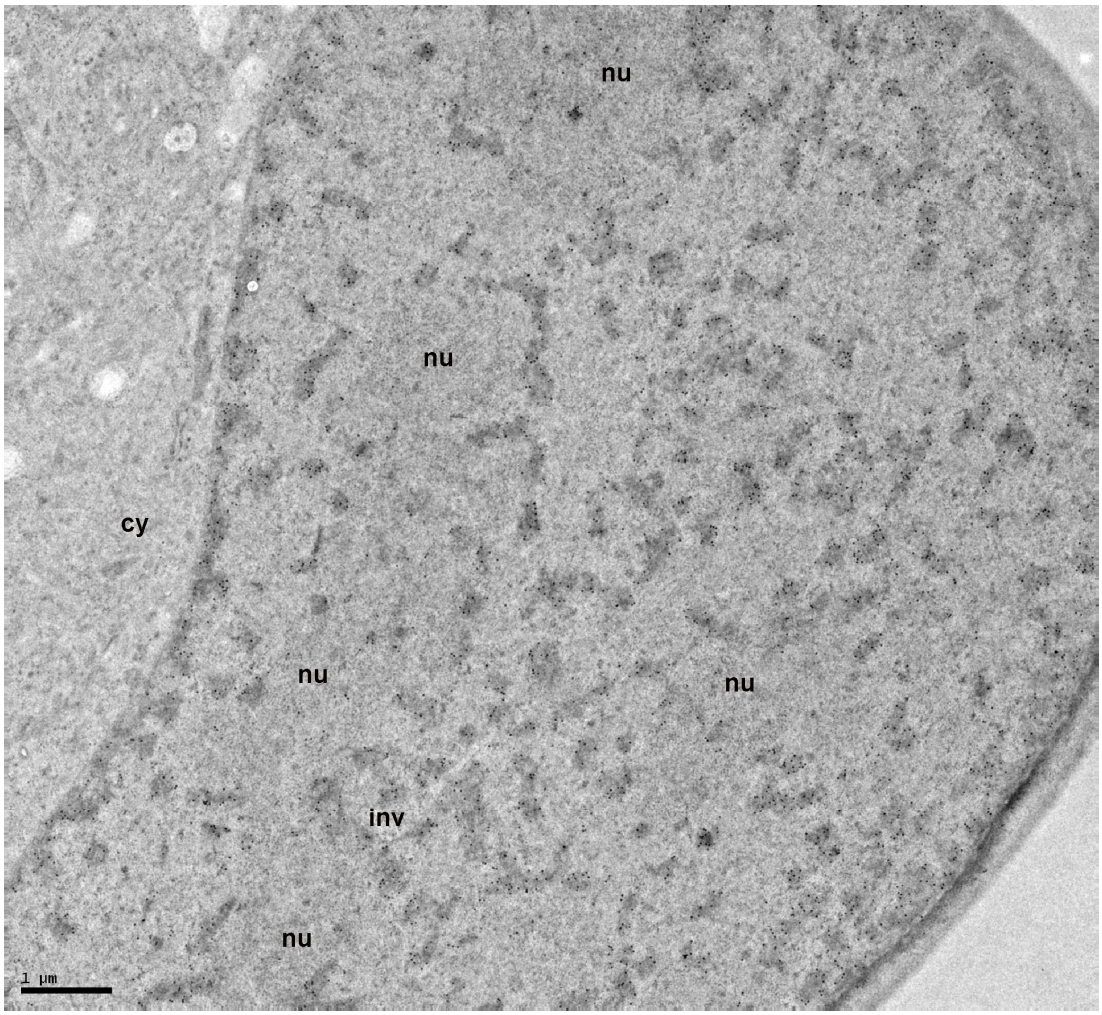

Figure 4.S2. BMI1 protein immunogold labeling of transfected U2-OS cells. Heterochromatin structures (electron-dense areas in the nucleus) are specifically enriched in the immunogold label (15 nm gold particles) all over the thin sectioned nucleus. Note a variety of preserved structures depicted in the cytoplasm (cy) after high-pressure freezing/cryosubstitution of cells. Nucleoli (nu); invagination of the nuclear envelope (inv).

Figures 4.S3-4.S5 are included in the Supplementary Material. to describe in more detail the identification of the nuclear domain corresponding to the "PcG body."

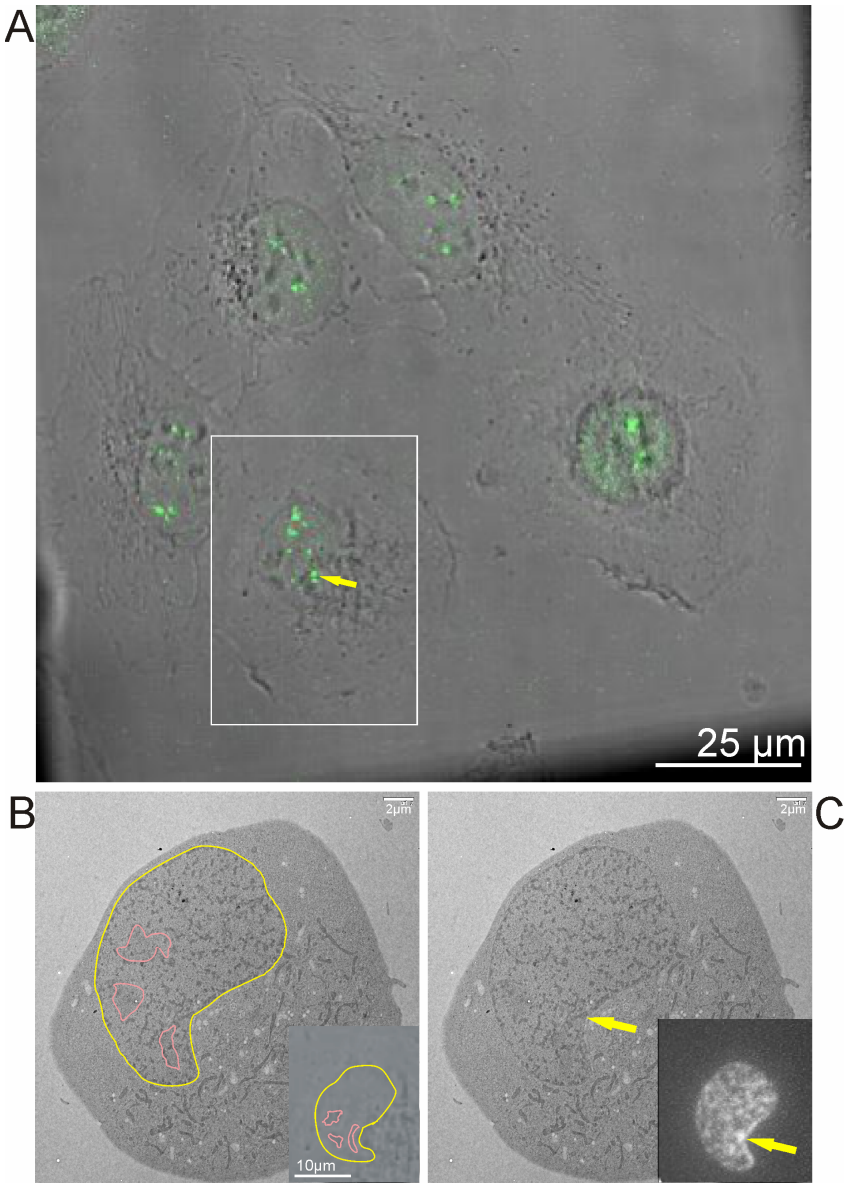

Figure 4.S3. An overview of the correlation from the main results. (**A**) An overview image (merge of fluorescence and phase contrast) of the cell used for CLEM; the maximum intensity projection of fluorescence is shown. The cell of the interest is delineated in the rectangle. (**B**) The same, but embedded and thin sectioned cell (shown already in Fig. 4.3B of the main results). The nucleus is delineated by a yellow line and the nucleoli with pink lines. In the insert, the cell shown **A** is shown in phase contrast only. The nucleus also is delineated with a yellow line and the nucleoli by pink lines. (**C**) The same, but embedded and thin sectioned cell (shown already in Fig. 4.3B of the main results). Yellow arrow points to the nuclear region (domain) that corresponds to a section through the "PcG body." This thin section was first used for on-section immunofluorescence mapping of the BMI1 protein (insert); the same insert is already shown in Fig. 4.3B of the main results, with the yellow arrow pointing to the section through the fluorescent "PcG body."

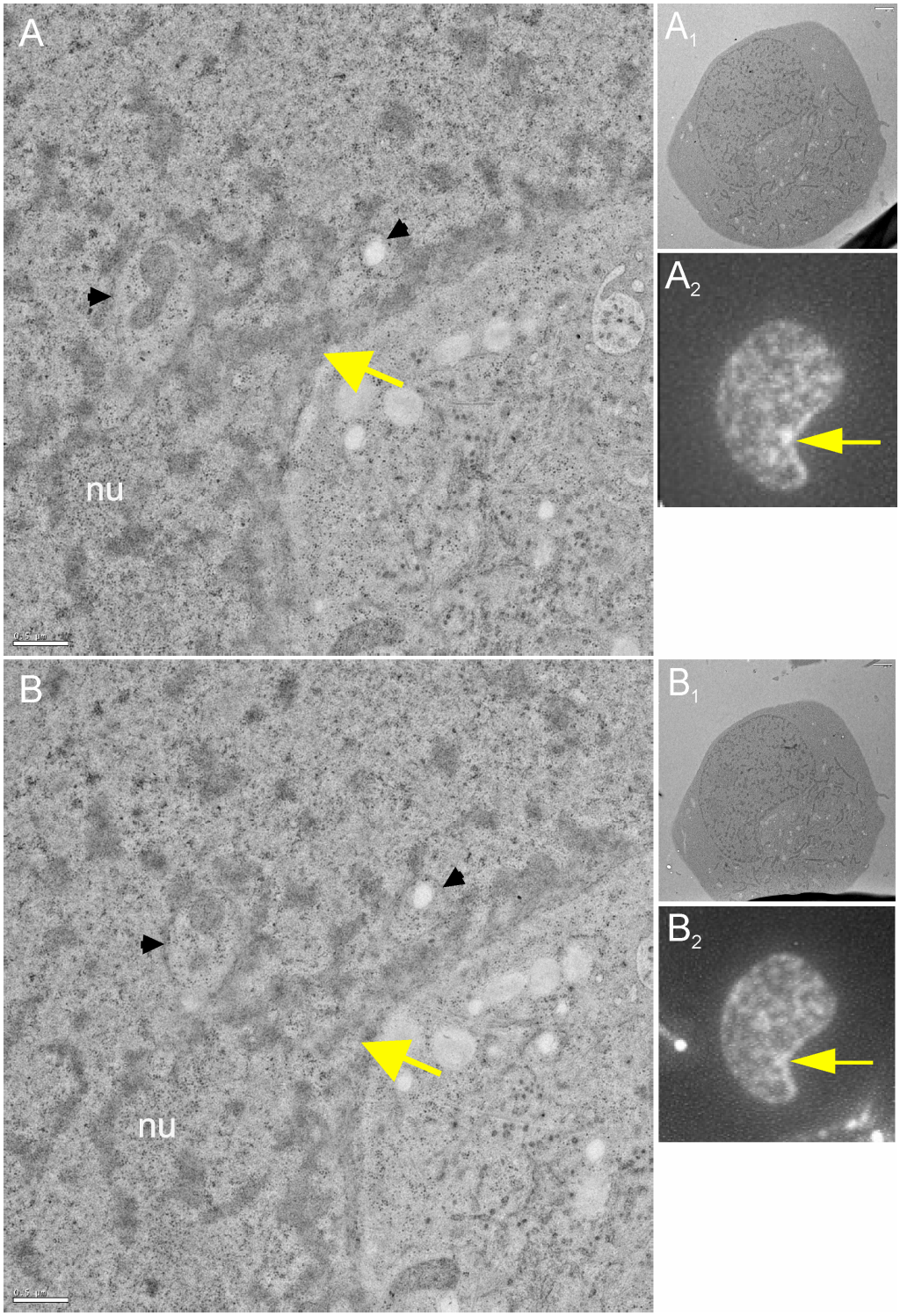

Figure. 4.S4. Higher magnification of Figs. 4.3B and 4.3C from the main results. (**A, B**) The yellow arrow points to the nuclear region/domain corresponding to the "PcG body" seen in the electron microscope in two consecutive serial sections. Nucleolus (nu), invaginations of the nuclear envelope (black arrowheads). (**A1, B1**) The low magnification of the thin sections shown in **A** and **B**. (**A2, B2**) The on-section 2-D immunofluorescence labeling of the BMI1 protein in the two serial thin resin sections. Fig. 4.S4A2 was already shown in Figs. 4.3B and 4.S3C, Fig. 4.S4B2 in Fig.4.3C.

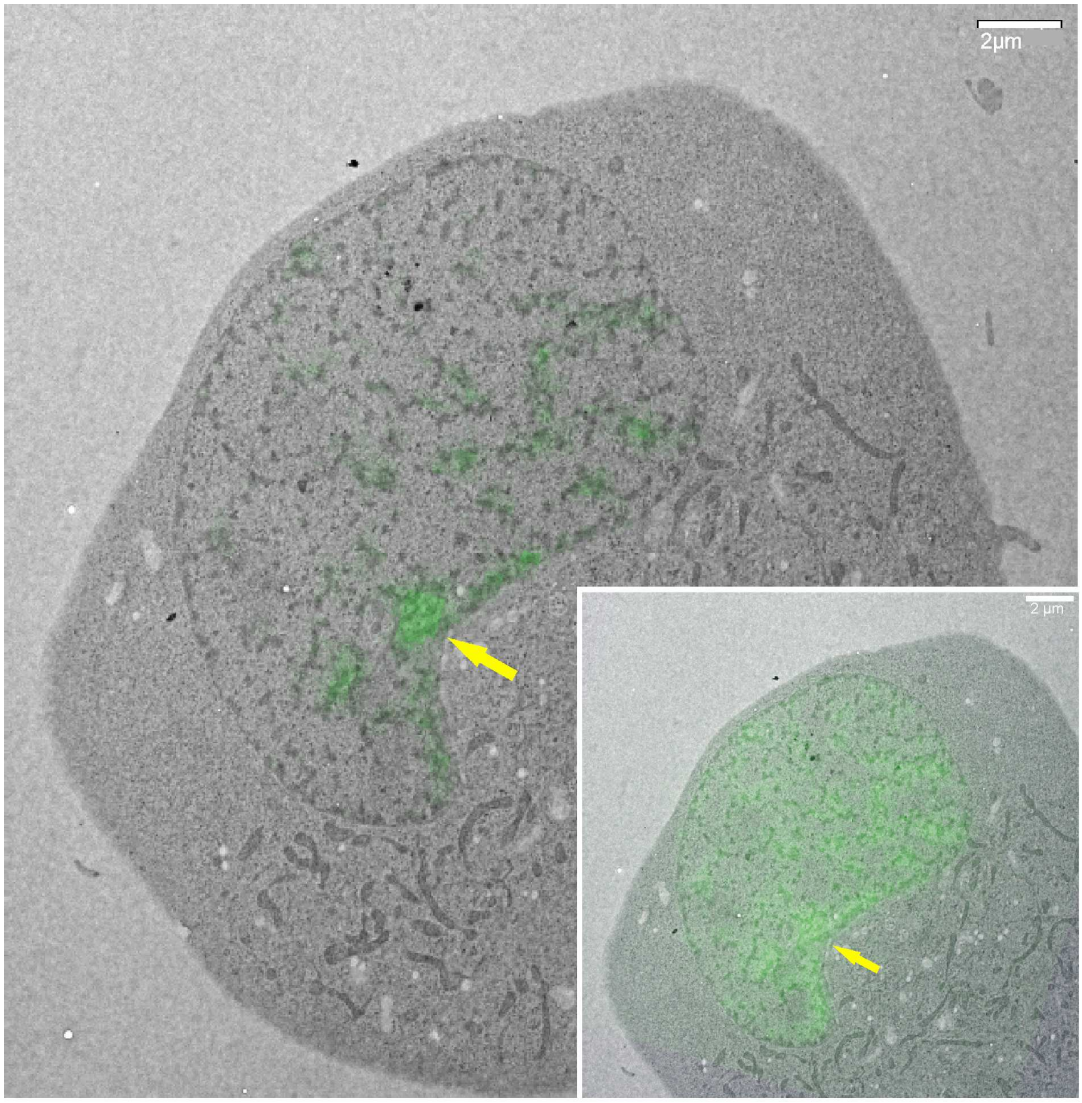

Figure 4.S5. Overlay of immunofluorescence (in green) and electron microscopic image on the same resin section shown in Figs. 4.3B, 4.S3C and 4.S4A. In the lower magnification image, the ovelay is performed using original, unadjusted fluorescence image. The yellow arrow points to the nuclear region/domain corresponding to the "PcG body. In the higher magnification image, we applied a threshold such that only the highest intensities are displayed. Yellow arrow points to (a section through) the "PcG body" as identified by green fluorescence. The "PcG body" corresponds to a local accumulation of heterochromatin fascicles. A higher magnification of the region/domain corresponding to this "PcG body" is provided in Fig. 4.S4A.

To further expand our findings with the CLEM in which HPF and freeze substitution was implemented, we provide here two other CLEM approaches (Figs. 4.S6, 4.S7) that lead, with a help of the pre-embedding labeling, to the identification of the "PcG bodies."

CLEM with pre-embedding labeling

To mimic the immunofluorescence procedure of the cell processing (Raska, 2003), and thus to also achieve the 3-D immunolabeling of cells, we immunolabeled cells prior to their embedding into resin (Fig. 4.S6). Because of the weak (and relatively slow) fixation, subsequent permeabilization/extraction, numerous washing steps and rather abrupt dehydration, the ultrastructure of cytoplasm and nuclei was largely affected.

However, via CLEM, and despite the presence of a non-specific silver label, the "PcG bodies" could be identified in a straightforward way through their very intense labeling (Figs. 4.S6B-D). Silver particles apparently completely labeled three distinct nuclear domains of the three "PcG bodies" (Fig. 4.S6), with two "PcG bodies" being associated with nucleoli. However, the "PcG bodies" were compacted and their fine structure was ruined. Interestingly enough, the implementation of CLEM would likely not be necessary for the identification of the "PcG bodies" in this pre-embedding approach as the "PcG bodies" are in the sectioned resin embedded cells noticed immediately in a straightforward way.

CLEM with pre-embedding labeling of cells extracted prior fixation

In the next approach to identify "PcG bodies" at the ultrastructural level, we used even a more invasive method with respect to the previous approach - extraction of cells prior fixation (Fig. 4.S7). This approach was originally introduced in order to visualize rather stable structures like cytoskeleton, with many other cellular components being extracted (Fey et al., 1986).

Here, the living cells were extracted with a hyperosmotic cytoskeleton CSK buffer containing detergent prior fixation and pre-embeding labeling (Fig. 4.S7). In such processed cells, the preservation of the cellular ultrastructures was even more affected than with the previous pre-embedding approach. The "PcG bodies" were, however, still easily identified through the more intense silver label (Fig. 4.S7), but their fine structure was extensively affected.

The labeling pattern observed differed from that of the previous approach. Here, silver particles decorated the periphery of the "PcG bodies", indicating a high aggregation/compaction of the heterochromatin structures giving rise to such a "body." Immunoprobes apparently did not penetrate such compacted structures as other heterochromatin structures also appeared to be labeled on the outer surface.

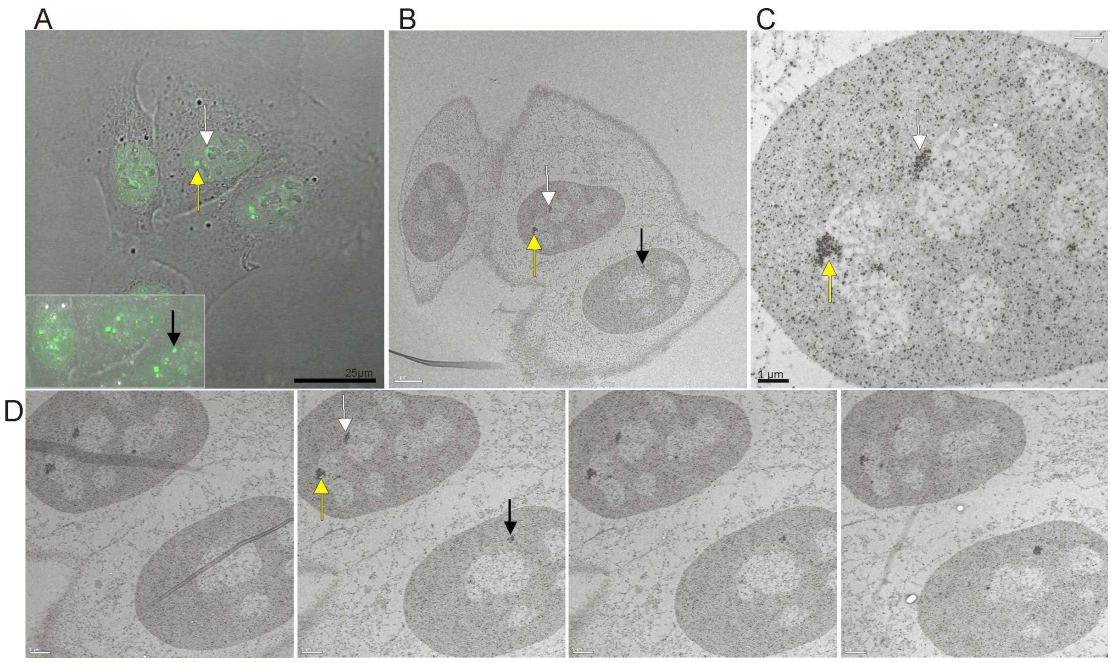

Figure 4.S6. CLEM with pre-embedding procedure. U-2 OS cells were imaged for BMI1-GFP signals on the gridded Petri dishes. Yellow, white and black arrows point to the signals corresponding to three "PcG bodies." (**A**) One optical section and in the insert maximum intensity projection of all optical sections through the cells. Merge of fluorescence and phase contrast is shown. (**B**) Electron micrograph of the same group of cells after the pre-embedding procedure. (**C**) Detailed view showing accumulations of silver enhanced ultrasmall gold particles (in the preembedding labeling of BMI1 protein) corresponding to the fluorescent PcG foci. (**D**) Four consecutive serial sections depicting "PcG bodies" (arrows pointing to the three "PcG bodies" are drawn in the second serial section). The pre-embedding CLEM allowed, at the EM level, to identify the "PcG bodies" as detected by fluorescence.

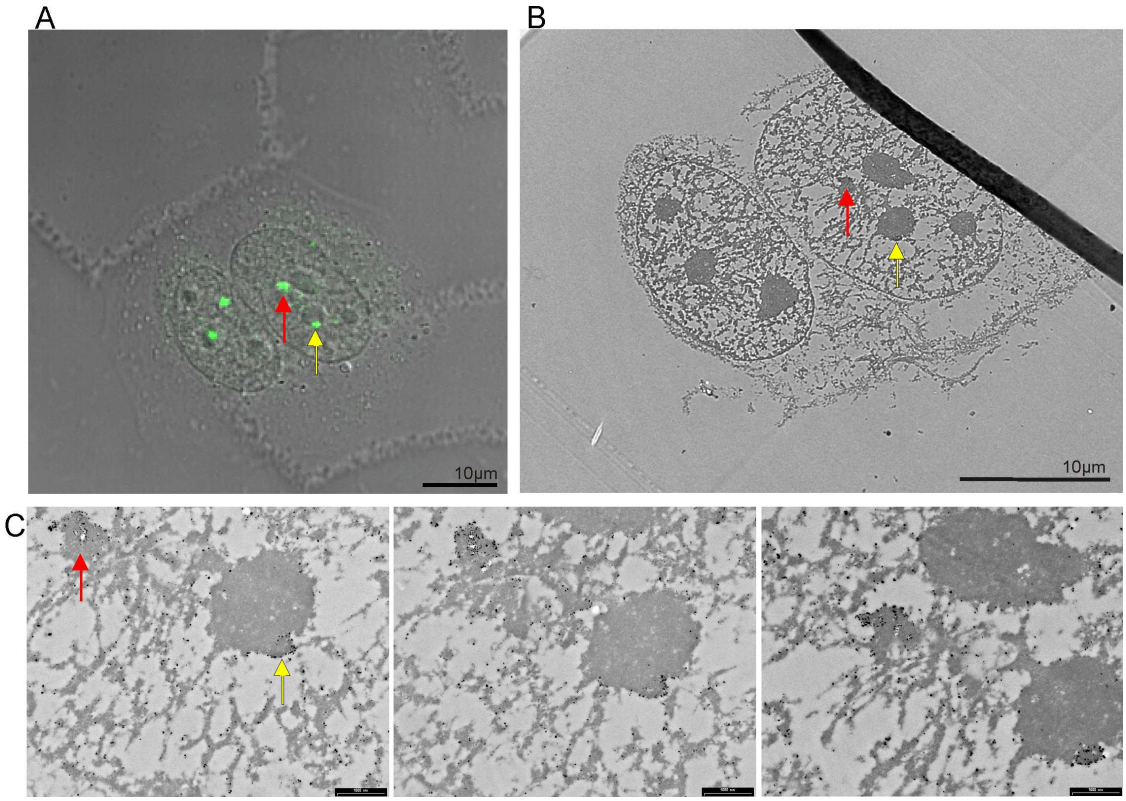

Figure 4.S7. CLEM of extracted cells prior fixation and pre-embedding labeling. U-2 OS BMI1-GFP cells were, after extraction with CSK buffer containing detergent and fixation with 2% formaldehyde, imaged on CELLocate coverslips in the fluorodishes. Yellow and red arrows point to two "PcG bodies. " (**A**) Merge of GFP fluorescence and phase contrast images; one optical section. (**B**) The same cells as imaged by the electron microscope. (**C**) The structures corresponding to the fluorescence PcG bodies (yellow and red arrows in the first serial section) in the three serial ultrathin sections immunolabeled for BMI1 protein (pre-embedding, silver enhancement). The heterochromatin corresponding to the "PcG body" fluorescence signal is found associated with the nucleoli.

Supplementary I Discussion

We identified the "PcG body" in the two other CLEM approaches in which a chemical fixation of cells was used. These two approaches led to an identification of the "PcG bodies" at the ultrastructural level due to a higher labeling density, one throughout the "PcG body" and the other decorating the outer surface of the "PcG body." These approaches, especially the second one, revealed the presence of more aggregated/compacted heterochromatin structures correlating with the respective fluorescent PcG foci.

It has to be emphasized here that chromatin is very complex and highly dynamic, and its structure exhibits extraordinary sensitivity to environmental factors (Dubochet

and Sartori-Blanc, 2001). The molecular composition of chromatin, that necessarily involves numerous modifications of its components, is of course related to the highly dynamic *in situ* structure of chromatin in living cells. At the same time, the composition of ions, particularly of the polyvalent ions, and osmolarity are very important factors. The weak (and relatively slow) chemical fixation, change in ionic conditions, change of osmolarity, permeabilization/extraction, various washing procedures, and abrupt dehydration do affect the structure of chromatin. This is apparently due to both extraction of molecules and pronounced structural changes, particularly aggregation of molecules, including their sticking to pre-existiting structures (Richter et al., 2007). To establish the fine structure of the large scale chromatin organization in a convenient way, it is crucial to minimize such effects that lead to structural changes. And even though such changes are not resolved by light microscopy (Fig. 4.1), they are put in evidence by electron microscopy. In the context of this study, we consider only the results obtained in the HPF and cryosubstitution approach (Figs. 4.2, 4.3) as appropriate for both the identification, and for the description of the fine stucture of the "PcG bodies."

4.2. Paper II

Behaviour of PcG chromatin domains under conditions of molecular crowding.

Jana Šmigová, Pavel Juda, Eva Bártová and Ivan Raška

Manuscript submitted

Abstract

A Polycomb body was considered to be a genuine structure, a novel nuclear body, in the cell nucleus. In our previous work we defined a "PcG body" as a chromatin domain rather than a nuclear body. We found out that the essence of the fluorescent PcG foci is associated with the local accumulation of heterochromatin fascicles with the same labeling density against BMI1 protein per area of dense chromatin throughout the nucleus. Here, we studied the behaviour of PcG foci under molecular crowding conditions. Molecular crowding is known to represent a convenient experimental model to manipulate the chromatin condensation or to study the formation/reassembly of nuclear bodies. Because of PcG proteins as chromatin modifiers as well as because of the "PcG bodies", we discuss both of these effects. For most of our experiments we applied correlation of live cell imaging before and after hyperosmotic treatment with imaging of immunolabeled cells. By this approach, we observed that PcG foci as BMI1 protein accumulations in cells grown in hyperosmotic medium reversibly disappeared. Interestingly, (PcG) chromatin domains under molecular crowding persisted. The same PcG foci disappearance phenomenon without the influence of the chromatin condensation in the (PcG) chromatin domains was observed by immunolabeling against RING1a protein of the PRC1 complex. The PcG foci pattern disappeared whatever type of hyperosmotic agent (with a final osmolarity of 320 mOsm) was used and also after release of BMI protein from chromatin by DRAQ5. We showed that the nature of PcG foci is rather in condensed chromatin that shows no dependance on studied PRC1 proteins to stay condensed under (not only) molecular crowding conditions.

Results II

In this study, we decided to follow the behaviour of PcG chromatin domains within the frame of the experimental model of molecular crowding. Nuclear subcompartments or domains are not separated from their surrounding by biological membranes (Taddei et al., 2004) and the overall structural stability of the nucleus is largely generated by the stochastic interaction of its components (Hubner and Spector, 2010; Dundr, 2011). The forces that assemble complexes mostly arise from macromolecular crowding (Hancock, 2004a, b). Generaly, molecular crowding represents a convenient experimental model to study the reassembly and formation of nuclear bodies (Hancock, 2004a, b) as well as manipulation of chromatin compaction (Richter et al., 2007). Importantly, it was shown (Richter et al., 2007) that the incubation of cells in medium supplemented with sucrose induces overall chromatin compaction, but the hyperosmotic shock re-organizes the nucleus within the realms of its natural potential. Here, we focused on the compaction aspect of the chromatin accumulated into PcG foci.

We performed live cell imaging followed by fixation and immunolabeling. This approach allowed us to follow the changes induced by the incubation of cells in hyperosmotic medium at the single cell level. We compared the signals from hyperosmotically treated cells with the signals from the same cells grown under physiological conditions. For live cell experiments we used U-2 OS cells stably expressing BMI1-GFP fusion protein (Hernandez-Munoz et al., 2005). The U-2 OS cell line represents a mammalian model to study PcG proteins since it contains a number of well distinguished "PcG bodies" at the fluorescence level (e.g. see Saurin et al., 1998; Voncken et al., 1999; Hernandez-Munoz et al., 2005). The immunofluorescence experiments without live cell imaging were performed also on non-transfected U-2 OS cells. For Western blot analysis Hep G2 cells were also used.

The experiments described below induced extensive changes in the localization of BMI1 (as well as RING1a) protein. Therefore, we use following three terms to describe these changes: "PcG foci", "PcG chromatin domain" and "(PcG) chromatin domain." The term "PcG foci" is used to describe the accumulations of PcG proteins and in fact it represents PcG bodies as described originally. The term "PcG

chromatin domain" is used if it is necessary to emphasize to the chromatin nature of the PcG body. The PcG chromatin domain with the released BMI1 (or RING1a) protein is termed the "(PcG) chromatin domain."

4.2.1. The "PcG bodies" as BMI1 protein accumulations disappear under molecular crowding conditions

To study the behaviour of PcG bodies in hyperosmotic medium, we incubated live cells in growth medium supplemented with a dilution of 1.6 M sucrose in growth medium to yield either 320 mOsm or 640 mOsm final concentration of sucrose (further termed 320 or 640 mOsm sucrose). The cells were treated for different time intervals ranging from 5 minutes to 2 hours (not all data are shown). According to the results obtained, we used 320 mOsm sucrose for further experiments, as this concentration was sufficient to efficiently evoke the changes in chromatin condensation as well as in PcG protein accumulations.

After incubation in medium supplemented with sucrose, the cells were immediately fixed and immunolabeled with mouse monoclonal anti-BMI1 (BMI1) and rabbit polyclonal anti-3meK27H3 (3meK27H3) antibodies and stained with distamycin A/DAPI (DA/DAPI). We observed that with increasing incubation time the PcG bodies as BMI1 protein accumulations (see control, BMI1 in Fig. 4.4A) reduced their size gradually up to their total disappearance (see BMI1 in Fig. 4.4B-D). Disappearance of the BMI1 signal from the original PcG foci (see also Fig. 4.6) was detected starting after 20 minutes of incubation in hyperosmotic medium (Fig. 4.4B). However, the remnants of BMI1 foci were still detected in most of the cells incubated in hyperosmotic medium for 20 minutes (Fig. 4.4B; white arrowheads). The total disappearance of BMI1 foci in most cells in culture was observed after 30-60 minutes incubation in hyperosmotic medium (Fig. 4.4C-D; BMI1), total disappearance in all cells after 60 minutes (Fig. 4.4D, BMI1). Similar PcG foci disappearance phenomenon was observed by immunolabeling against the RING1a protein of the PRC1 complex (see Fig. 4.8S).

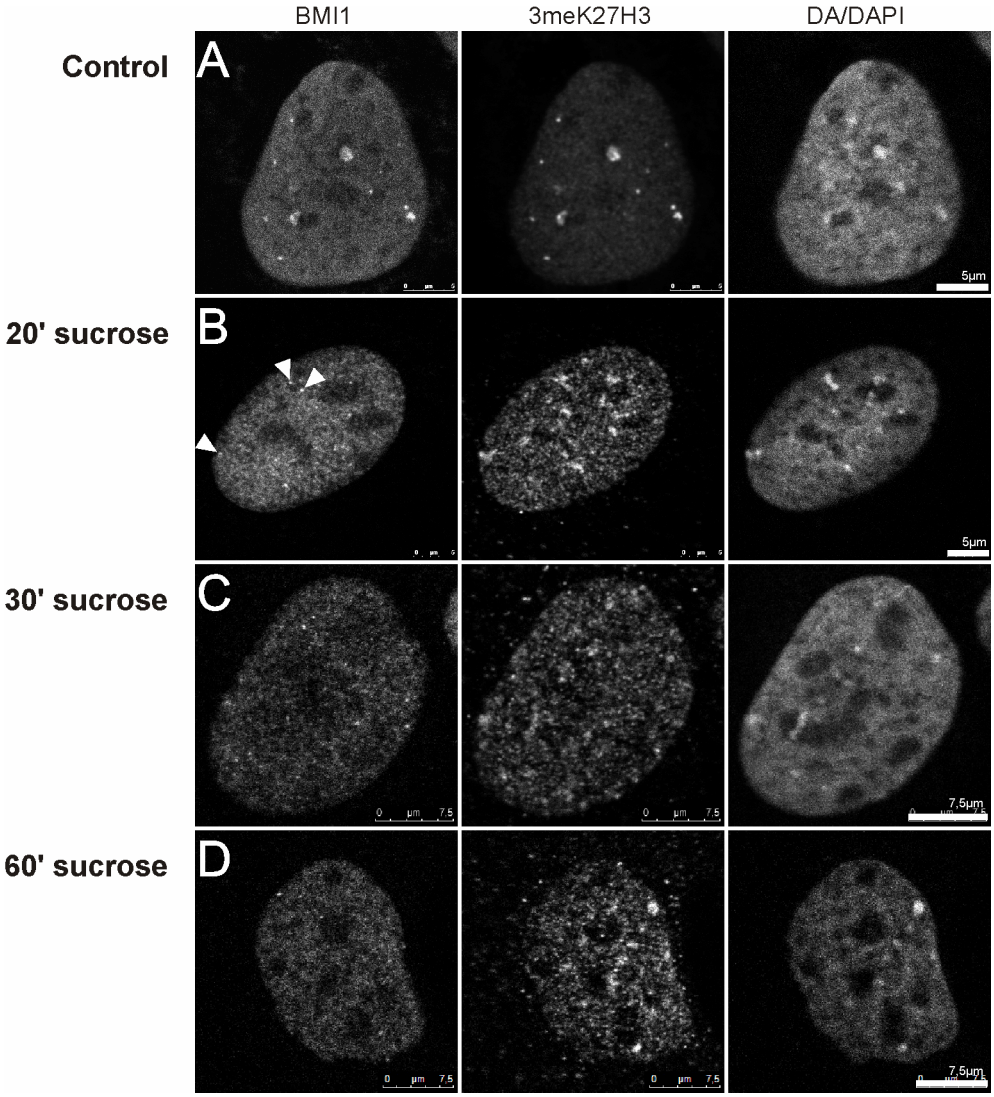

Figure 4.4. The influence of molecular crowding on BMI1 accumulations. (**A**) U-2 OS cells grown in medium with normal (290 mOsm) osmolarity. (**B-D**) U-2 OS cells that were incubated in hyperosmotic medium formed by supplementation of sucrose to its final osmolarity 320 mOsm for different time intervals: (**B**) 20 minutes, (**C**) 30 minutes or (**D**) 60 minutes. The cells were immunolabeled with anti-BMI1 (BMI1) and anti-3meK27H3 (3meK27H3) antibodies and DA/DAPI stained (DA/DAPI). Note that the PcG foci reduced their size gradually with increasing incubation time (see white arrowheads in **B**), up to their total disappearance (see BMI, **C-D**). Despite sucrose-induced hypercondensation of chromatin (see DA/DAPI pattern, **B-D**) and BMI1 foci gradual disappearance (see BMI1, **B-D**), 3meK27H3 and DA/DAPI accumulations persist after sucrose treatment (see 3meK27H3, DA/DAPI in **B-D**).

4.2.2. Different hyperosmotic agents generate the PcG foci disappearance phenomenon

The hyperosmotic agents do not act in the same ways (e.g. Richter et al., 2007). It has been established that whereas some of them (e.g. sucrose or sorbitol) cannot freely permeate membranes of living cells and their effect results from the the osmotic loss of water from cells, others (sodium and chloride ions) can cross the membrane barrier across ion channels (e.g. Richter et al., 2007).

To test the effect of different hyperosmotic agents, the U-2 OS cells were incubated for 30 minutes in hyperosmotic media with added sucrose (Fig. 4.5A), sorbitol (Fig. 4.5B) or NaCl (Fig. 4.5C) to reach their osmolarity of 320 mOsm in DMEM. Then the cells were fixed and imunolabeled with anti-BMI1 antibody (BMI1) and stained with DA/DAPI. DA/DAPI staining showed the evident hypercondensation of chromatin in such treated cells. Concerning BMI1 signal, the PcG foci pattern disappeared whatever type of hyperosmotic agent (with a final osmolarity of 320 mOsm) was used. Also, we observed that in the cells grown under molecular crowding conditions the BMI1 signal was often localized into the periphery of the cell nucleus (e.g. see Fig. 4.5B) and such a labeled peripheral domain lacked DA/DAPI staining. These data are in agreement with findings of Richter et al. (2007) which observed that hyperosmotic treatment causes the separation of peripheral chromatin from the nuclear lamina, giving rise a new nuclear compartment, the peripheral layer, which is free of chromatin. Also, we observed that the peripheral layer in the cells treated with sorbitol or NaCl was formed more rapidly than in cells treated with sucrose of the same osmolarity.

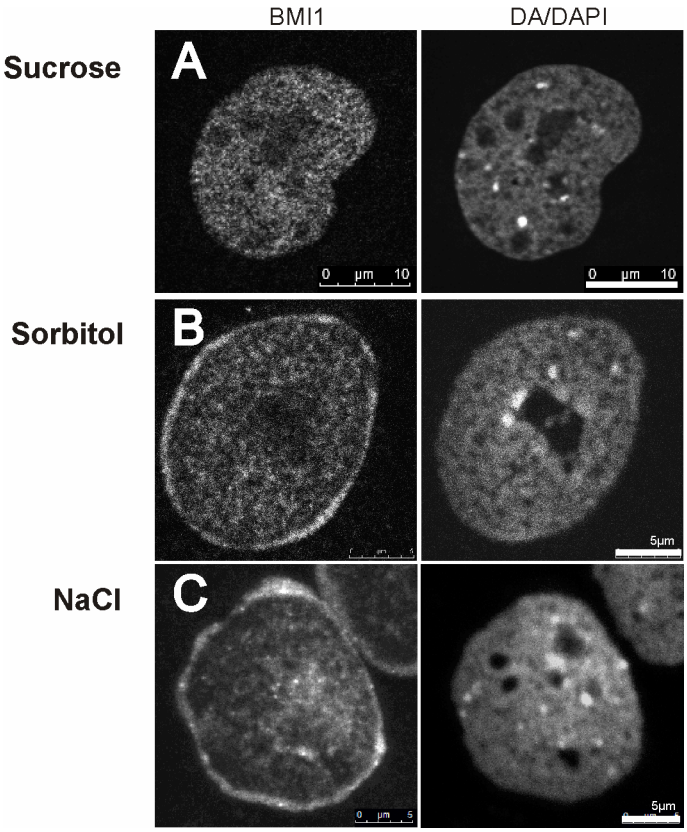

Figure 4.5. The disappearance phenomenon was observed after treatment with different hyperosmotic agents. U-2 OS cells were incubated for 30 minutes in hyperosmotic media formed by adding (**A**) sucrose, (**B**) sorbitol or (**C**) NaCl. The cells were then immunolabeled for BMI1 protein (BMI1) and stained with DA/DAPI (DA/DAPI). The disappearance of BMI1 protein accumulations from PcG chromatin domains was observed (see pattern in BMI1 column) whatever type of hyperosmotic agent was used.

4.2.3. PcG bodies as chromatin accumulations persist after sucrose treatment

As already shown (e.g. Richter et al., 2007), hyperosmotic treatment did not denature the cells. Even gross re-arrangements, such as formation of the peripheral layer, reversibly relaxed within minutes of the re-incubation in normal medium. The initial, heterogeneous pattern of chromatin distribution remains preserved (Richter et al., 2007; Albiez et al., 2006). Segregation patterns observable upon hyperosmotic treatment may thus represent the imposed expression of regular, functional organization (Richter et al., 2007).

Accordingly, we were interested in what happens to PcG chromatin domains when PRC1 proteins as chromatin regulators that should stably maintain their compaction are redistributed (released from chromatin; Figs. 4.4, 4.8S).

Chromatin compaction after 45 minutes of incubation with 320 mOsm sucrose in DMEM was followed by DAPI staining in combination with distamycin A (DA/DAPI staining). DA/DAPI staining was used to overcome the problem of probe (e.g. DAPI, antibodies) penetration/epitope accessibility within compacted chromatin areas. In U-2 OS cells cultivated under physiological conditions, DNA (after permeabilization with 2% TritonX-100) and DA/DAPI signals co-localized and the highest densities of DNA and DA/DAPI were localized with PcG foci (Fig. 4.S9, control; see also Fig. 4.1). Here, we also show the co-localization of DNA and DA/DAPI signals after sucrose treatment (Fig. 4.S9, sucrose). Because DNA and DA/DAPI co-localized before as well as after sucrose treatment, we used DA/DAPI staining as a quantitative measure of DNA density.

To correlate the BMI1-GFP fluorescent signals before and after sucrose treatment with signals from the same cells which were immediately fixed and immunolabeled with anti-GFP and anti-BMI1 antibodies as well as stained with DA/DAPI, we used transfected U-2 OS BMI-GFP cells grown on gridded Petri dishes. Using this approach, we also showed that BMI1-GFP fluorescent signals (Fig. 4.6B) are compatibile with signals from the same cells which were immediately fixed and immunolabeled with anti-GFP (Fig. 4.6C) and anti-BMI1 (Fig. 4.6D) antibodies.

In sucrose treated cells, we observed hypercondensation of chromatin (e.g. Fig. 4.6E, H). However, the highest densities of DA/DAPI staining persisted at sites of the original PcG foci (compare the signals in Fig. 4.6A with signals in Fig. 4.6E; yellow arrows). Our results are consistent with data on the preservation of the global patern of chromatin distribution after sucrose treatment (Richter et al., 2007). Thus, we observed that PcG chromatin domains persisted despite PcG foci disappearance (Fig. 4.6B-D, G and see Fig. 4.S8 for RING1a) and BMI1 release into the interchromatin compartment (see Fig. 4.6B, E, white arrowheads and Fig. 4.6F-H). The obtained results strongly support the chromatin nature of the PcG foci. But also, they question whether the PRC1 complex, specifically its BMI1 protein, is essential for the maintenance of chromatin compaction.

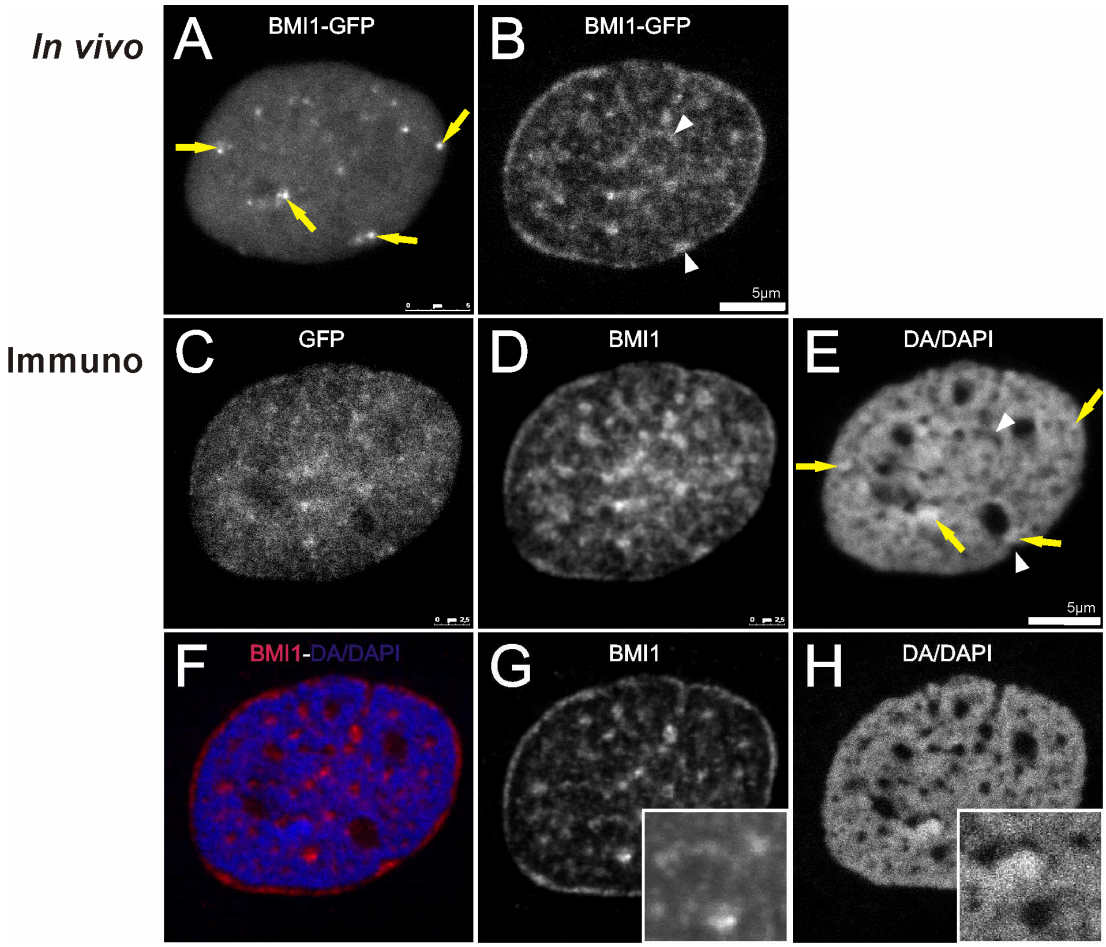

Figure 4.6. The influence of molecular crowding on the PcG chromatin domains appearance. (**A-E**) Correlation of the live cell imaging signals before and after 320 mOsm sucrose treatment and the signals after immunofluorescence and DA/DAPI staining. Maximum intensity projections of signals are shown. (**A**) U-2 OS BMI1-GFP cells imaged *in vivo* before sucrose treatment (physiological conditions). The yellow arrows point to the PcG foci. (**B**) The same cell was imaged after 30 minutes of sucrose treatment. BMI1 protein foci in cells incubated in hyperosmotic medium disappeared. (**C-D**) The same cell after fixation and immunolabeling with anti-GFP (**C**) and anti-BMI1 (**D**) antibodies and counterstaining with DA/DAPI (**E**). The highest densities of DA/DAPI persist in the sites of original PcG foci (compare **A** and **E**; yellow arrows). (**F-H**) The localization of translocated BMI1 protein is also shown in images of middle optical section. In cells incubated in hyperosmotic conditions, the BMI1 signal was detected in the interchromatin compartment (**F**- merge of **G** and **H**). For details of BMI1 localization into the interchromatin compartment (areas free of DA/DAPI staining) are seen in insets in **G**, **H**.

4.2.4. PcG foci disappearance phenomenon is reversible

It was shown that in sucrose treated cells, nuclear functions such as DNA replication, RNA synthesis or division of mitotic cells are stalled, but after returning to normal conditions they are immediatly recovered (Albiez et al., 2006). The cells could be kept up to 60 minutes in hypertonic conditions without any significant sign of cell suffering or increased cell death rate. Even, after returning of sensitive mitotic cells to normal conditions and subsequent long-term incubation (>17 hours), cells survive and continue cell cycle progression (Albiez et al., 2006).

To study the reversibility of PcG foci disappearance, the BMI1-GFP signal was followed through hyperosmotic incubation–washing cycles. We observed that upon re-incubation of cells with normal growth medium (290 mM), PcG protein accumulations recovered to their initial state (Fig. 4.7). The size, number and position of the re-formed PcG foci appeared to be the same as before treatment (compare Fig. 4.7C_1, C_2 with Fig. 4.7A). Further, we observed that after repeated hyperosmotic incubation (Fig. 4.7D_1, D_2), BMI1 protein accumulations disappeared more quickly; within 10 minutes instead of more than 20 minutes (compare Fig. 4.7B and D_1). After 20 minutes of the second cycle of incubation in hyperosmotic medium, the PcG accumulations in the interchromatin compartment (compare Fig. 4.7E and Fig. 4.7F, G; see also Fig. 4.6) became visible. When we correlated these BMI1-GFP fluorescent signals (Fig. 4.7D_2) with BMI1 and GFP signals from the same cells which were immediately fixed and immunolabeled (Fig. 4.7F, G), they were consistent. On the other hand, the (PcG) chromatin domains (DA/DAPI, Fig. 4.7E) and 3meK27H3 (Fig. 4.7H), that should act as PRC1 binding sites, even after repeated treatment persisted and were consistent with PcG foci signals seen before the treatment (Fig. 4.7A).

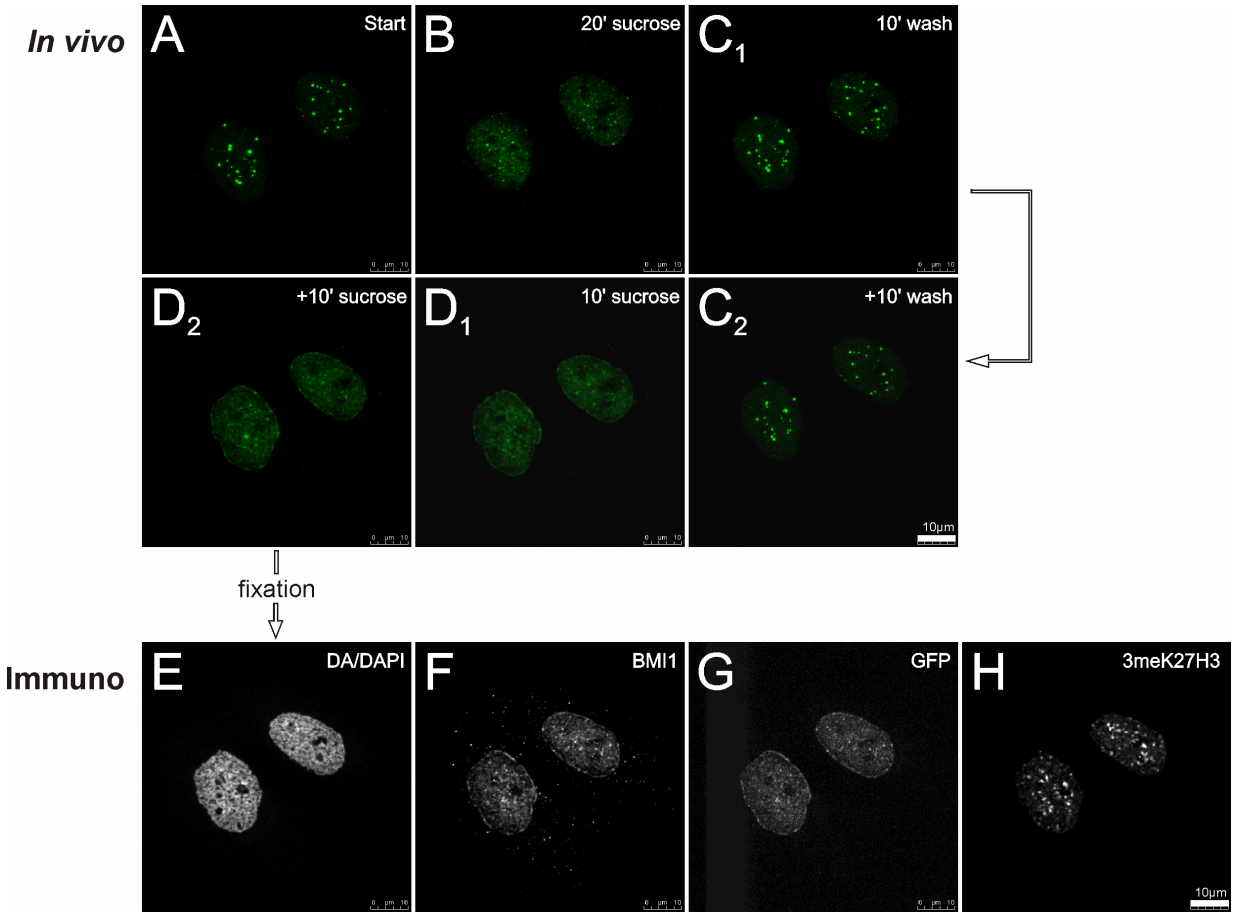

Figure 4.7. Reversibility of the PcG fluorescent foci disappearance phenomenon. Transfected U-2 OS cells were imaged *in vivo* for BMI1-GFP signal in the gridded Petri dishes. (**A**) In the cells grown in normal growth medium, the BMI1 accumulations into PcG foci are visible. (**B**) In the cells incubated in hyperosmotic medium (320mOsm sucrose), BMI1 foci disappeared. (**C1, C2**) The PcG body disappearance was reversible. When the cells were returned to normal growth medium, BMI1 foci recovered to original phenotype. The BMI1-GFP signal after 10 minutes (**C1**) / 20 minutes (**C2**) incubation of the cells in normal growth medium. (**D1, D2**) U-2 OS BMI1-GFP cells after 10 minutes (**D1**) / 20 minutes (**D2**) re-incubation in hyperosmotic medium. (**E-H**) Then the cells were fixed and immunolabeled with anti-BMI1 (**F**) and anti-3meK27H3 (**H**) antibodies and stained with DA/DAPI (**E**). Also, the cells were captured for fixed BMI1-GFP signal (**G**).

4.2.5. BMI1 foci disappearance correlates with its (hyper-)phosphorylation status

We asked whether the disappearance of BMI1 accumulations and BMI1 release from chromatin after sucrose treatment is physiologically regulated, or whether it just represents a mechanical release of less tightly bound BMI from chromatin.

By comparing of lyzates from cells grown under normal versus hyperosmotic conditions, we observed a difference in the migration speed of BMI1 in SDS-PAGE

gels. In both treated and untreated cells four isoforms of BMI1 (ranging from 40-44 kDa) in two different cell lines (U-2 OS BMI1-GFP and Hep G2) were detected. However, in cells incubated in normal growth medium, the majority of BMI1 appeared as the faster migrating bands (U, H in Figs. 4.8A, B), whereas in sucrose-treated cells, the most abundant species corresponded to the slower migrating form of BMI1 (Us, Us1, Hs1 in Figs. 4.8A, B). The same results were obtained with RING1a protein from PRC1 (compare Us– and U– in Fig. 4.8D).

To find out whether the differences in mobility result from phosphorylation of BMI1 (and RING1a), we treated the cell lyzates with Calf Intestinal Alkaline Phosphatase (CIAP; +). The incubation of cell lyzates in buffer containing CIAP resulted in a gradual shift in the mobility of the BMI1 bands. We observed that by removal of phosphate groups, the slow migration BMI1 bands disappeared, whereas the faster bands became more obvious (compare U/Us1+ to U/Us1– in Fig. 4.8C). Similarly, RING1a protein occurs mostly in hypo-phosphorylated form in cells incubated in normal growth medium and mostly in hyper-phosphorylated form in cells incubated in hyperosmotic medium.

Together, our data provides an evidence that BMI1 foci disappearance in cells grown in hyperosmotic conditions and BMI1 release from chromatin is under the control of the cell and it correlates with the phosphorylation status of BMI1 (or RING1a; Figs. 4.8C, D).

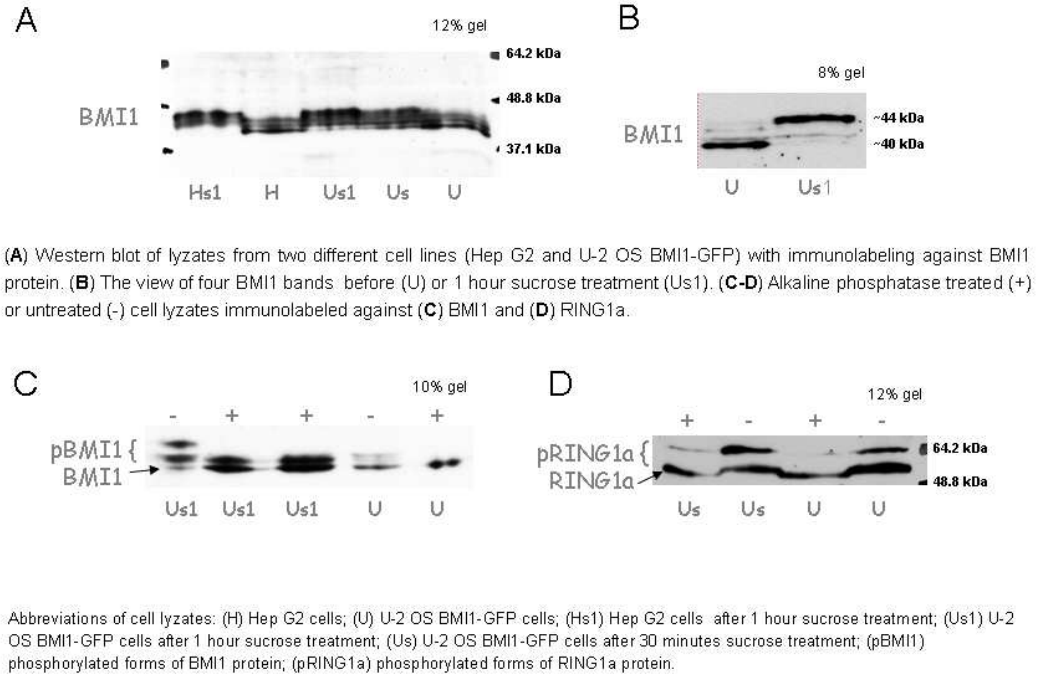

Figure 4.8. Hyperosmotic treatment induces changes in the phosphorylation of BMI1 and RING1a proteins. (**A**) To study the phosphorylation changes of BMI1, two different cell lines, U-2 OS BMI1-GFP (U) and HepG2 (H), were used. The cells incubated in hyperosmotic media are designated with the letter S (30 minutes incubation) or S1 (60 minutes incubation). (**B**) In both treated and untreated cells the four isoforms of BMI1 (ranging from 40-44 kDa) were clearly detected in less concentrated (8%) polyacrylamide gel. After sucrose treatment decreasing the amount of the slower migrating form and increasing the amount of the faster migrating form of BMI1 was detected in both cell lines (**A, B**). The observed changes were more obvious in Hep G2 cells with respect to U-2 OS BMI1-GFP cells (see Hs1 in **A**). (**C**) Alkaline phosphatase treatment revealed that the changes are associated with the hyper-phosphorylation of BMI1 protein in sucrose treated cells. (**D**) Therefore, the sucrose treatment evoked changes in phosphorylation were also observed with RING1a protein of the PRC1 complex. Note: anti-RING1a antibody showed a difference in sensitivity to unphosphorylated form of RING1a that was detected in CIAP treated lyzates.

4.2.6. DRAQ5 treatment releases BMI1 protein from chromatin, but (PcG) chromatin domains remain condensed

Because heterochromatin maintenance could be facilitated by crowding (Bancaud et al., 2009), to verify the unimportance of BMI1 protein for the maintenace of chromatin condensation, we applied entirely different approach with respect to hypercondensation caused dislocation of BMI1 protein. We used the DNA dye

DRAQ5 (Fig. 4.9) that is known for its effect to change DNA-binding capacity of chromatin-associated proteins such as polymerases, repair proteins, transcription factors and even some histones and release them from chromatin (Mari et al., 2010; Richard et al., 2011), while non-DNA-binding factors, such as non-fused GFP, are not affected (Mari et al., 2010; Richard et al., 2011). Although initially DRAQ5 was considered to be a highly useful DNA marker in living cells because of its photostability, deep red fluorescence and independence on transfectability of the cells (Martin et al., 2005; Edward, 2009), nowadays it is known that 30 minutes exposure to DRAQ5 induces irreversible changes in U-2 OS cells and their death 24 hours later (Richard et al., 2011).

To be able to follow DRAQ5 induced release of BMI1 from chromatin, we applied correlative microscopy. With transfected U-2 OS cells, we correlated *in vivo* BMI1-GFP fluorescent signal (Fig. 4.9A) with immunofluorescence/staining signals from the same cells after 30 minutes staining of live cells with 5 mM DRAQ5 (Fig. 4.9B-E). We found DRAQ5 association with chromatin (compare Fig. 4.9D and 4.9C) and dislocation of BMI1 protein from chromatin (Fig. 4.9A) to the interchromatin compartment (Fig. 4.9B, E). Importantly, we found that although DRAQ5 staining of living cells lead to BMI1 release from chromatin, the (PcG) chromatin domains remained the same (compare Fig. 4.9 C and 4.9A; red arrows).

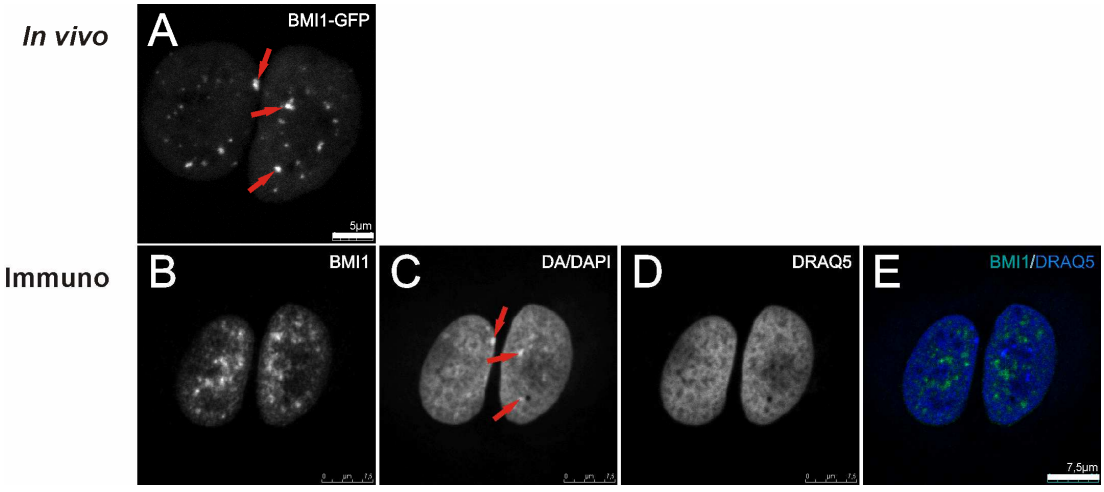

Figure 4.9. DRAQ5 induced releasing of BMI1 proteins from chromatin. (**A**) U-2 OS BMI1-GFP cells imaged for BMI1-GFP signal before treatment. Then the live cells were stained with a DNA dye DRAQ5 (5 mM) for 30 minutes. (**B-E**) The same, however fixed and immunolabeled cells after incubation with DRAQ5 dye. DRAQ5 (**D**) intercalates into DNA stained with DA/DAPI (**C**) and causes the dislocation of BMI1 protein (**B**) from chromatin to interchromatin compartment. In (**E**)

merge image of BMI1 and DA/DAPI is shown. Importantly, despite BMI1 release from chromatin, DA/DAPI signal colocalizes with original BMI1 foci (compare **A** and **C**; red arrows), i.e. this signal corresponds to (PcG) chromatin domains.

4.2.7. Supplementary figures II

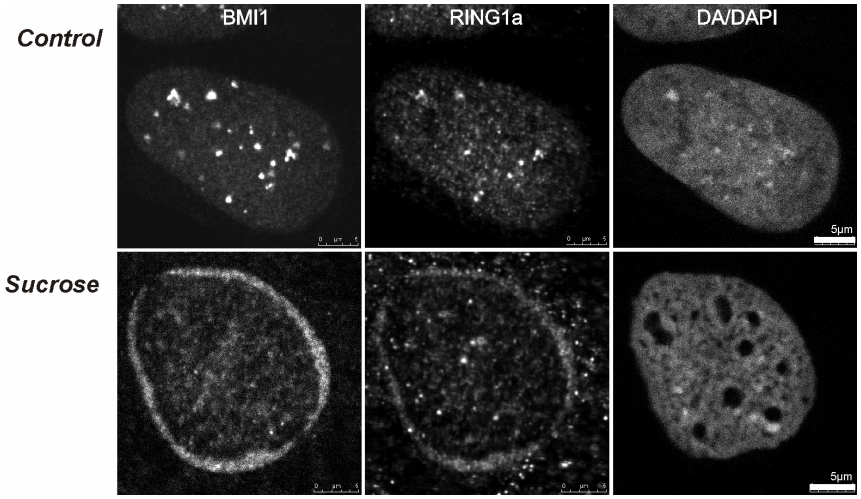

Figure 4.S8. The PcG foci disappearance phenomenon observed by immunolabeling against BMI1 and RING1a proteins of the PRC1 complex. U-2 OS cells were grown in medium with normal osmolarity (Control) or in hyperosmotic medium formed by adding sucrose for 45 minutes (Sucrose). The cells were immunolabeled with anti-BMI1 (BMI1) and anti-RING1a (RING1a) antibodies and counterstained with DA/DAPI. Whereas in control cells BMI1 and RING1a signals co-localized in PcG foci and they corresponded to the sites with the highest DA/DAPI densities, in sucrose treated cells PcG foci disappeared and BMI1 and RING1a signals were detected in the interchromatin compartment.

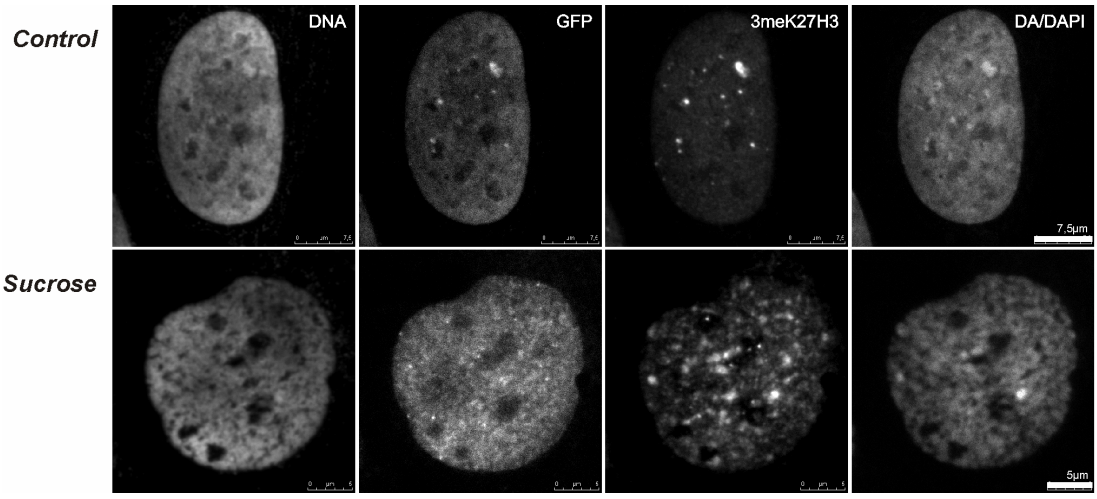

Figure 4.S9. DNA-rich (PcG) chromatin domains persist after sucrose treatment. U-2 OS BMI1-GFP cells were incubated under normal (Control) or for 45 minutes hypercondensed (Sucrose) conditions. The cells were immunolabeled with anti-DNA (DNA), anti-GFP (GFP), anti-3meK27H3 (3meK27H3) antibodies and stained with DA/DAPI. In control cells, all signals co-localized and the PcG foci represent the sites with the highest densities of DNA, DA/DAPI as well as 3meK27H3. In

sucrose treated cells, the PcG foci disappeared, however, the highest densities of DNA, DA/DAPI and 3meK27H3 persisted in co-localization in the (PcG) chromatin domain.

4.2.8. Discussion II

Here, we have experimentally shown, using a molecular crowding approach, that PcG bodies are chromatin domains rather than proteinaceous nuclear bodies localized in interchromatin compartment. These data are consistent with our previous work on the ultrastructure of the "PcG body" (Smigova et al., 2011). Hyperosmotic induced compaction of chromatin differs from compaction of chromatin caused after local binding of chromatin-regulatory proteins (e.g. PcG proteins). However, despite of this fact, molecular crowding represents a convenient experimental model to study chromatin and manipulate its compaction (e.g. Richter et al., 2007).

We found that the behaviour of PcG foci under increased crowding conditions vastly differs from the behaviour of typical nuclear bodies. Whereas nuclear bodies like PML nuclear bodies and nucleoli are formed/reassembled under hyperosmotic treatment (Hancock, 2004a, b), PcG foci under crowding conditions disassemble. Further, in agreement with previous studies (Albiez et al., 2006; Richter et al., 2007; Martin and Cardoso, 2010; Finan et al., 2011) by staining of DNA, we clearly detected after hyperosmotic treatment the condensation of chromatin. Importantly, we also observed that the pattern of the (PcG) chromatin domains remained the same. This is consistent with the data on the preservation of the global patern of chromatin distribution after sucrose treatment (Richter et al., 2007). However, because of the release of PRC1 proteins from chromatin and PcG protein foci disappearance, such a result was surprising. The similar result was obtained also using DRAQ5 staining of living cells. Here rises a question whether BMI1 (and also RING1a) protein is essential for the maintenance of chromatin condensation.

Here, we found out that the cells react to hypertonic treatment by hyper-phosphorylation of BMI1 (and also RING1a) protein. Thus, the BMI1 release from chromatin seems to be not only the consequence of mechanical disruption of BMI1 binding after hyperosmotic treatment. Phosphorylation reflects the functional state of BMI1 protein rather than its localization (Voncken et al., 1999). The correlation between BMI1 hyperphosphorylation and its dissociation from chromatin was detected by Voncken et al. (1999) in mitotic cells. As observed by Martin and Cardoso (2010), mitosis and hyperosmolarity (equivalent to a 500 mM saline solution), the levels of chromatin compaction are comparable (Martin and Cardoso, 2010).

We also observed that BMI1 foci disappearance in hyperosmotic conditions is a reversible process. Upon re-incubation of the cells treated by high molar sucrose in normal growth medium, PcG foci recovered to their initial state. The rapid recovery of BMI1 protein into the PcG foci was also allowed by chromatin modifications (and condensations) in the (PcG) chromatin domains. The reversibility signifies that the disappearance phenomenon is under the control of the cell, which is consistent with the findings on reversible chromatin compaction obtained by Richter et al. (2008). According to these authors, the hyperosmotically induced chromatin compaction is not caused by the precipitation of denatured matter, but rather the cell reacts within its physiological realms (Richter et al., 2007).

Together, in this study we have experimentally shown that the behaviour of the PcG body, concerning chromatin compaction and preservation of its chromatin pattern distribution, is similar to the behaviour of chromatin. Moreover, we found that molecular crowding, despite the hyperosmosis caused release of the studied PRC1 proteins (BMI1, RING1a), does not influence the presence of the (PcG) chromatin domain. This indicates not-essential nature of the studied PRC1 proteins for the maintenance of the (PcG) chromatin domain condensation in mammalian cells.

5. General discussion

The cell nucleus has a compartmentalized structure made up of the chromatin domains and the interchromatin compartment. Whereas the chromatin basically consists of euchromatin and heterochromatin, the interchromatin compartment is enriched in a number of various structures containing no or just little of DNA, such as nuclear bodies (Raska, 1995; Lamond and Earnshaw, 1998; Spector, 2001; Gall, 2003; Craig, 2005; Matera et al., 2009; Zhao et al., 2009).

The term nuclear body is used for a nuclear domain that is morphologically distinct from its surroundings when observed by transmission electron microscopy (Raska, 1995; Matera et al., 2009). Nuclear bodies are dynamic, mainly ribonucleoproteinaceous structures that form at sites of specific activities associated with gene expression and genome maintenance. Their formation is driven by non-random, biologically determined initial seeding events followed by stochastic self-assembly (Dundr, 2011). Nuclear bodies such as nucleoli, Cajal bodies and PML bodies are well characterized, even at the ultrastructural level (Matera et al., 2009). In this respect, so far less well studied are the structures containing transcriptional regulators or RNA-binding proteins (Carmo-Fonseca et al., 2010). These structures are also termed orphan nuclear bodies. The group of orphan nuclear bodies includes the clastosome, the cleavage body, the OPT domain, the SUMO body, the Sam68 body, and also the PcG body (Carmo-Fonseca et al., 2010). Even though the PcG bodies were described 15 years ago, no ultrastructural study on the PcG body architecture has been provided to date.

Nowadays, all existed models of the PcG body arise mainly from the biochemical and fluorescence microscopy studies (e.g. Cavalli, 2007; Sexton et al., 2007). The Polycomb body has been considered to be a genuine structure, a novel nuclear body within the nucleus and has been compared to transcription factories in these hypothetical models (Cavalli, 2007; Bantignies et al., 2011; Hodgson and Brock, 2011). Concerning composition, the Polycomb body was thought to be formed by accumulation of PcG proteins and non-coding RNAs, localized in the interchromatin compartment where genes are looped into it to be co-silenced (Cavalli, 2007; Bantignies et al., 2011; Hodgson and Brock, 2011; see also Fig. 5.1). It was also termed "gene silencing factory" (Bantignies et al., 2011; Hodgson and Brock, 2011).

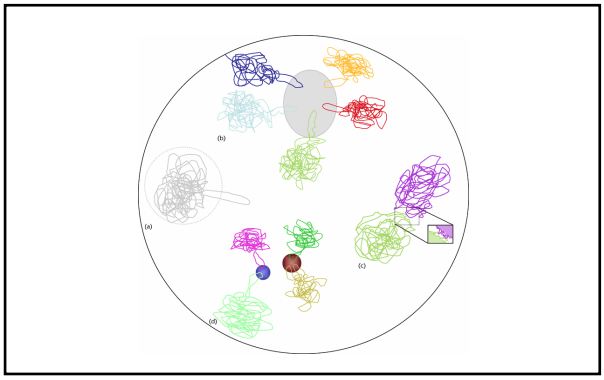

Figure 5.1. Nuclear positioning of looped-genes: (a) looping out of specific locus upon activation, (b) concentration of rDNA loci located on different chromosomes to form nucleolus, (c) natural intermingling between different chromosome territories and (d) long-distance chromosomal interactions between two loci into repressive bodies (blue, e.g. Polycomb bodies), or into active RNA factories (red). Adapted from Grimaud (2011).

In our first study, we established the fine structure of the "PcG body." The essence of the "PcG body," at the electron microscopy level, was associated with locally accumulated and BMI1 labeled heterochromatin fascicles. Thus, the concept that the PcG body is a typical nuclear body situated in the interchromatin compartment is not correct (Smigova et al., 2011). In the second study, by using molecular crowding approach, the chromatin nature of the PcG body was shown experimentally.

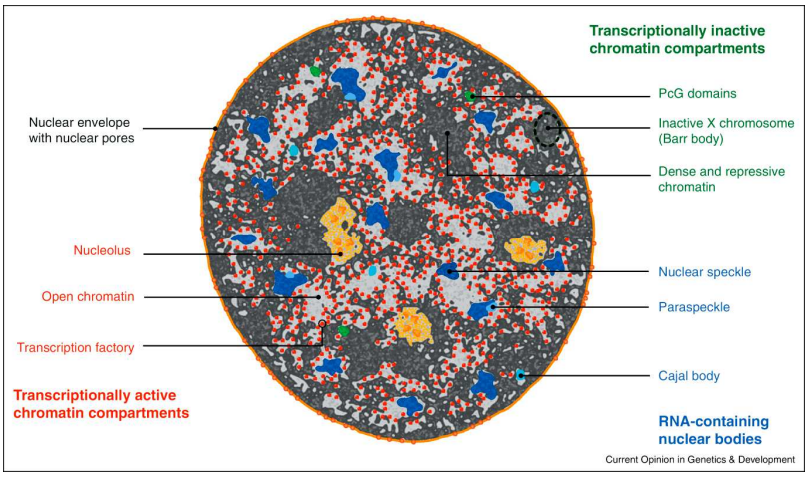

Figure 5.2. Based on our results, PcG bodies were classified as repressive chromatin domains. The figure represents a scheme of nuclear architecture with subcompartments that involve RNA for their structural integrity. These comprise DNA-free mobile nuclear bodies (blue) and chromatin compartments. The latter are subdivided into transcriptionally active (red) and inactive (green) chromatin regions as well as the boundaries between these. Adapted from Caudron-Herger and Rippe (2012).

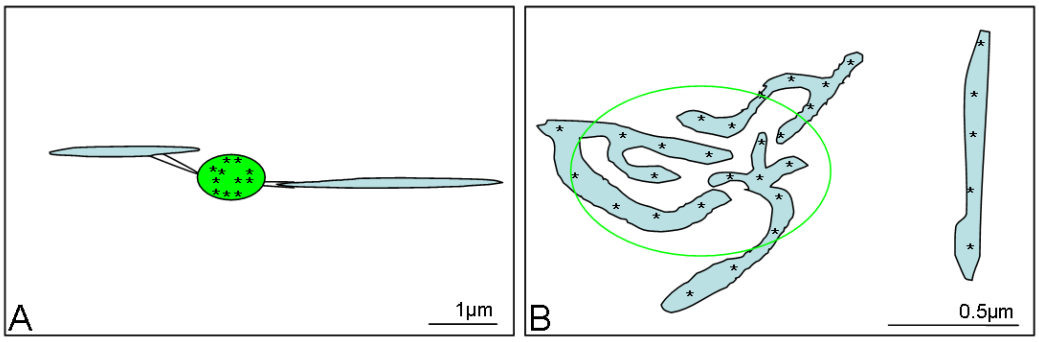

Figure 5.3. An previous vs. a new "PcG body" model. Condensed chromatin fascicle (blue), BMI1 protein (black asterisk), PcG body (green ellipse in A, respectively a green line in the form of ellipse delimitig a "PcG body" in B). In previous models (A), PcG foci were considered to be the typical nuclear bodies formed by accumulations of PcG proteins in the interchromatin compartment. In our model (B), PcG foci represent the chromatin domains formed by an accumulation of condensed chromatin (heterochromatin) fascicles.

The term "PcG body" was replaced with the term "PcG chromatin domain" (Smigova etal., 2011; Caudron-Herger and Rippe, 2012; see Fig. 5.2) and a new "PcG body" model was generated (see Fig. 5.3B).

Simultaneously, the importance of a topological rather than sequence-based mechanism for PcG target interactions was shown by Tolhuis et al. (2011). It is known that certain genomic loci that are distinct in the linear genome may come together in nuclear space by folding of the chromosome fiber. Previously, such interaction was found in *Drosophila* for two PcG target genomic loci spaced 10 Mb apart (Bantignies et al., 2011). Tolhuis et al. (2011) mapped the long-range chromatin interactions among PcG target genes on a genome-wide scale. They showed that PcG target sites extensively and specifically interact with each other even when they are separated by megabases of sequence, but they also found that these long-range interactions occur almost exclusively on the same chromosome arm. Although results of both studies more or less demonstrate the long-range interactions between PcG target genes, they are interpreted differently. Whereas Bantignies et al. (2011) presented their result to reflect the role of the labeled PcG foci as a gene silencing factory, Tolhuis et al. (2011) did not generalize their results and rather highlighted the importance of the chromosome architecture for PcG target interactions.

Our result has also a straightforward importance for further research. Whereas earlier studies documented that the PcG foci as ribonucleoproteinaceous structures, the more recent research rather focus on the distribution of PcG target genes in the cell nucleus and the role of nuclear compartmentalization in Polycomb regulation. The traditional model (nowadays called as an alternative model) where PcG foci has been considered to be a nucleation sites onto which PcG target genes move to become silenced (Fig. 5.3A) was replaced by a more recent view that PcG foci are formed by PcG proteins binding to their target chromatin (Figs. 5.4, 5.5A). It is thought that PcG proteins enrichments in PcG foci depend on the length of genomic domains coated by PcG proteins (Cheutin and Cavalli, 2012). The idea is that PcG complexes are concentrated in certain nuclear neighborhoods simply because their targets are clustered in genomic neighborhoods (Fig. 5.4a) or are physically co-localizing in the nucleus (Fig. 5.4b) (Pirrotta and Li, 2011).

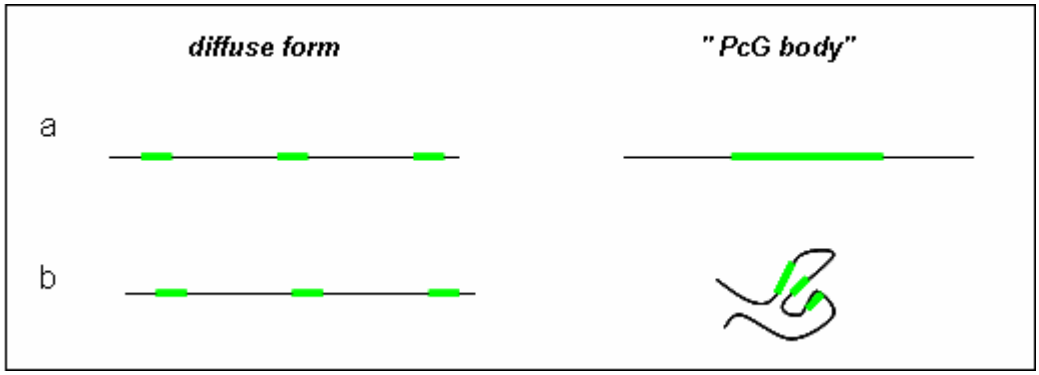

Figure 5.4. Two different hypothetical views on the PcG target genes clustering. The PcG foci are thought to be formed by (a) genomic or (b) spatial accumulation of PcG proteins binding to their target genes. Linear DNA (black line), PcG target genes occupied by PcG proteins (green line).

Both new hypotheses emphasize the importance of PcG target genes for PcG foci nature and are closer to our electron microscopy result (Smigova et al., 2011) where BMI1 label was detected to be enriched within condensed chromatin fascicles throughout the nucleus and the accumulation of label in PcG foci was shown to be generated by the local accumulation of heterochromatin fascicles in space. However, we are of the opinion that the clustering of PcG target genes in PcG foci is rather of the spatial than genomic origin. As shown by morphometric analysis of gold label, PcG target sites are specifically enriched over condensed chromatin (heterochromatin) and more or less evenly distributed throughout the nucleus

(Smigova et al., 2011). The spatial clustering theory is also in agreement with the results on long-range interactions between PcG target genes (e.g. Bantignies et al., 2011; Tolhuis et al., 2011). Importantly, our results also show that PcG foci correspond to chromatin domains formed by accumulations of condensed chromatin fascicles rather than to accumulations of looped genes in the interchromatin compartment. Also, it is hard to imagine a DNA poor environment (e.g. Raska, 1995) with the accumulation of PcG target genes that could form such large and intensive fluorescent structures as PcG foci are.

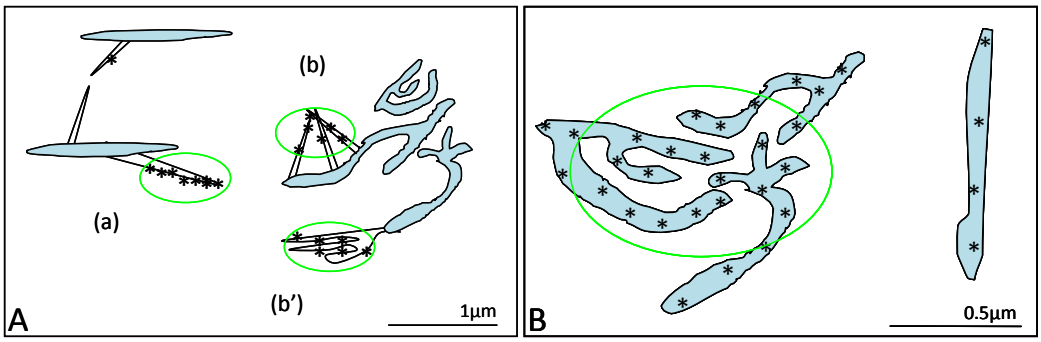

Figure 5.5. Different views on the "PcG body" formed by (a) genomic or (b, b´, B) spatial clustering of PcG target genes. Condensed chromatin fascicle (blue), BMI1 protein (black asterisk), PcG body (a green line in the form of ellipse delimitig a "PcG body"). (A) In some new models, PcG foci are thought to be formed by PcG proteins binding to their target chromatin but they are still localized in the interchromatin compartment. (B) In our model, PcG proteins are localized in the condensed chromatin fascicles throught the nucleus and PcG foci represent the chromatin domains formed by accumulations of the condensed chromatin fascicles. The chromatin nature of the PcG foci was also shown by molecular crowding experiments.

Concerning the diffuse form, it is thought to be the result of the isolated distribution of PcG complexes (Pirrotta and Li, 2011). Two scenarios why PcG complexes are isolated exist. In the first scenario, PcG complexes are isolated because they are not closely linked with others on the genome. In the second scenario, they have transiently looped away from the other PcG sites (reviewed in Pirrotta and Li, 2011). Based on our results, where PcG proteins were exclusively detected in condensed chromatin fascicles and distributed more or less evenly throughout the condensed chromatin (Smigova et al., 2011), the third scenario should be created. The distribution of the PcG target genes, in the context whether they are or are not accumulated into PcG foci, should be perceived in the three-dimensional space of the cell nucleus with its subcompartments. According to our results, the diffuse form of

PcG complexes represents the PcG labeled heterochromatin fascicles that are not accumulated in space so much as they are accumulated at the sites of PcG foci. Because of the structural identity of both PcG forms, to establish the fine structure of the PcG body was difficult and without the using of the CLEM technique even impossible.

The correlation between the enrichment of PcG proteins and the enrichment of genomic regions was later also shown by Cheutin and Cavalli (2012). They calculated the ratio between the maximum intensity of PC-GFP (PC, Polycomb protein is a member of PRC1) measured within PcG bodies and the average PC-GFP intensity of the cell nucleus within optical sections of epidermal cells in *Drosophila* embryos. To test wheather the intensity of PcG foci correlates with the length of genomic regions associated with PcG proteins, they performed immuno-FISH experiments using antibodies against PcG proteins and DNA probes that hybridize to genomic gene clusters coated with PcG proteins. By measurements of fluorescence intensities, they found that the amount of PcG proteins within a PcG body depends on the linear size of the genomic region coated by PcG proteins binding to their target chromatin. However, the question is whether the used FISH technique and the experiments based on the measurements of fluorescence intensities are sufficient enough to solve this problem. Further, according to DAPI poor staining and time-lapse chromatin motion experiments, where they found that PcG bodies move within volumes slightly larger than those of condensed chromatin domains, they still localize the PcG bodies into euchromatin. They highlight that their co-localization is consistent with the electron microscopy study of Cmarko et al. (2003) where in mammalian cells PRC1 proteins were localized in the perichromatin region (see Discussion I). This is in contrast with our results where BMI1 protein was clearly localized into condensed chromain fascicles and PcG bodies were described as DNA rich domains (Smigova et al., 2011). Concerning DNA detection, there is a known problem due to the probe (e.g. DAPI, antibodies) penetration/epitope accessibility within compacted chromatin structures (Smigova et al., 2011). This is the reason why the most condensed chromatin areas appear to be DAPI poor. Therefore, to overcome this problem, in our study we used rather distamycin A/DAPI staining than DAPI alone. Alternatively, immunocytochemistry with antibody against DNA with increased concentration of detergent was used. Moreover, our research was done

at electron microscopy level which allows to clearly distinguish the condensed labeled fascicles. Contrary to the study of Cmarko et al. (2003), the strength of our study is also based on the high and clear-cut BMI1 immunogold labeling. Here, we would also like to touch the matter of the perichromatin region. The perichromatin region was originally established by Monneron and Bernhard (1969) as a region rich in fibrogranular material, where dispersed chromatin cannot be morphologically distinguished from ribonucleoprotein perichromatin fibrils that are considered to be the primary products of transcription (Monneron and Bernhard, 1969; Bouchet-Marquis et al., 2006; Fakan and van Driel, 2007). Later, the width of the perichromatin region has been estimated to be about 100-200 nm, according to the length of chromatin fibers looping out from the higher order chromatin (reviewed in Fakan and van Driel., 2007). Also, gene silencing was localized into this compartment (Cmarko et al., 2003). However, the estimated length of looped chromatin fibers disproves the existence of long-range loops that could expand up to several µm and are considered to be essential for gene silencing as well as questions the existence of the perichromatin region as defined in Fakan and van Driel (2007).

Further, although PcG proteins are mostly studied during development (e.g. also Bantignies et al., 2011, Cheutin and Cavalli, 2012), our study was performed on decided cells. In early development, PcG function seems to be largely restricted to the regulation of developmental genes and as such predicted to play a pivotal part in integrating signals that determine lineage choices (Pietersen and Lohuizen, 2008). Most of PcG proteins in stem cells occupy the bivalent chromatin domains and allow the postponement of lineage choices until the appropriate signals are received (Pietersen and Lohuizen, 2008). Bivalent domains in mouse and human cells represent the chromatin domains with coexistence of repressive marks (H3K27me3) and activating marks (H3K4me3) (Azuara et al. 2006; Bernstein et al. 2006; Lee et al. 2006). Therefore, in embryonic stem cell, the label of H3K27me3 does not immediately means the repressive domain. Moreover, concerning PcG proteins, bivalent genes bound by both PRC1 and PRC2 are more refractory to the repressive H3K27me3 mark loss compared with those bound by PRC2 alone (Ku et al., 2008; Delest et al., 2012). In *Drosophila*, H3K27me3/H3K4me3 overlapping regions are rarely observed (Schuettengruber et al., 2009), but other varieties of bivalent domains have been detected (e.g. H3K27me3/H3K27ac) (Schwartz et al., 2010).

Under the electron microscope, chromatin marked by bivalent domains has a structure of 10 nm chromatin fiber (Ahmed et al., 2009). Compact chromatin domains, consisting of densely packed 10 nm fibers, become to be detected from two-cell stage embryos during mouse development, they disappear in eight-cell stage embryos and then they appear again (Ahmed et al., 2009). Although these cells contain the same amount of genetic material, there are clear and dramatic differences in the way the genetic material is organized (Fussner et al., 2011). The effective length of the genome must be shortened, but since the fractional volume of the nucleus occupied by chromatin is typically less than 50%, the decision to compact chromatin has more to do with the creation of functional domains that characterize different cell types rather than to fit the DNA into the nucleus (Rapkin et al., 2012). The changes in chromatin architecture should also include the formation of typical functional PcG chromatin domains, instead of the PcG labeled bivalent chromatin foci. Perhaps, this is also the reason why PcG proteins were observed to be dispersed and the foci resembling PcG foci disappeared during embryonic stem cell differentiation (Ren et al., 2008). Despite the presence of PcG foci in embryonic stem cells, however, because of the enormous number of unknowns and the unstable chromatin state, we do not consider the stem cells to be a right model (nowadays) to study the nature of the real PcG foci. Rather, embryonic stem cells offer the possibility to study the variabilities in expression of PcG target genes and represent an ideal genetic model. Thus, unfortunately, transformed cell lines have appeared as the only possible model to be used to study the nature of the so-called PcG body. In primary cells, PcG foci are much less distinct (Voncken et al., 1999; Ren et al., 2008) and not convenient for microscopy analysis.

Although the chromatin domains are better to be studied in decided cells, generally, the higher order chromatin structure remains poorly understood up to date. In our work, PcG bodies were shown to correspond to the separated condensed chromatin fascicles. Moreover, we observed that they appear to represent the most dense chromatin domains in the nucleus of the U-2 OS cells. However, the detailed architecture of the chromatin organized into PcG bodies remains to be elucidated. New data (van Holde and Zlatanova, 1995; Eltsov et al., 2008; Ahmed et al., 2009; Fussner et al., 2011) suggest that the organization of the genome based on 10 nm chromatin fibers is sufficient to describe the complexities of nuclear organization, including compact chromatin domains that structurally should represent densely

packed 10 nm chromatin fibers (Ahmed et al., 2009). However, recently, other papers where the authors stand up the existence of the 30 nm chromatin fiber have been published (e.g. Kizilyaprak et al., 2011; Scheffer et al., 2011; Bian and Belmont, 2012). This clearly documents that the higher order chromatin fiber folding is difficult and still unresolved task. Also, the future research should be foccused on how to distinguish among phenotypes of different types of heterochromatin by electron microscopy (if possible, also euchromatin). Recently, this was partially resolved using DamID technique (van Steensel et al., 2001; Filion and van Steensel, 2010). Based on the presence of unique combinations of histone marks and chromatin-binding proteins, van Steensel´s group (van Steensel, 2011) distinguished five distinct chromatin types in *Drosophila*. Whereas active housekeeping genes were asigned to YELLOW chromatin, active tissue specific genes were allocated to RED chromatin. On the other side, inactive tissue specific genes were allocated to BLACK chromatin and traditionally called heterochromatin was assigned to GREEN chromatin. Type of chromatin that is characterized by the presence of Polycomb proteins was called BLUE chromatin.

The highest contribution to our research comes from the correlative microscopy. At the light microscopy level, we correlated BMI1-GFP fluorescent signals with signals from the same cells which were immediately fixed and immunolabeled. This approach allowed us to find the enrichment of the PcG foci in DNA or to follow the changes in (PcG) chromatin domains appearance in cells grown under hyperosmotic treatment. To establish the fine structure of the PcG body, the different approaches of the correlative light-electron microscopy were used. However, we consider only the results obtained by correlative light-electron microscopy with implemented high-pressure freezing and freeze substitution approach as appropriate for both the identification, and for the description of the fine stucture of the PcG foci. Importantly, by using the correlative microscopy, our research was performed at the single cell level. Because populations of cells are almost always heterogeneous in structure, function and fate, single cell analysis has recently emerged as an important field of research. At microscopy level, it allows to capture spatio-temporal information within the one cell and thus, to understand the organization or biological processes at better level. In our research, correlative microscopy was also essential to follow the spatio-temporal changes induced in PcG foci in cells grown under

increased molecular crowding conditions (see Results II). Crowding forces vastly increase the association constants for intermolecular interactions and can segregate different macromolecules into discrete phases (Hancock, 2004a). The model that they play a role in compartmentalization of the nucleus is consistent with the properties of compartments (Hancock, 2004a). Generally, molecular crowding represents a convenient experimental model to study the formation/reassembly of nuclear bodies as well as to manipulate the chromatin condensation (Hancock, 2004b). Here, the molecular crowding was used to uncover the nature of the PcG foci, and the chromatin nature of PcG foci was established. We therefore consider a debate on the nature of the PcG foci as irrelevant (e.g. Delest et al., 2012). In our experiments we applied correlation of live cell imaging before and after hyperosmotic treatment with imaging of immunolabeled cells. By this approach, we found that the behaviour of PcG foci under increased crowding conditions vastly differs from the behaviour of typical nuclear bodies. Whereas nuclear bodies like PML nuclear bodies and nucleoli are formed/reassembled under hyperosmotic treatment (Hancock, 2004a, b), PcG foci under molecular crowding conditions disassembled (see Results II). The PcG foci pattern disappeared whatever type of hyperosmotic agent was used and also after release of BMI1 protein from chromatin by DRAQ5. Importantly, we also observed that the pattern of the (PcG) chromatin domains remained the same. Thus, also by experimental approach, the structural basis of the PcG foci was clearly shown to represent rather a condensed chromatin domain than accumulations of PcG proteins.

Concerning gene silencing, our structural data do not allow to contribute much to the mechanism of silencing itself. However, according to our results on the localization of the BMI1 protein into condensed chromatin, it seems that PcG-mediated silencing (its maintenance, if occurs) is rather similar to the Xist-mediated X chromosome inactivation (see Fig. 5.6) than to the suggested hypothetical silencing factory where genes are looped into it to be co-silenced. But to uncover the principle of the PcG-mediated gene silencing, it is important to follow also components of PRC2 complex and target DNA simultaneously. The other question is whether PcG proteins are the only essential gene repressors of the BLUE heterochromatin. For example, (PcG) chromatin domains showed no dependence on PRC1 proteins (BMI1, RING1a) to stay condensed under (not only) molecular crowding conditions (see Results II).

On the other side, the reversibility of the PcG foci disappearance in cells re-incubated in normal growth medium (together in the conserved viability of cells) documents the functional importance of the presence of PRC1 proteins in the condensed (PcG) chromatin domains. The reversibility could signify the possible role of PRC1 proteins in competitive binding of (PcG) chromatin domains in the transcriptionally active nucleus or their role in cellular memory (e.g. see Ringrose and Paro, 2004), rather than the PRC1 importance for the mainenance of the condensed state of chromatin (Wang et al., 2004; Cao et al., 2005; in Martin-Perez et al., 2010).

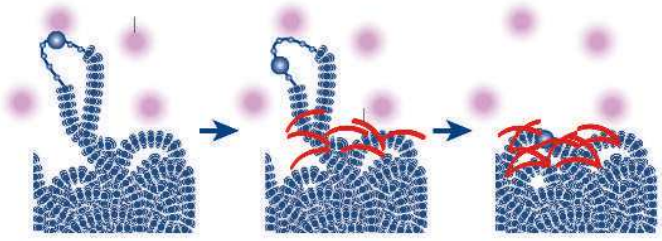

Figure 5.6. The coating of the inactive X chromosome by Xist RNA molecules. Genes initially located outside the domain (purple circles) coated by *Xist* RNA are retracted back inside the *Xist* compartment as they become silenced. Adapted from Fraser and Bickmore (2007).

All together, we identified and established the new nuclear domain (Results I) and described its behaviour under the molecular crowding conditions (see Results II). We are of the opinion that our results have brought a new information into the field of nuclear architecture, specifically in the context of the PcG foci. We have also showed the importance of combining the different microscopical techniques at the single cell level.

6. Conclusions

- In both presented studies, by using correlative imaging, investigations at the **single cell level** were performed. In the first study, **the ultrastructure of the "PcG body"** was characterized. In the second study, the **behaviour of the "PcG body"** under the molecular crowding conditions was established.
- By correlation at fluorescence microscopy level, the PcG foci were shown to represent **DNA-rich structures**.
- Correlative light-electron microscopy (CLEM) with implemented pre-embedding labeling led to a straightforward **identification of the PcG foci**, but their ultrastructure was biased.
- In contrast, using CLEM with implemented high-pressure freezing followed by cryosubstitution, the convenient **structural preservation of the cell** and **high efficiency of the post-embedding immunocytochemistry** was achieved.
- Post-embedding immunogold **BMI1 label** was specifically enriched within **heterochromatin fascicles throughout the nucleus**.
- A nuclear region/domain with a locally increased post-embedding immunogold **label present outside of the heterochromatin structures** was **never** observed.
- Using **correlative light-electron microscopy** (CLEM) with cryosubstituted cells allowed to correlate the live cell imaging of the localization of BMI1-GFP with imaging at the ultrastructural level and thus enabled to **establish the ultrastructure of the PcG body**.
- The nature of the PcG body was associated with **locally accumulated heterochromatin fascicles**, but **not** with a **nuclear body.** A better term to be used is **the PcG chromatin domain.**
- PcG chromatin domains were frequently **associated with the nuclear envelope, together with its invaginations, and with nucleoli**. It is well known that these nuclear areas are frequently associated with heterochromatin structures.
- As shown by morphometric analysis, the **number of gold particles** per unit area of heterochromatin fascicles **outside and inside the PcG chromatin domain** was about **the same**.

- By applying molecular crowding, PcG bodies were **shown to be chromatin domains** rather than typical nuclear bodies localized in the interchromatin compartment.
- Under increased crowding conditions, in comparison with the typical nuclear bodies, vastly **different behaviour of the „PcG bodies" was observed.** Whereas typical nuclear bodies are formed/reassembled under hyperosmotic treatment, **PcG bodies**, concerning spatial PcG proteins accumulation, under crowding conditions **disassembled**.
- In sucrose treated cells, the **translocation of BM1 protein** from chromatin to the **interchromatin compartment** was detected. Using **DRAQ5** staining of living cells, a **similar result** was obtained.
- PcG foci disappearance in hyperosmotic conditions was shown to be a **reversible** process. Upon re-incubation of cells with normal growth medium, PcG protein accumulations recovered apparently to their initial state. **The size, number and position of the re-formed PcG foci were the same as before treatment.**
- PcG foci disappearance and BMI1 release from chromatin was correlated with **hyper-phosphorylation** of BMI1 protein.
- Whereas "PcG bodies" as spatial BMI1 **protein accumulations** under crowding conditions **disassembled,** the pattern of the PcG chromatin **domains remained the same.**
- A similar PcG foci disappearance phenomenon with preservation of PcG chromatin domains was observed by immunolabeling against **another member of the PRC1 complex** (the RING1a protein).
- The generated **new model of the "PcG body"** may help to rectify, and expand the information about, the view how PcG proteins mediated gene silencing occurs.

7. References

Aggarwal, B., D. Chromatin suppression and structural integrity. http://www.abcam.com/index.html?pageconfig=resource&rid=10189&pid=5

Ahmed, K., H. Dehghani, P. Rugg-Gunn, E. Fussner, J. Rossant, and D.P. Bazett-Jones. 2010. Global chromatin architecture reflects pluripotency and lineage commitment in the early mouse embryo. PLoS One. 5:e10531.

Ahmed, K., R. Li, and D.P. Bazett-Jones. 2009. Electron spectroscopic imaging of the nuclear landscape. Methods Mol Biol. 464:415-23.

Albiez, H., M. Cremer, C. Tiberi, L. Vecchio, L. Schermelleh, S. Dittrich, K. Kupper, B. Joffe, T. Thormeyer, J. von Hase, S. Yang, K. Rohr, H. Leonhardt, I. Solovei, C. Cremer, S. Fakan, and T. Cremer. 2006. Chromatin domains and the interchromatin compartment form structurally defined and functionally interacting nuclear networks. Chromosome Res. 14:707-33.

Alkema, M.J., M. Bronk, E. Verhoeven, A. Otte, L.J. van 't Veer, A. Berns, and M. van Lohuizen. 1997. Identification of Bmi1-interacting proteins as constituents of a multimeric mammalian polycomb complex. Genes Dev. 11:226-40.

Amouroux, R., A. Campalans, B. Epe, and J.P. Radicella. 2010. Oxidative stress triggers the preferential assembly of base excision repair complexes on open chromatin regions. Nucleic Acids Res. 38:2878-90.

Azuara, V., P. Perry, S. Sauer, M. Spivakov, H.F. Jorgensen, R.M. John, M. Gouti, M. Casanova, G. Warnes, M. Merkenschlager, and A.G. Fisher. 2006. Chromatin signatures of pluripotent cell lines. Nat Cell Biol. 8:532-8.

Bancaud, A., S. Huet, N. Daigle, J. Mozziconacci, J. Beaudouin, and J. Ellenberg. 2009. Molecular crowding affects diffusion and binding of nuclear proteins in heterochromatin and reveals the fractal organization of chromatin. Embo J. 28:3785-98.

Bannister, A.J., P. Zegerman, J.F. Partridge, E.A. Miska, J.O. Thomas, R.C. Allshire, and T. Kouzarides. 2001. Selective recognition of methylated lysine 9 on histone H3 by the HP1 chromo domain. Nature. 410:120-4.

Bantignies, F., V. Roure, I. Comet, B. Leblanc, B. Schuettengruber, J. Bonnet, V. Tixier, A. Mas, and G. Cavalli. 2011. Polycomb-dependent regulatory contacts between distant Hox loci in *Drosophila*. Cell. 144:214-26.

Barski, A., S. Cuddapah, K. Cui, T.Y. Roh, D.E. Schones, Z. Wang, G. Wei, I. Chepelev, and K. Zhao. 2007. High-resolution profiling of histone methylations in the human genome. Cell. 129:823-37.

Bartlett, J., J. Blagojevic, D. Carter, C. Eskiw, M. Fromaget, C. Job, M. Shamsher, I.F. Trindade, M. Xu, and P.R. Cook. 2006. Specialized transcription factories. Biochem Soc Symp:67-75.

Beck, J.S. 1961. Variations in the morphological patterns of "autoimmune" nuclear fluorescence. Lancet. 1:1203-5.

Bednar, J., R.A. Horowitz, S.A. Grigoryev, L.M. Carruthers, J.C. Hansen, A.J. Koster, and C.L. Woodcock. 1998. Nucleosomes, linker DNA, and linker histone form a unique structural motif that directs the higher-order folding and compaction of chromatin. Proc Natl Acad Sci U S A. 95:14173-8.

Berger, S.L. 2007. The complex language of chromatin regulation during transcription. Nature. 447:407-12.

Bernardi, R., and P.P. Pandolfi. 2007. Structure, dynamics and functions of promyelocytic leukaemia nuclear bodies. Nat Rev Mol Cell Biol. 8:1006-16.

Bernstein, B.E., T.S. Mikkelsen, X. Xie, M. Kamal, D.J. Huebert, J. Cuff, B. Fry, A. Meissner, M. Wernig, K. Plath, R. Jaenisch, A. Wagschal, R. Feil, S.L. Schreiber, and E.S. Lander. 2006. A bivalent chromatin structure marks key developmental genes in embryonic stem cells. Cell. 125:315-26.

Bian, Q., and A.S. Belmont. 2012. Revisiting higher-order and large-scale chromatin organization. Curr Opin Cell Biol. 24:359-66.

Boisvert, F.M., S. van Koningsbruggen, J. Navascues, and A.I. Lamond. 2007. The multifunctional nucleolus. Nat Rev Mol Cell Biol. 8:574-85.

Bouchet-Marquis, C., J. Dubochet, and S. Fakan. 2006. Cryoelectron microscopy of vitrified sections: a new challenge for the analysis of functional nuclear architecture. Histochem Cell Biol. 125:43-51.

Boukarabila, H., A.J. Saurin, E. Batsche, N. Mossadegh, M. van Lohuizen, A.P. Otte, J. Pradel, C. Muchardt, M. Sieweke, and E. Duprez. 2009. The PRC1 Polycomb group complex interacts with PLZF/RARA to mediate leukemic transformation. Genes Dev. 23:1195-206.

Bouteille, M., Laval, M., Dupuy-Coin, A.M. 1974. Localization of nuclear functions as revealed by ultrastructural autoradiography and cytochemistry. In: Busch, H. (Ed.), Cell Nucl., vol. 1, pp. 3 –7.

Boveri, T. 1909. Die Blastomerenkerne von Ascaris megalocephala und die Theorie der Chromosomenindividualität. Arch. Zellforsch. 3, 181–268.

Brown, E., J. Mantell, D. Carter, G. Tilly, and P. Verkade. 2009. Studying intracellular transport using high-pressure freezing and Correlative Light Electron Microscopy. Semin Cell Dev Biol. 20:910-9.

Buchenau, P., J. Hodgson, H. Strutt, and D.J. Arndt-Jovin. 1998. The distribution of polycomb-group proteins during cell division and development in *Drosophila* embryos: impact on models for silencing. J Cell Biol. 141:469-81.

Cao, R., Y. Tsukada, and Y. Zhang. 2005. Role of Bmi-1 and Ring1A in H2A ubiquitylation and Hox gene silencing. Mol Cell. 20:845-54.

Cao, R., L. Wang, H. Wang, L. Xia, H. Erdjument-Bromage, P. Tempst, R.S. Jones, and Y. Zhang. 2002. Role of histone H3 lysine 27 methylation in Polycomb-group silencing. Science. 298:1039-43.

Carmo-Fonseca, M., M.T. Berciano, and M. Lafarga. 2010. Orphan nuclear bodies. Cold Spring Harb Perspect Biol. 2:a000703.

Caron, H., B. van Schaik, M. van der Mee, F. Baas, G. Riggins, P. van Sluis, M.C. Hermus, R. van Asperen, K. Boon, P.A. Voute, S. Heisterkamp, A. van Kampen, and R. Versteeg. 2001. The human transcriptome map: clustering of highly expressed genes in chromosomal domains. Science. 291:1289-92.

Caudron-Herger, M., and K. Rippe. 2012. Nuclear architecture by RNA. Curr Opin Genet Dev. 22:179-87.

Cavalli, G. 2007. Chromosome kissing. Curr Opin Genet Dev. 17:443-50.

Cavalli, G., and R. Paro. 1998. The *Drosophila* Fab-7 chromosomal element conveys epigenetic inheritance during mitosis and meiosis. Cell. 93:505-18.

Cmarko, D., J. Smigova, L. Minichova, and A. Popov. 2008. Nucleolus: the ribosome factory. Histol Histopathol. 23:1291-8.

Cmarko, D., P.J. Verschure, T.E. Martin, M.E. Dahmus, S. Krause, X.D. Fu, R. van Driel, and S. Fakan. 1999. Ultrastructural analysis of transcription and splicing in the cell nucleus after bromo-UTP microinjection. Mol Biol Cell. 10:211-23.

Cmarko, D., P.J. Verschure, A.P. Otte, R. van Driel, and S. Fakan. 2003. Polycomb group gene silencing proteins are concentrated in the perichromatin compartment of the mammalian nucleus. J Cell Sci. 116:335-43.

Cook, P.R. 1999. The organization of replication and transcription. Science. 284:1790-5.

Craig, J.M. 2005. Heterochromatin--many flavours, common themes. Bioessays. 27:17-28.

Cremer, T., and C. Cremer. 2006. Rise, fall and resurrection of chromosome territories: a historical perspective. Part II. Fall and resurrection of chromosome territories during the 1950s to 1980s. Part III. Chromosome territories and the functional nuclear architecture: experiments and models from the 1990s to the present. Eur J Histochem. 50:223-72.

Cremer, T., A. Kurz, R. Zirbel, S. Dietzel, B. Rinke, E. Schrock, M.R. Speicher, U. Mathieu, A. Jauch, P. Emmerich, H. Scherthan, T. Ried, C. Cremer, and P. Lichter. 1993. Role of chromosome territories in the functional compartmentalization of the cell nucleus. Cold Spring Harb Symp Quant Biol. 58:777-92.

Czermin, B., R. Melfi, D. McCabe, V. Seitz, A. Imhof, and V. Pirrotta. 2002. *Drosophila* enhancer of Zeste/ESC complexes have a histone H3 methyltransferase activity that marks chromosomal Polycomb sites. Cell. 111:185-96.

Dehghani, H., G. Dellaire, and D.P. Bazett-Jones. 2005. Organization of chromatin in the interphase mammalian cell. Micron. 36:95-108.

Delest, A., T. Sexton, and G. Cavalli. 2012. Polycomb: a paradigm for genome organization from one to three dimensions. Curr Opin Cell Biol. 24:405-14.

Dellaire, G., R.W. Ching, H. Dehghani, Y. Ren, and D.P. Bazett-Jones. 2006. The number of PML nuclear bodies increases in early S phase by a fission mechanism. J Cell Sci. 119:1026-33.

Dellino, G.I., Y.B. Schwartz, G. Farkas, D. McCabe, S.C. Elgin, and V. Pirrotta. 2004. Polycomb silencing blocks transcription initiation. Mol Cell. 13:887-93.

Derenzini, M. 1979. Fine structure of chromatin as visualized in thin sections with the Gautier selective stain for DNA. J Ultrastruct Res. 69:239-48.

Derenzini, M., A. Viron, and E. Puvion. 1984. Structural organization of rat hepatocyte chromatin as visualized in thin frozen sections selectively stained for DNA. Eur J Cell Biol. 33:148-56.

Dubochet, J., and N. Sartori Blanc. 2001. The cell in absence of aggregation artifacts. Micron. 32:91-9.

Dundr, M. 2011. Seed and grow: a two-step model for nuclear body biogenesis. J Cell Biol. 193:605-6.

Edward, R. 2009. Use of DNA-specific anthraquinone dyes to directly reveal cytoplasmic and nuclear boundaries in live and fixed cells. Mol Cells. 27:391-6.

Ekstrom, J., L. www.bch.msu.edu/faculty/ekstrom.htm

Eltsov, M., K.M. Maclellan, K. Maeshima, A.S. Frangakis, and J. Dubochet. 2008. Analysis of cryo-electron microscopy images does not support the existence of 30-nm chromatin fibers in mitotic chromosomes *in situ*. Proc Natl Acad Sci U S A. 105:19732-7.

Enderle, D., C. Beisel, M.B. Stadler, M. Gerstung, P. Athri, and R. Paro. 2011. Polycomb preferentially targets stalled promoters of coding and noncoding transcripts. Genome Res. 21:216-26.

Fakan, S. 1994. Perichromatin fibrils are *in situ* forms of nascent transcripts. Trends Cell Biol. 4:86-90.

Fakan, S. 2004. The functional architecture of the nucleus as analysed by ultrastructural cytochemistry. Histochem Cell Biol. 122:83-93.

Fakan, S., G. Leser, and T.E. Martin. 1984. Ultrastructural distribution of nuclear ribonucleoproteins as visualized by immunocytochemistry on thin sections. J Cell Biol. 98:358-63.

Fakan, S., and R. van Driel. 2007. The perichromatin region: a functional compartment in the nucleus that determines large-scale chromatin folding. Semin Cell Dev Biol. 18:676-81.

Faro-Trindade, I., and P.R. Cook. 2006. Transcription factories: structures conserved during differentiation and evolution. Biochem Soc Trans. 34:1133-7.

Fey, E.G., G. Krochmalnic, and S. Penman. 1986. The nonchromatin substructures of the nucleus: the ribonucleoprotein (RNP)-containing and RNP-depleted matrices analyzed by sequential fractionation and resinless section electron microscopy. J Cell Biol. 102:1654-65.

Filion, G.J., and B. van Steensel. 2010. Reassessing the abundance of H3K9me2 chromatin domains in embryonic stem cells. Nat Genet. 42:4; author reply 5-6.

Finan, J.D., H.A. Leddy, and F. Guilak. 2011. Osmotic stress alters chromatin condensation and nucleocytoplasmic transport. Biochem Biophys Res Commun. 408:230-5.

Francis, N.J., R.E. Kingston, and C.L. Woodcock. 2004. Chromatin compaction by a polycomb group protein complex. Science. 306:1574-7.

Fraser, P., and W. Bickmore. 2007. Nuclear organization of the genome and the potential for gene regulation. Nature. 447:413-7.

Fricker, M., M. Hollinshead, N. White, and D. Vaux. 1997. Interphase nuclei of many mammalian cell types contain deep, dynamic, tubular membrane-bound invaginations of the nuclear envelope. J Cell Biol. 136:531-44.

Fussner, E., R.W. Ching, and D.P. Bazett-Jones. 2011. Living without 30nm chromatin fibers. Trends Biochem Sci. 36:1-6.

Gall, J.G. 2003. The centennial of the Cajal body. Nat Rev Mol Cell Biol. 4:975-80.

Gasser, S.M., and U.K. Laemmli. 1987. Improved methods for the isolation of individual and clustered mitotic chromosomes. Exp Cell Res. 173:85-98.

Gil, J., and G. Peters. 2006. Regulation of the INK4b-ARF-INK4a tumour suppressor locus: all for one or one for all. Nat Rev Mol Cell Biol. 7:667-77.

Gilbert, N., S. Boyle, H. Fiegler, K. Woodfine, N.P. Carter, and W.A. Bickmore. 2004. Chromatin architecture of the human genome: gene-rich domains are enriched in open chromatin fibers. Cell. 118:555-66.

Gorisch, S.M., M. Wachsmuth, C. Ittrich, C.P. Bacher, K. Rippe, and P. Lichter. 2004. Nuclear body movement is determined by chromatin accessibility and dynamics. Proc Natl Acad Sci U S A. 101:13221-6.

Grandjean, V., L. O'Neill, T. Sado, B. Turner, and A. Ferguson-Smith. 2001. Relationship between DNA methylation, histone H4 acetylation and gene expression in the mouse imprinted Igf2-H19 domain. FEBS Lett. 488:165-9.

Grimaud, C. 2011. Chromatin Structure and Domains. In: eLS. John Wiley & Sons Ltd, Chichester.
http://www.els.net [doi: 10.1002/9780470015902.a0005279.pub2]

Grimaud, C., F. Bantignies, M. Pal-Bhadra, P. Ghana, U. Bhadra, and G. Cavalli. 2006. RNAi components are required for nuclear clustering of Polycomb group response elements. Cell. 124:957-71.

Gunster, M.J., F.M. Raaphorst, K.M. Hamer, J.L. den Blaauwen, E. Fieret, C.J. Meijer, and A.P. Otte. 2001. Differential expression of human Polycomb group proteins in various tissues and cell types. J Cell Biochem Suppl. Suppl 36:129-43.

Gunster, M.J., D.P. Satijn, K.M. Hamer, J.L. den Blaauwen, D. de Bruijn, M.J. Alkema, M. van Lohuizen, R. van Driel, and A.P. Otte. 1997. Identification and characterization of interactions between the vertebrate polycomb-group protein BMI1 and human homologs of polyhomeotic. Mol Cell Biol. 17:2326-35.

Hancock, R. 2004. Internal organisation of the nucleus: assembly of compartments by macromolecular crowding and the nuclear matrix model. Biol Cell. 96:595-601.

Hancock, R. 2004. A role for macromolecular crowding effects in the assembly and function of compartments in the nucleus. J Struct Biol. 146:281-90.

Heitz, E. 1928. Das Heterochromatin der Moose. Jarbuch Wiss. Bot. 69:762–780

Heride, C., M. Ricoul, K. Kieu, J. von Hase, V. Guillemot, C. Cremer, K. Dubrana, and L. Sabatier. 2010. Distance between homologous chromosomes results from chromosome positioning constraints. J Cell Sci. 123:4063-75.

Hernandez-Munoz, I., P. Taghavi, C. Kuijl, J. Neefjes, and M. van Lohuizen. 2005. Association of BMI1 with polycomb bodies is dynamic and requires PRC2/EZH2 and the maintenance DNA methyltransferase DNMT1. Mol Cell Biol. 25:11047-58.

Hernandez-Verdun, D. 2006. The nucleolus: a model for the organization of nuclear functions. Histochem Cell Biol. 126:135-48.

Hodgson, J.W., and H.W. Brock. 2011. Are polycomb group bodies gene silencing factories? Cell. 144:170-1.

Horard, B., C. Tatout, S. Poux, and V. Pirrotta. 2000. Structure of a polycomb response element and *in vitro* binding of polycomb group complexes containing GAGA factor. Mol Cell Biol. 20:3187-97.

Hu, Y., I. Kireev, M. Plutz, N. Ashourian, and A.S. Belmont. 2009. Large-scale chromatin structure of inducible genes: transcription on a condensed, linear template. J Cell Biol. 185:87-100.

Hubner, M.R., and D.L. Spector. 2010. Chromatin dynamics. Annu Rev Biophys. 39:471-89.

Chen, D., M. Dundr, C. Wang, A. Leung, A. Lamond, T. Misteli, and S. Huang. 2005. Condensed mitotic chromatin is accessible to transcription factors and chromatin structural proteins. J Cell Biol. 168:41-54.

Cheutin, T., and G. Cavalli. 2012. Progressive polycomb assembly on H3K27me3 compartments generates polycomb bodies with developmentally regulated motion. PLoS Genet. 8:e1002465.

Jackson, D.A., F.J. Iborra, E.M. Manders, and P.R. Cook. 1998. Numbers and organization of RNA polymerases, nascent transcripts, and transcription units in HeLa nuclei. Mol Biol Cell. 9:1523-36.

Jaenisch, R., and A. Bird. 2003. Epigenetic regulation of gene expression: how the genome integrates intrinsic and environmental signals. Nat Genet. 33 Suppl:245-54.

Jenuwein, T., and C.D. Allis. 2001. Translating the histone code. Science. 293:1074-80.

Kalmarova, M., E. Smirnov, M. Masata, K. Koberna, A. Ligasova, A. Popov, and I. Raska. 2007. Positioning of NORs and NOR-bearing chromosomes in relation to nucleoli. J Struct Biol. 160:49-56.

Kizilyaprak, C., D. Spehner, D. Devys, and P. Schultz. 2011. The linker histone H1C contributes to the SCA7 nuclear phenotype. Nucleus. 2:444-54.

Kouzarides, T. 2007. Chromatin modifications and their function. Cell. 128:693-705.

Krause, S., S. Fakan, K. Weis, and E. Wahle. 1994. Immunodetection of poly(A) binding protein II in the cell nucleus. Exp Cell Res. 214:75-82.

Kreth, G., J. Finsterle, J. von Hase, M. Cremer, and C. Cremer. 2004. Radial arrangement of chromosome territories in human cell nuclei: a computer model approach based on gene density indicates a probabilistic global positioning code. Biophys J. 86:2803-12.

Ku, M., R.P. Koche, E. Rheinbay, E.M. Mendenhall, M. Endoh, T.S. Mikkelsen, A. Presser, C. Nusbaum, X. Xie, A.S. Chi, M. Adli, S. Kasif, L.M. Ptaszek, C.A. Cowan, E.S. Lander, H. Koseki, and B.E. Bernstein. 2008. Genomewide analysis of PRC1 and PRC2 occupancy identifies two classes of bivalent domains. PLoS Genet. 4:e1000242.

Kurz, A., S. Lampel, J.E. Nickolenko, J. Bradl, A. Benner, R.M. Zirbel, T. Cremer, and P. Lichter. 1996. Active and inactive genes localize preferentially in the periphery of chromosome territories. J Cell Biol. 135:1195-205.

Kuzmichev, A., T. Jenuwein, P. Tempst, and D. Reinberg. 2004. Different EZH2-containing complexes target methylation of histone H1 or nucleosomal histone H3. Mol Cell. 14:183-93.

Kuzmichev, A., R. Margueron, A. Vaquero, T.S. Preissner, M. Scher, A. Kirmizis, X. Ouyang, N. Brockdorff, C. Abate-Shen, P. Farnham, and D. Reinberg. 2005. Composition and histone substrates of polycomb repressive group complexes change during cellular differentiation. Proc Natl Acad Sci U S A. 102:1859-64.

Lafarga, M., M.T. Berciano, E. Pena, I. Mayo, J.G. Castano, D. Bohmann, J.P. Rodrigues, J.P. Tavanez, and M. Carmo-Fonseca. 2002. Clastosome: a subtype of nuclear body enriched in 19S and 20S proteasomes, ubiquitin, and protein substrates of proteasome. Mol Biol Cell. 13:2771-82.

Lachner, M., D. O'Carroll, S. Rea, K. Mechtler, and T. Jenuwein. 2001. Methylation of histone H3 lysine 9 creates a binding site for HP1 proteins. Nature. 410:116-20.

Lamond, A.I., and W.C. Earnshaw. 1998. Structure and function in the nucleus. Science. 280:547-53.

Langowski, J., and D.W. Heermann. 2007. Computational modeling of the chromatin fiber. Semin Cell Dev Biol. 18:659-67.

Larsson, S.H., J.P. Charlieu, K. Miyagawa, D. Engelkamp, M. Rassoulzadegan, A. Ross, F. Cuzin, V. van Heyningen, and N.D. Hastie. 1995. Subnuclear localization of WT1 in splicing or transcription factor domains is regulated by alternative splicing. Cell. 81:391-401.

Lee, M.G., C. Wynder, D.A. Bochar, M.A. Hakimi, N. Cooch, and R. Shiekhattar. 2006. Functional interplay between histone demethylase and deacetylase enzymes. Mol Cell Biol. 26:6395-402.

Levine, S.S., I.F. King, and R.E. Kingston. 2004. Division of labor in polycomb group repression. Trends Biochem Sci. 29:478-85.

Lewis, E.B. 1978. A gene complex controlling segmentation in Drosophila. Nature. 276:565-70.

Li, L., K. Roy, S. Katyal, X. Sun, S. Bleoo, and R. Godbout. 2006. Dynamic nature of cleavage bodies and their spatial relationship to DDX1 bodies, Cajal bodies, and gems. Mol Biol Cell. 17:1126-40.

Liang, Z., and M.D. Biggin. 1998. Eve and ftz regulate a wide array of genes in blastoderm embryos: the selector homeoproteins directly or indirectly regulate most genes in *Drosophila*. Development. 125:4471-82.

Luger, K., and J.C. Hansen. 2005. Nucleosome and chromatin fiber dynamics. Curr Opin Struct Biol. 15:188-96.

Lund, A.H., and M. van Lohuizen. 2004. Polycomb complexes and silencing mechanisms. Curr Opin Cell Biol. 16:239-46.

Maertens, G.N., S. El Messaoudi-Aubert, T. Racek, J.K. Stock, J. Nicholls, M. Rodriguez-Niedenfuhr, J. Gil, and G. Peters. 2009. Several distinct polycomb complexes regulate and co-localize on the INK4a tumor suppressor locus. PLoS One. 4:e6380.

Mahy, N.L., P.E. Perry, S. Gilchrist, R.A. Baldock, and W.A. Bickmore. 2002. Spatial organization of active and inactive genes and noncoding DNA within chromosome territories. J Cell Biol. 157:579-89.

Maniatis, T., and R. Reed. 2002. An extensive network of coupling among gene expression machines. Nature. 416:499-506.

Mao, Y.S., B. Zhang, and D.L. Spector. 2011. Biogenesis and function of nuclear bodies. Trends Genet. 27:295-306.

Mari, P.O., V. Verbiest, S. Sabbioneda, A.M. Gourdin, N. Wijgers, C. Dinant, A.R. Lehmann, W. Vermeulen, and G. Giglia-Mari. 2010. Influence of the live cell DNA marker DRAQ5 on chromatin-associated processes. DNA Repair (Amst). 9:848-55.

Martin, R.M., and M.C. Cardoso. 2010. Chromatin condensation modulates access and binding of nuclear proteins. FASEB J. 24:1066-72.

Martin, R.M., H. Leonhardt, and M.C. Cardoso. 2005. DNA labeling in living cells. Cytometry A. 67:45-52.

Martinez, A.M., and G. Cavalli. 2006. The role of polycomb group proteins in cell cycle regulation during development. Cell Cycle. 5:1189-97.

Martini, E., D.M. Roche, K. Marheineke, A. Verreault, and G. Almouzni. 1998. Recruitment of phosphorylated chromatin assembly factor 1 to chromatin after UV irradiation of human cells. J Cell Biol. 143:563-75.

Martin-Perez, D., M.A. Piris, and M. Sanchez-Beato. 2010. Polycomb proteins in hematologic malignancies. Blood. 116:5465-75.

Matera, A.G. 1999. Nuclear bodies: multifaceted subdomains of the interchromatin space. Trends Cell Biol. 9:302-9.

Matera, A.G., M. Izaguire-Sierra, K. Praveen, and T.K. Rajendra. 2009. Nuclear bodies: random aggregates of sticky proteins or crucibles of macromolecular assembly? Dev Cell. 17:639-47.

McDonald, K.L., M. Morphew, P. Verkade, and T. Muller-Reichert. 2007. Recent advances in high-pressure freezing: equipment- and specimen-loading methods. Methods Mol Biol. 369:143-73.

Mikkelsen, T.S., M. Ku, D.B. Jaffe, B. Issac, E. Lieberman, G. Giannoukos, P. Alvarez, W. Brockman, T.K. Kim, R.P. Koche, W. Lee, E. Mendenhall, A. O'Donovan, A. Presser, C. Russ, X. Xie, A. Meissner, M. Wernig, R. Jaenisch, C. Nusbaum, E.S. Lander, and B.E. Bernstein. 2007. Genome-wide maps of chromatin state in pluripotent and lineage-committed cells. Nature. 448:553-60.

Mintz, P.J., S.D. Patterson, A.F. Neuwald, C.S. Spahr, and D.L. Spector. 1999. Purification and biochemical characterization of interchromatin granule clusters. Embo J. 18:4308-20.

Mishra, R.K. and Karch, F. 1999. Boundaries that demarcate structural and functional domains of chromatin. J. Biosci. 24, 377–399.

Misteli, T. 2000. Cell biology of transcription and pre-mRNA splicing: nuclear architecture meets nuclear function. J Cell Sci. 113 (Pt 11):1841-9.

Misteli, T. 2001. Protein dynamics: implications for nuclear architecture and gene expression. Science. 291:843-7.

Misteli, T., and D.L. Spector. 1998. The cellular organization of gene expression. Curr Opin Cell Biol. 10:323-31.

Miyoshi, D., and N. Sugimoto. 2008. Molecular crowding effects on structure and stability of DNA. Biochimie. 90:1040-51.

Monneron, A., and W. Bernhard. 1969. Fine structural organization of the interphase nucleus in some mammalian cells. J Ultrastruct Res. 27:266-88.

Mortillaro, M.J., B.J. Blencowe, X. Wei, H. Nakayasu, L. Du, S.L. Warren, P.A. Sharp, and R. Berezney. 1996. A hyperphosphorylated form of the large subunit of RNA polymerase II is associated with splicing complexes and the nuclear matrix. Proc Natl Acad Sci U S A. 93:8253-7.

Muller, W.G., D. Rieder, T.S. Karpova, S. John, Z. Trajanoski, and J.G. McNally. 2007. Organization of chromatin and histone modifications at a transcription site. J Cell Biol. 177:957-67.

Muller-Reichert, T., M. Srayko, A. Hyman, E.T. O'Toole, and K. McDonald. 2007. Correlative light and electron microscopy of early *Caenorhabditis elegans* embryos in mitosis. Methods Cell Biol. 79:101-19.

Navascues, J., R. Bengoechea, O. Tapia, J.P. Vaque, M. Lafarga, and M.T. Berciano. 2007. Characterization of a new SUMO-1 nuclear body (SNB) enriched in pCREB, CBP, c-Jun in neuron-like UR61 cells. Chromosoma. 116:441-51.

Noguchi, K., R. Shiurba, and T. Higashinakagawa. 2002. Nuclear translocation of mouse polycomb m33 protein in regenerating liver. Biochem Biophys Res Commun. 291:508-15.

Nye, A.C., R.R. Rajendran, D.L. Stenoien, M.A. Mancini, B.S. Katzenellenbogen, and A.S. Belmont. 2002. Alteration of large-scale chromatin structure by estrogen receptor. Mol Cell Biol. 22:3437-49.

Osborne, C.S., L. Chakalova, K.E. Brown, D. Carter, A. Horton, E. Debrand, B. Goyenechea, J.A. Mitchell, S. Lopes, W. Reik, and P. Fraser. 2004. Active genes dynamically colocalize to shared sites of ongoing transcription. Nat Genet. 36:1065-71.

Otte, A.P., and T.H. Kwaks. 2003. Gene repression by Polycomb group protein complexes: a distinct complex for every occasion? Curr Opin Genet Dev. 13:448-54.

Pan, G., S. Tian, J. Nie, C. Yang, V. Ruotti, H. Wei, G.A. Jonsdottir, R. Stewart, and J.A. Thomson. 2007. Whole-genome analysis of histone H3 lysine 4 and lysine 27 methylation in human embryonic stem cells. Cell Stem Cell. 1:299-312.

Parada, L., and T. Misteli. 2002. Chromosome positioning in the interphase nucleus. Trends Cell Biol. 12:425-32.

Pederson, T. 1998. The plurifunctional nucleolus. Nucleic Acids Res. 26:3871-6.

Peric-Hupkes, D., W. Meuleman, L. Pagie, S.W. Bruggeman, I. Solovei, W. Brugman, S. Graf, P. Flicek, R.M. Kerkhoven, M. van Lohuizen, M. Reinders, L. Wessels, and B. van Steensel. 2010. Molecular maps of the reorganization of genome-nuclear lamina interactions during differentiation. Mol Cell. 38:603-13.

Phair, R.D., P. Scaffidi, C. Elbi, J. Vecerova, A. Dey, K. Ozato, D.T. Brown, G. Hager, M. Bustin, and T. Misteli. 2004. Global nature of dynamic protein-chromatin interactions *in vivo*: three-dimensional genome scanning and dynamic interaction networks of chromatin proteins. Mol Cell Biol. 24:6393-402.

Pietersen, A.M., B. Evers, A.A. Prasad, E. Tanger, P. Cornelissen-Steijger, J. Jonkers, and M. van Lohuizen. 2008. Bmi1 regulates stem cells and proliferation and differentiation of committed cells in mammary epithelium. Curr Biol. 18:1094-9.

Pietersen, A.M., and M. van Lohuizen. 2008. Stem cell regulation by polycomb repressors: postponing commitment. Curr Opin Cell Biol. 20:201-7.

Pirrotta, V., and H.B. Li. 2011. A view of nuclear Polycomb bodies. Curr Opin Genet Dev. 22:101-9.

Platero, J.S., T. Hartnett, and J.C. Eissenberg. 1995. Functional analysis of the chromo domain of HP1. Embo J. 14:3977-86.

Plath, K., D. Talbot, K.M. Hamer, A.P. Otte, T.P. Yang, R. Jaenisch, and B. Panning. 2004. Developmentally regulated alterations in Polycomb repressive complex 1 proteins on the inactive X chromosome. J Cell Biol. 167:1025-35.

Politz, J.C., R.A. Tuft, T. Pederson, and R.H. Singer. 1999. Movement of nuclear poly(A) RNA throughout the interchromatin space in living cells. Curr Biol. 9:285-91.

Pombo, A., P. Cuello, W. Schul, J.B. Yoon, R.G. Roeder, P.R. Cook, and S. Murphy. 1998. Regional and temporal specialization in the nucleus: a transcriptionally-active nuclear domain rich in PTF, Oct1 and PIKA antigens associates with specific chromosomes early in the cell cycle. Embo J. 17:1768-78.

Rajapakse, I., and M. Groudine. 2011. On emerging nuclear order. J Cell Biol. 192:711-21.

Rapkin, L.M., D.R. Anchel, R. Li, and D.P. Bazett-Jones. 2012. A view of the chromatin landscape. Micron. 43:150-8.

Raska, I. 1995. Nuclear ultrastructures associated with the RNA synthesis and processing. J Cell Biochem. 59:11-26.

Raska, I. 2003. Oldies but goldies: searching for Christmas trees within the nucleolar architecture. Trends Cell Biol. 13:517-25.

Raska, I., B.L. Armbruster, J.R. Frey, and K. Smetana. 1983. Analysis of ring-shaped nucleoli in serially sectioned human lymphocytes. Cell Tissue Res. 234:707-11.

Raska, I., M. Dundr, K. Koberna, I. Melcak, M.C. Risueno, and I. Torok. 1995. Does the synthesis of ribosomal RNA take place within nucleolar fibrillar centers or dense fibrillar components? A critical appraisal. J Struct Biol. 114:1-22.

Raska, I., K. Koberna, J. Malinsky, H. Fidlerova, and M. Masata. 2004. The nucleolus and transcription of ribosomal genes. Biol Cell. 96:579-94.

Raska, I., R.L. Ochs, L.E. Andrade, E.K. Chan, R. Burlingame, C. Peebles, D. Gruol, and E.M. Tan. 1990. Association between the nucleolus and the coiled body. J Struct Biol. 104:120-7.

Raska, I., Z. Rychter, and K. Smetana. 1983. Fibrillar centres and condensed nucleolar chromatin in resting and stimulated human lymphocytes. Z Mikrosk Anat Forsch. 97:15-32.

Raska, I., P.J. Shaw, and D. Cmarko. 2006. New insights into nucleolar architecture and activity. Int Rev Cytol. 255:177-235.

Ren, X., C. Vincenz, and T.K. Kerppola. 2008. Changes in the distributions and dynamics of polycomb repressive complexes during embryonic stem cell differentiation. Mol Cell Biol. 28:2884-95.

Reynolds, E.S. 1963. The use of lead citrate at high pH as an electron-opaque stain in electron microscopy. J Cell Biol. 17:208-12.

Richard, E., S. Causse, C. Spriet, N. Fourre, D. Trinel, X. Darzacq, B. Vandenbunder, and L. Heliot. 2011. Short exposure to the DNA intercalator DRAQ5 dislocates the transcription machinery and induces cell death. Photochem Photobiol. 87:256-61.

Richter, K., M. Nessling, and P. Lichter. 2007. Experimental evidence for the influence of molecular crowding on nuclear architecture. J Cell Sci. 120:1673-80.

Richter, K., M. Nessling, and P. Lichter. 2008. Macromolecular crowding and its potential impact on nuclear function. Biochim Biophys Acta. 1783:2100-7.

Ringrose, L., and R. Paro. 2004. Epigenetic regulation of cellular memory by the Polycomb and Trithorax group proteins. Annu Rev Genet. 38:413-43.

Rinn, J.L., M. Kertesz, J.K. Wang, S.L. Squazzo, X. Xu, S.A. Brugmann, L.H. Goodnough, J.A. Helms, P.J. Farnham, E. Segal, and H.Y. Chang. 2007. Functional demarcation of active and silent chromatin domains in human HOX loci by noncoding RNAs. Cell. 129:1311-23.

Rouquette, J., C. Cremer, T. Cremer, and S. Fakan. 2010. Functional nuclear architecture studied by microscopy: present and future. Int Rev Cell Mol Biol. 282:1-90.

Satijn, D.P., M.J. Gunster, J. van der Vlag, K.M. Hamer, W. Schul, M.J. Alkema, A.J. Saurin, P.S. Freemont, R. van Driel, and A.P. Otte. 1997. RING1 is associated with the polycomb group protein complex and acts as a transcriptional repressor. Mol Cell Biol. 17:4105-13.

Saurin, A.J., C. Shiels, J. Williamson, D.P. Satijn, A.P. Otte, D. Sheer, and P.S. Freemont. 1998. The human polycomb group complex associates with pericentromeric heterochromatin to form a novel nuclear domain. J Cell Biol. 142:887-98.

Sawarkar, R., and R. Paro. 2010. Interpretation of developmental signaling at chromatin: the Polycomb perspective. Dev Cell. 19:651-61.

Sexton, T., D. Umlauf, S. Kurukuti, and P. Fraser. 2007. The role of transcription factories in large-scale structure and dynamics of interphase chromatin. Semin Cell Dev Biol. 18:691-7.

Scheffer, M.P., M. Eltsov, and A.S. Frangakis. 2011. Evidence for short-range helical order in the 30-nm chromatin fibers of erythrocyte nuclei. Proc Natl Acad Sci U S A. 108:16992-7.

Schneider, R., and R. Grosschedl. 2007. Dynamics and interplay of nuclear architecture, genome organization, and gene expression. Genes Dev. 21:3027-43.

Schoenfelder, S., T. Sexton, L. Chakalova, N.F. Cope, A. Horton, S. Andrews, S. Kurukuti, J.A. Mitchell, D. Umlauf, D.S. Dimitrova, C.H. Eskiw, Y. Luo, C.L. Wei, Y. Ruan, J.J. Bieker, and P. Fraser. 2009. Preferential associations between co-regulated genes reveal a transcriptional interactome in erythroid cells. Nat Genet. 42:53-61.

Schoenfelder, S., I. Clay, and P. Fraser. 2010. The transcriptional interactome: gene expression in 3D. Curr Opin Genet Dev. 20:127-33.

Schoorlemmer, J., C. Marcos-Gutierrez, F. Were, R. Martinez, E. Garcia, D.P. Satijn, A.P. Otte, and M. Vidal. 1997. Ring1A is a transcriptional repressor that interacts with the Polycomb-M33 protein and is expressed at rhombomere boundaries in the mouse hindbrain. EMBO J. 16:5930-42.

Schubeler, D. 2010. Chromatin in multicolor. Cell. 143:183-4.

Schuettengruber, B., M. Ganapathi, B. Leblanc, M. Portoso, R. Jaschek, B. Tolhuis, M. van Lohuizen, A. Tanay, and G. Cavalli. 2009. Functional anatomy of polycomb and trithorax chromatin landscapes in *Drosophila* embryos. PLoS Biol. 7:e13.

Schul, W., B. Groenhout, K. Koberna, Y. Takagaki, A. Jenny, E.M. Manders, I. Raska, R. van Driel, and L. de Jong. 1996. The RNA 3' cleavage factors CstF 64 kDa and CPSF 100 kDa are concentrated in nuclear domains closely associated with coiled bodies and newly synthesized RNA. Embo J. 15:2883-92.

Schul, W., R. van Driel, and L. de Jong. 1998. A subset of poly(A) polymerase is concentrated at sites of RNA synthesis and is associated with domains enriched in splicing factors and poly(A) RNA. Exp Cell Res. 238:1-12.

Schwartz, Y.B., T.G. Kahn, P. Stenberg, K. Ohno, R. Bourgon, and V. Pirrotta. 2010. Alternative epigenetic chromatin states of polycomb target genes. PLoS Genet. 6:e1000805.

Schweizer, D., and P.F. Ambros. 1994. Chromosome banding. Stain combinations for specific regions. Methods Mol Biol. 29:97-112.

Simon, J.A., and R.E. Kingston. 2009. Mechanisms of polycomb gene silencing: knowns and unknowns. Nat Rev Mol Cell Biol. 10:697-708.

Smetana, K., I. Daskal, and H. Busch. 1979. Further cytochemical studies on the perichromatin granules. Histochemistry. 61:327-34.

Smigova, J., P. Juda, D. Cmarko, and I. Raska. 2011. Fine structure of the "PcG body" in human U-2 OS cells established by correlative light-electron microscopy. Nucleus. 2:219-28.

Sparmann, A., and M. van Lohuizen. 2006. Polycomb silencers control cell fate, development and cancer. Nat Rev Cancer. 6:846-56.

Spector, D.L. 1990. Higher order nuclear organization: three-dimensional distribution of small nuclear ribonucleoprotein particles. Proc Natl Acad Sci U S A. 87:147-51.

Spector, D.L. 1993. Nuclear organization of pre-mRNA processing. Curr Opin Cell Biol. 5:442-7.

Spector, D.L. 2001. Nuclear domains. J Cell Sci. 114:2891-3.

Spector, D.L. 2006. SnapShot: Cellular bodies. Cell. 127:1071.

Spector, D.L., X.D. Fu, and T. Maniatis. 1991. Associations between distinct pre-mRNA splicing components and the cell nucleus. Embo J. 10:3467-81.

Spellman, P.T., and G.M. Rubin. 2002. Evidence for large domains of similarly expressed genes in the *Drosophila* genome. J Biol. 1:5.

Stack, S.M., D.B. Brown, and W.C. Dewey. 1977. Visualization of interphase chromosomes. J Cell Sci. 26:281-99.

Stadler, S., V. Schnapp, R. Mayer, S. Stein, C. Cremer, C. Bonifer, T. Cremer, and S. Dietzel. 2004. The architecture of chicken chromosome territories changes during differentiation. BMC Cell Biol. 5:44.

Stock, J.K., S. Giadrossi, M. Casanova, E. Brookes, M. Vidal, H. Koseki, N. Brockdorff, A.G. Fisher, and A. Pombo. 2007. Ring1-mediated ubiquitination of H2A restrains poised RNA polymerase II at bivalent genes in mouse ES cells. Nat Cell Biol. 9:1428-35.

Strickfaden, H., A. Zunhammer, S. van Koningsbruggen, D. Kohler, and T. Cremer. 2010. 4D chromatin dynamics in cycling cells: Theodor Boveri's hypotheses revisited. Nucleus. 1:284-97.

Taddei, A., F. Hediger, F.R. Neumann, C. Bauer, and S.M. Gasser. 2004. Separation of silencing from perinuclear anchoring functions in yeast Ku80, Sir4 and Esc1 proteins. EMBO J. 23:1301-12.

Tolhuis, B., M. Blom, R.M. Kerkhoven, L. Pagie, H. Teunissen, M. Nieuwland, M. Simonis, W. de Laat, M. van Lohuizen, and B. van Steensel. 2011. Interactions among Polycomb domains are guided by chromosome architecture. PLoS Genet. 7:e1001343.

Trojer, P., and D. Reinberg. 2007. Facultative heterochromatin: is there a distinctive molecular signature? Mol Cell. 28:1-13.

Tuckfield, A., D.R. Clouston, T.M. Wilanowski, L.L. Zhao, J.M. Cunningham, and S.M. Jane. 2002. Binding of the RING polycomb proteins to specific target genes in complex with the grainyhead-like family of developmental transcription factors. Mol Cell Biol. 22:1936-46.

Tumbar, T., G. Sudlow, and A.S. Belmont. 1999. Large-scale chromatin unfolding and remodeling induced by VP16 acidic activation domain. J Cell Biol. 145:1341-54.

Turner, B.M. 2007. Defining an epigenetic code. Nat Cell Biol. 9:2-6.

van Driel, R., P.F. Fransz, and P.J. Verschure. 2003. The eukaryotic genome: a system regulated at different hierarchical levels. J Cell Sci. 116:4067-75.

van Holde, K., and J. Zlatanova. 1995. Chromatin higher order structure: chasing a mirage? J Biol Chem. 270:8373-6.

van Steensel, B. 2011. Chromatin: constructing the big picture. Embo J. 30:1885-95.

van Steensel, B., J. Delrow, and S. Henikoff. 2001. Chromatin profiling using targeted DNA adenine methyltransferase. Nat Genet. 27:304-8.

Verkade, P. 2008. Moving EM: the Rapid Transfer System as a new tool for correlative light and electron microscopy and high throughput for high-pressure freezing. J Microsc. 230:317-28.

Verschure, P.J., I. Van Der Kraan, J.M. Enserink, M.J. Mone, E.M. Manders, and R. Van Driel. 2002. Large-scale chromatin organization and the localization of proteins involved in gene expression in human cells. J Histochem Cytochem. 50:1303-12.

Verschure, P.J., I. van der Kraan, E.M. Manders, D. Hoogstraten, A.B. Houtsmuller, and R. van Driel. 2003. Condensed chromatin domains in the mammalian nucleus are accessible to large macromolecules. EMBO Rep. 4:861-6.

Verschure, P.J., I. van Der Kraan, E.M. Manders, and R. van Driel. 1999. Spatial relationship between transcription sites and chromosome territories. J Cell Biol. 147:13-24.

Villa, R., D. Pasini, A. Gutierrez, L. Morey, M. Occhionorelli, E. Vire, J.F. Nomdedeu, T. Jenuwein, P.G. Pelicci, S. Minucci, F. Fuks, K. Helin, and L. Di Croce. 2007. Role of the polycomb repressive complex 2 in acute promyelocytic leukemia. Cancer Cell. 11:513-25.

Visser, A.E., F. Jaunin, S. Fakan, and J.A. Aten. 2000. High resolution analysis of interphase chromosome domains. J Cell Sci. 113 (Pt 14):2585-93.

Volpi, E.V., E. Chevret, T. Jones, R. Vatcheva, J. Williamson, S. Beck, R.D. Campbell, M. Goldsworthy, S.H. Powis, J. Ragoussis, J. Trowsdale, and D. Sheer. 2000. Large-scale chromatin organization of the major histocompatibility complex and other regions of human chromosome 6 and its response to interferon in interphase nuclei. J Cell Sci. 113 (Pt 9):1565-76.

Voncken, J.W., D. Schweizer, L. Aagaard, L. Sattler, M.F. Jantsch, and M. van Lohuizen. 1999. Chromatin-association of the Polycomb group protein BMI1 is cell cycle-regulated and correlates with its phosphorylation status. J Cell Sci. 112 (Pt 24):4627-39.

Wang, H., L. Wang, H. Erdjument-Bromage, M. Vidal, P. Tempst, R.S. Jones, and Y. Zhang. 2004. Role of histone H2A ubiquitination in Polycomb silencing. Nature. 431:873-8.

Whitcomb, S.J., A. Basu, C.D. Allis, and E. Bernstein. 2007. Polycomb Group proteins: an evolutionary perspective. Trends Genet. 23:494-502.

Woodcock, C.L. 2006. Chromatin architecture. Curr Opin Struct Biol. 16:213-20.

Woodcock, C.L., and R.P. Ghosh. 2010. Chromatin higher-order structure and dynamics. Cold Spring Harb Perspect Biol. 2:a000596.

Yap, K.L., S. Li, A.M. Munoz-Cabello, S. Raguz, L. Zeng, S. Mujtaba, J. Gil, M.J. Walsh, and M.M. Zhou. 2010. Molecular interplay of the noncoding RNA ANRIL and methylated histone H3 lysine 27 by polycomb CBX7 in transcriptional silencing of INK4a. Mol Cell. 38:662-74.

Zeng, C., E. Kim, S.L. Warren, and S.M. Berget. 1997. Dynamic relocation of transcription and splicing factors dependent upon transcriptional activity. Embo J. 16:1401-12.

Zhang, T., Y. Sun, E. Tian, H. Deng, Y. Zhang, X. Luo, Q. Cai, H. Wang, J. Chai, and H. Zhang. 2006. RNA-binding proteins SOP-2 and SOR-1 form a novel PcG-like complex in *C. elegans.* Development. 133:1023-33.

Zhao, R., M.S. Bodnar, and D.L. Spector. 2009. Nuclear neighborhoods and gene expression. Curr Opin Genet Dev. 19:172-9.

Zhao, X.D., X. Han, J.L. Chew, J. Liu, K.P. Chiu, A. Choo, Y.L. Orlov, W.K. Sung, A. Shahab, V.A. Kuznetsov, G. Bourque, S. Oh, Y. Ruan, H.H. Ng, and C.L. Wei. 2007. Whole-genome mapping of histone H3 Lys4 and 27 trimethylations reveals distinct genomic compartments in human embryonic stem cells. Cell Stem Cell. 1:286-98.

Zink, B., and R. Paro. 1989. *In vivo* binding pattern of a trans-regulator of homoeotic genes in *Drosophila* melanogaster. Nature. 337:468-71.

8. List of publications

Slamenova D, Sramkova M, Chalupa I, Smigova J, Kogan G. Reduction of genotoxic effects of N-nitrosomorpholine in human hepatoma cells and hamster lung cells by carboxymethyl chitin-glucan. Neoplasma. 2008;55(4):280-5. IF 1,449

Cmarko D, Smigova J, Minichova L, Popov A. Nucleolus: the ribosome factory. Histol Histopathol. 2008; 23(10):1291-8. IF 2,502

Krejcí J, Uhlírová R, Galiová G, Kozubek S, Smigová J, Bártová E. Genome-wide reduction in H3K9 acetylation during human embryonic stem cell differentiation. J Cell Physiol. 2009 Jun;219(3):677-87. IF 3,986

Gancarcíková M, Zemanová Z, Brezinová J, Berková A, Vcelíková S, Smigová J, Michalová K. The role of telomeres and telomerase complex in haematological neoplasia: the length of telomeres as a marker of carcinogenesis and prognosis of disease. Prague Med Rep. 2010;111(2):91-105.

Šmigová J, Juda P, Cmarko D, Raška I. Fine structure of the "PcG body" in human U-2 OS cells established by correlative light-electron microscopy. Nucleus 2011 May/June; 2(3):219-28; a new journal

Šmigová J, Juda P, Bártová E, Raška I. Behaviour of PcG chromatin domain under conditions of molecular crowding, manuscript submitted 2012.